

**ORIENTATIONAL CONTROL OF CHEMICAL REACTIVITY
IN
LIQUID CRYSTALLINE SOLVENTS**

**By
DAVID SCOTT MITCHELL, B.Sc.**

**Submitted to the School of Graduate Studies
in Partial Fulfilment of the Requirements
for the Degree
Doctor of Philosophy**

McMaster University

(c) Copyright by David Scott Mitchell, October 1990

BIMOLECULAR REACTIVITY IN LIQUID CRYSTALLINE SOLVENTS

DOCTOR OF PHILOSOPHY (1991)
(Chemistry)

McMASTER UNIVERSITY
Hamilton, Ontario

TITLE: Orientational Control of Chemical Reactivity
 in Liquid Crystalline Solvents

AUTHOR: David Scott Mitchell, B.Sc. (McMaster University)

SUPERVISOR: Professor W. J. Leigh

NUMBER OF PAGES: xiii, 178

ABSTRACT

The effect of cholesteric and smectic liquid crystalline solvent order on the regiochemical control of a thermal bimolecular reaction has been investigated. The cycloaddition reaction of cholesta-5,7-dien-3 β -yl acetate with rigid enophiles has been shown to yield several 1:1 cycloadducts. The relative product yields for this reaction have been determined in a number of isotropic solvents, two cholesteric liquid crystals and a highly ordered smectic B phase. In ordered media, the relative yield of one product is enhanced at the expense of the others. The magnitude of this effect is highly dependent on the rod-like shape of the enophile and on the ordered nature of the solvent. We rationalize these results in terms of how the average orientation of the reactants within the liquid crystal influences the energetics of reaction. The enhanced adduct occurs *via* a transition state orientation that, compared to the other products, is much more compatible with liquid crystalline order. In ordered media, this pathway becomes energetically favoured. The largest effects on reactivity are seen when the reactants are rod-like in shape, the reactive centres are conformationally immobile and the solvent is highly ordered. This is explained in terms of how reactant shape and solvent order influence the average orientation of the solutes within the liquid crystal. It appears that more rod-like reactants are better oriented, resulting in a larger influence on reaction energetics. The more ordered smectic mesogen exerts a larger influence on regiochemical control than the more fluid cholesteric phases, presumably due to a better average orientation of the reactant(s). Activation parameters and thermal microscopy data indicate that while the orientational control of reactivity is greater in the smectic phase, the reactants may experience a heterogeneous environment.

ACKNOWLEDGEMENTS

First, and foremost, I would like to thank my research supervisor, Dr. William J. Leigh, for all of his guidance and support throughout my project. His enthusiastic approach to research and his "never say die" attitude have helped to make me a better scientist. I would also like to thank Willie for his friendship and understanding in more personal matters over the years.

The members of my supervisory committee, Dr. B.E. McCarry, Dr. O.E. Hileman and, more recently, Dr. P. Harrison have been very generous with their time and I would like to thank them for all their suggestions and assistance.

I would also like to thank the staff of both the n.m.r. and mass spec. facilities for their kind assistance. Dr. D. Hughes and Mr. B. Sayer were always willing to squeeze me in to their busy schedule and to assist with n.m.r. problems while Dr. R. Smith and Mr. F. Ramelan were particularly helpful in completing some rather troublesome high resolution mass spec. work.

My lab-mates over the years have certainly added some very colourful memories. Many thanks to Brad Clark, Brian Fahie, Mark Workentin, Greg Sluggett, Al Postigo, Nien Nguyen and Kangcheng Zheng who have each contributed in their own way to making the past few years so enjoyable.

Finally, I would like to thank my entire family, particularly my mother and father, for their support (both personal and financial) and for putting up with my (occasionally) temperamental personality. My wife Sarah has also borne the brunt of a few senseless tirades and I thank her for putting up with me over the past few months.

TABLE OF CONTENTS

CHAPTER 1: INTRODUCTION

1.1.	Reactions in Ordered Media	1
1.2.	Introduction to Liquid Crystals	2
1.2.1.	General	2
1.2.2.	Classification of Liquid Crystals	3
1.2.3.	Viscosity and Diffusion in Liquid Crystals	6
1.3.	Organic Reactions in Liquid Crystals	9
1.3.1.	General	9
1.3.2.	Unimolecular Reactions in Liquid Crystalline Solvents	10
1.3.3.	Summary: Unimolecular Reactions in Liquid Crystalline Solvents	21
1.3.4.	Bimolecular Reactions in Liquid Crystalline Solvents	22
1.3.5.	Summary: Bimolecular Reactions in Liquid Crystalline Solvents	32
1.3.6.	Purpose of our Study	33

CHAPTER 2: REACTION OF N-ARYLMALEIMIDES WITH CHOLESTA-5,7-DIENE-3 β -YL ACETATE (I)

2.1.	Introduction	36
2.2.	Selection of a Suitable Bimolecular Reaction	36

2.2.1.	The Reaction of <u>1</u> with Dimethyl- -Acetylenedicarboxylate (DMAD)	36
2.2.2.	The Reaction of <u>1</u> with N-Arylmaleimides	40
2.3.	Structural Identification of Cycloaddition Adducts	42
2.3.1.	Introduction	42
2.3.2.	Structural Assignments; Adducts of <u>1</u> with (DMAD)	43
2.3.3.	Structural Assignments; Adducts of <u>1</u> with N-Biphenylmaleimide	46
2.3.4.	Product Identification; Adduct B5	47
2.3.5.	Product Identification; Adducts B4a and B4b	54
2.3.6.	Product Identification; Adduct B3	64
2.4.	Summary: Chapter 2	70
CHAPTER 3: ORIENTATIONAL CONTROL OF REACTIVITY IN LIQUID CRYSTALLINE SOLVENTS: THE REACTION OF <u>1</u> WITH N-ARYLMALEIMIDES		
3.1.	Introduction	72
3.2.	Results	73
3.2.1.	Solvent Selection and Transition Temperatures	73
3.2.2.	Cycloaddition Reaction of <u>1</u> with N-Arylmaleimides in Liquid Crystalline Solvents	76
3.2.3.	Relative Activation Parameters for the Reaction of <u>1</u> with TPMI in Liquid Crystalline Solvents	81
3.3.	Discussion: Reaction of <u>1</u> with N-Arylmaleimides in Liquid Crystalline Solvents	87
3.3.1.	General: The Influence of Orientational Order on Chemical Reactivity-How Much Can We Expect?	87

3.3.2.	Reaction of 1 with N-Arylmaleimides in Cholesteric Liquid Crystalline Solvents	93
3.3.3.	Relative Activation Parameters for the Reaction of 1 with TPMI in Cholesteric Liquid Crystalline Solvents	95
3.3.4.	Structural Studies: The Influence of Enophile Length on the Control of Chemical Reactivity in Cholesteric Solvents	98
3.3.5.	Reaction of 1 with N-Arylmaleimides in Smectic Liquid Crystalline Solvents	103
3.3.6.	Activation Parameters for the Reaction of 1 with TPMI in Smectic Liquid Crystalline Solvents	104
3.3.7.	Heterogeneous Solubilization of Reactants in Smectic Liquid Crystalline Solvents	106
3.3.8.	Thermal Microscopy: 1 with TPMI in S1544	108

CHAPTER 4: SUMMARY AND CONCLUSIONS

4.1.	Contributions of Our Study	112
4.2.	Future Work	114

CHAPTER 5: EXPERIMENTAL SECTION

5.1.	General	116
5.2.	Solvents	117
5.3.	Preparation and Purification of Compounds	118
5.3.1.	Preparation of Liquid Crystalline and Model Isotropic Solvents	118
5.3.2.	Preparation and Purification of Reactants	120
5.4.	Thermolyses of 1 with N-Arylmaleimides	123
5.4.1.	General Sample Preparation	123

5.4.2.	Reaction of <u>1</u> with N-Arylmaleimides	124
Appendix 1		131
Appendix 2a		134
Appendix 2b		137
Appendix 2c		144
Appendix 2d		156
Appendix 3a		162
Appendix 3b		164
Appendix 3c		166
Appendix 3d		168
Appendix 4		170
CHAPTER 6: REFERENCES		171

LIST OF SCHEMES

1.1.	Claisen rearrangement of allyl phenyl ethers.	11
1.2.	Cis-trans isomerization of a bulky olefin.	12
1.3.	Hindered rotation of dimethylamino group.	13
1.4.	Isomerization of photochromic merocyanine	15
1.5.	Remote hydrogen abstraction in linked phenolic ketones	17
1.6.	Intermolecular exciplex formation in β -phenyl ketones	20
1.7.	The fate of photogenerated benzyl radicals	24
1.8.	Dissociation equilibrium of 4-methoxytriphenyltrifluoroacetate	25
1.9.	Esterification of a chiral anhydride	26
1.10.	Diels-Alder reaction of substituted cyclopentadienone with various rigid dienophiles	27
1.11.	Competitive excimer/exciple formation	28
1.12.	Photodimerization of acenaphthalene	29
1.13.	Isomerization of benzene sulphonate esters	30
2.1.	Reaction of <u>1</u> with <u>DMAD</u>	37
2.2.	Transition states to <u>1/DMAD</u> products	38
2.3.	Reaction of <u>1</u> with N-arylmaleimides	40
2.4.	Transition states to <u>1/N-arylmaleimide</u> products	41
2.5.	Hydrolysis of <u>II</u> and <u>X</u>	44

LIST OF FIGURES

1.1.	Representation of discotic liquid crystals	4
1.2.	Description of thermotropic liquid crystals	6
1.3.	CCH-n liquid crystals	18
1.4.	Smectic B liquid crystals used by Samori <i>et al</i>	31
1.5.	Cycloaddition reactions of a rod-like enophile with a steroidal diene	34
1.6.	Reactant orientations in liquid crystalline solvents	35
2.1.	Structures of rigid enophiles used in this work	39
2.2.	Structures of adducts <u>X</u> and <u>II</u>	43
2.3.	Structure of adduct <u>B5</u>	47
2.4.	Structures of adducts <u>B4a</u> and <u>B4b</u>	54
2.5.	Structure of adduct <u>B3</u>	64
3.1.	Eyring plot; reaction of <u>1</u> with <u>TPMI</u> in <u>C.B.</u> and <u>C.C.B.</u>	85
3.2.	Eyring plot; reaction of <u>1</u> with <u>TPMI</u> in <u>S1409</u> and <u>S1544</u>	86
3.3.	Percent yield of products for each enophile in isotropic, cholesteric and smectic solvents	94
3.4.	Ratio of <u>5</u> / <u>4a</u> in cholesteric and isotropic solvents vs number of phenyl groups on enophile	99
3.5.	Phase diagram for p-methoxy- β -phenylpropiophenone in <u>CCH-4</u> (0-30 mol%)	107

LIST OF TABLES

1.1.	Activation parameters for hindered rotation of dimethylamino group.	14
2.1.	^1H and ^{13}C chemical shifts (ppm) and important ^1H - ^1H correlations; ring A, adduct <u>B5</u>	49
2.2.	^1H and ^{13}C chemical shifts (ppm) and important ^1H - ^1H correlations; ring B, adduct <u>B5</u>	49
2.3.	^1H and ^{13}C chemical shifts (ppm) and important ^1H - ^1H correlations; ring C, adduct <u>B5</u>	50
2.4.	^1H and ^{13}C chemical shifts (ppm) and important ^1H - ^1H correlations; ring D, adduct <u>B5</u>	51
2.5.	^1H and ^{13}C chemical shifts (ppm) and important ^1H - ^1H correlations; succinimide portion and carbonyls, adduct <u>B5</u>	52
2.6.	^1H and ^{13}C chemical shifts (ppm) and important ^1H - ^1H correlations; alkyl chain and methyl groups, adduct <u>B5</u>	53
2.7.	^1H and ^{13}C chemical shifts (ppm) and important ^1H - ^1H correlations; ring A, adduct <u>B4b</u>	56
2.8.	^1H and ^{13}C chemical shifts (ppm) and important ^1H - ^1H correlations; ring B, adduct <u>B4b</u>	56
2.9.	^1H and ^{13}C chemical shifts (ppm) and important ^1H - ^1H correlations; ring C, adduct <u>B4b</u>	57
2.10.	^1H and ^{13}C chemical shifts (ppm) and important ^1H - ^1H correlations; ring D, adduct <u>B4b</u>	58
2.11.	^1H and ^{13}C chemical shifts (ppm) and important ^1H - ^1H correlations; succinimide portion and carbonyls, adduct <u>B4b</u>	58
2.12.	^1H and ^{13}C chemical shifts (ppm) and important ^1H - ^1H correlations; alkyl chain and methyl groups, adduct <u>B5</u>	59
2.13.	^1H and ^{13}C chemical shifts (ppm) and important ^1H - ^1H correlations; ring A, adduct <u>B4a</u>	60

2.14.	^1H and ^{13}C chemical shifts (ppm) and important ^1H - ^1H correlations; ring B, adduct <u>B4a</u>	61
2.15.	^1H and ^{13}C chemical shifts (ppm) and important ^1H - ^1H correlations; ring C, adduct <u>B4a</u>	61
2.16.	^1H and ^{13}C chemical shifts (ppm) and important ^1H - ^1H correlations; ring D, adduct <u>B4a</u>	62
2.17.	^1H and ^{13}C chemical shifts (ppm) and important ^1H - ^1H correlations; succinimide portion and carbonyls, adduct <u>B4a</u>	62
2.18.	^1H and ^{13}C chemical shifts (ppm) and important ^1H - ^1H correlations; alkyl chain and methyl groups, adduct <u>B4a</u>	63
2.19.	^1H and ^{13}C chemical shifts (ppm) and important ^1H - ^1H correlations; ring A, adduct <u>B3</u>	66
2.20.	^1H and ^{13}C chemical shifts (ppm) and important ^1H - ^1H correlations; ring B, adduct <u>B3</u>	67
2.21.	^1H and ^{13}C chemical shifts (ppm) and important ^1H - ^1H correlations; ring C, adduct <u>B3</u>	68
2.22.	^1H and ^{13}C chemical shifts (ppm) and important ^1H - ^1H correlations; ring D, adduct <u>B3</u>	69
2.23.	^1H and ^{13}C chemical shifts (ppm) and important ^1H - ^1H correlations; succinimide portion and carbonyls, adduct <u>B3</u>	69
2.24.	^1H and ^{13}C chemical shifts (ppm) and important ^1H - ^1H correlations; alkyl chain and methyl groups, adduct <u>B3</u>	70
3.1.	Structures of liquid crystalline solvents	74
3.2.	Transition temperatures for neat and solute doped cholesteric and model isotropic solvents	76
3.3.	Product yields (%); thermolysis of <u>1</u> with <u>NPMI</u>	78
3.4.	Product yields (%); thermolysis of <u>1</u> with <u>BPMI</u>	79
3.5.	Product yields (%); thermolysis of <u>1</u> with <u>TPMI</u>	80
3.6.	Product yields (%); thermolysis of <u>1</u> with <u>TPMI</u> at various temperatures between 180 and 240°C (solvent <u>C.B.</u>)	83

3.7.	Product yields (%); thermolysis of <u>1</u> with <u>TPMI</u> at various temperatures between 180 and 240°C (solvent <u>C.C.B.</u>)	83
3.8.	Product yields (%); thermolysis of <u>1</u> with <u>TPMI</u> at various temperatures between 180 and 240°C (solvent <u>S1409</u>)	84
3.9.	Product yields (%); thermolysis of <u>1</u> with <u>TPMI</u> at various temperatures between 180 and 240°C (solvent <u>S1544</u>)	84
3.10.	($\Delta G^*_{4a} - \Delta G^*_5$ (kcal/mol)) for the reaction of <u>1</u> with each enophile in <u>C.C.B.</u> and <u>C.B.</u>	100
3.11.	($\Delta G^*_{4a} - \Delta G^*_5$ (kcal/mol)) for the reaction of <u>1</u> with each enophile in <u>S1544</u> and <u>S1409</u>	104

CHAPTER 1: INTRODUCTION

1.1. Reactions in Ordered Media

Controlling the selectivity of chemical reactions is of great interest to many chemists. Whether it is an industrial chemist preparing compounds on a large scale or a synthetic chemist interested in isolating only a few crystals, increasing the yield of desired products is of prime importance. Altering chemical reactivity has traditionally been accomplished by utilizing electronic effects and/or steric factors. Molecular orientation and collision geometry usually remain random.

Another approach to controlling reactivity, that has received much interest recently, is to restrict molecular mobility and allow reactant interaction only along specific reaction profiles. Using this method, reactivity is limited to those pathways compatible with the imposed physical constraints.

A large number of systems have been investigated in which the translational or rotational motions of the reactive moieties are restricted.¹⁻⁸ Enzymes for example bind and orient the reactive species, restricting translational motion.^{1,2} This reduces the number of possible transition states to those which are compatible with the restrictions imposed by the organized medium. Inclusion compounds can also act as a restrictive medium. These porous materials contain discrete cavities or channel-like structures.³ The reactivity of guest molecules entering such a restrictive environment is altered due to reduced molecular mobility or limited access to other reactive species while inside the inclusion compound. Non-reactive surfaces such as silica gel can also be used to

restrict solute mobility. The reactant(s) are adsorbed onto the non-reactive surface causing a reduction in mobility and limiting access to reactive partners.^{2,7} Other systems used as constraining media include micelles, microemulsions and organic crystals. For a comprehensive review of these topics the reader should consult the cited references.¹⁻⁸

Our interest has been primarily in the use of liquid crystalline compounds to orient guest molecules. This method is particularly appealing because it is simple and potentially very useful. Separation of the liquid crystalline solvent from the reaction products can often be accomplished using chromatographic methods. Consequently, preparative scale syntheses in liquid crystals are quite feasible. Before such goals can be realized however, we need to be able to predict with some degree of certainty what the potential effect of liquid crystalline order might be on a given reactive system.

In the remainder of this chapter, an introduction to liquid crystals will be presented followed by a review of the current literature involving the use of these ordered solvents to alter chemical reactivity. Most of the work done to date has been aimed at better defining the potential of liquid crystalline solvents to alter chemical reactivity.

1.2. Introduction to Liquid Crystals

1.2.1. General

While the liquid crystalline phase has been known for over one hundred years, research into the nature of these compounds has only begun in earnest in the past twenty five years, due primarily to their potential applications as display devices.⁹ The unique properties of some liquid crystals such as their temperature sensitive colour

changes or their propensity to be aligned in magnetic fields have been utilized in applications such as thermometers, pocket calculators, and wrist watches. As well, a number of living systems have been found in which liquid crystalline phases control biological processes. There is also much interest in studying the basic nature of this state of matter, including its molecular ordering characteristics and phase transition behaviour.

1.2.2. Classification of Liquid Crystals

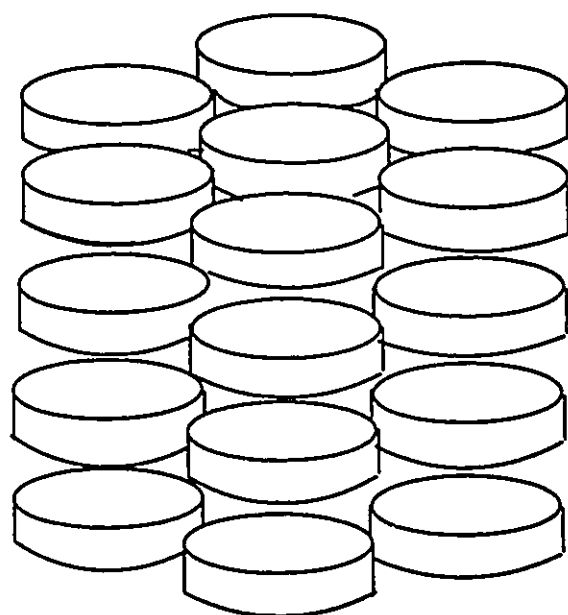
As the name implies, liquid crystals have properties intermediate between crystalline solids and isotropic liquids.⁹ Liquid crystals can be broadly divided into two classifications; lyotropic and thermotropic.

Lyotropic liquid crystalline phases are induced by adding polar solvents to amphiphilic compounds. Amphiphilic compounds contain a hydrophilic head group and a hydrophobic tail. By adding varying amounts of a polar solvent such as water, the amphiphile may exhibit several polymorphic phase types originating from a lamellar or cylindrical packing arrangement.⁹⁸

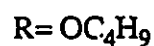
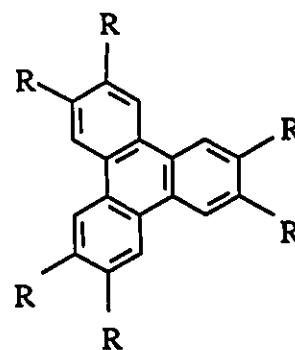
Our interest however, has been exclusively with thermotropic liquid crystals. Thermotropic liquid crystalline phases occur at temperatures intermediate between the crystalline solid and the isotropic liquid.

Thermotropic liquid crystals can be subdivided into four structural sub-classes; nematic (thread-like), cholesteric (usually cholesteryl esters), smectic (soap-like) or discotic.

Discotic liquid crystals, illustrated in Figure 1.1, are formed by flat "disk-like" molecules. The molecules are stacked into columns and packed in a hexagonal structure.



example;



Hexabutoxytriphenylene

Figure 1.1. Representation of discotic liquid crystals.

The interlayer spacing between molecules is variable and consequently, the columns are free to move laterally while translational order is maintained in the other two directions.

We are more interested in the types of liquid crystalline phases formed by molecules which have a rigid, rod-like structure. In the liquid crystalline phase, these molecules are oriented with their long axes, on average, parallel. In general such phases are seen in molecules that are cylindrical in shape. Polar groups are frequently found in the middle or at the extremities of molecules which exhibit liquid crystalline behaviour.⁹⁸

Nematic liquid crystals are the most fluid type of intermediate phase. They possess one degree of orientational order. The constituent molecules are aligned with their long axes, on average, parallel. There is no other translational or orientational order associated with nematic phases. They are essentially ordered fluids. *Cholesteric* phases are identical in terms of order to the nematic phase except that the molecules pack with a gradual twist to the direction of orientation. The period (or pitch) of this twist is on the order of the wavelength of light, resulting in the unique optical properties associated with cholesteric liquid crystals. *Smectic* liquid crystals can be much more ordered than nematics or cholesterics. Smectic phases have one degree of orientational order as well as one degree of translational order. The molecules are arranged with their long axes, on average, parallel as well as being stacked in layers. Due to this added translational order, smectic liquid crystals can exist in a number of different modifications of varying order depending on the nature of the layer packing and the angle of orientation of the molecules within the layer plane.¹⁰ In the more disordered types of smectic phases such as smectic A or smectic C, there is very little packing order within the layers. Intermolecular distances within the layers are inconsistent. As a result, these modifications are much more fluid like than some other smectic phases. The smectic B phase has a hexagonally close packed lattice within the layers making it a very ordered mesophase. There is usually no interlayer translational order in mesophases although recently discovered highly ordered crystal B phases do show some correlation between layers.¹⁰

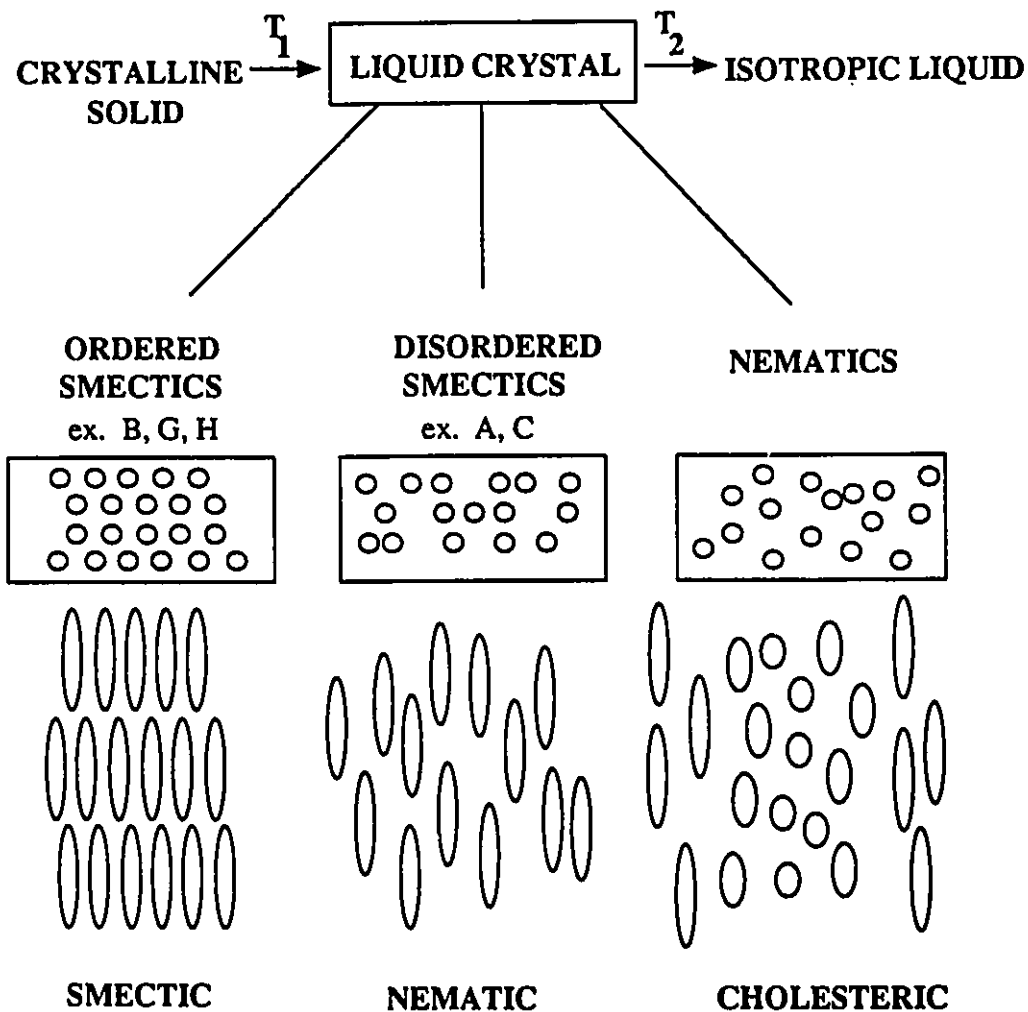


Figure 1.2. Description of thermotropic liquid crystals.

1.2.3. Viscosity and Diffusion in Liquid Crystals

Based on the oriented nature of liquid crystalline phases, it is not surprising that properties such as mass transport phenomena show anisotropic behaviour.^{9b,d,11-25}

Viscous flow of isotropic liquids is conventionally measured by the viscosity coefficient (η). Liquid crystals however require at least three shear viscosity

coefficients and a rotational viscosity coefficient to fully characterize the anisotropic flow behaviour.¹¹ Conventional viscometry can be used to measure the "apparent" viscosity of a liquid crystal without considering its anisotropic nature. The results have led to the general conclusion that nematics have flow characteristics similar to those of viscous fluids.^{9b,9d,12}

The "apparent" viscosity of the nematic phase of 4-methoxybenzylidene-4'-n-butylaniline (MBBA) has been measured by conventional viscometry and found to be on the order of 23 centipoises at 30°C while the isotropic phase of MBBA has a viscosity of 15 centipoises at 50°C.¹² For comparison, the viscosities of ethylene glycol and benzene at 20°C are 19.9 cP and 0.652 cP respectively.¹⁴

Directional anisotropies in the viscosity coefficients of nematic MBBA have been measured by several workers with differing results.^{13a-e} In general, the results indicate that solvent anisotropy can result in directional viscosity differences of ca. 10 or 20 centipoises. The inconsistencies in the measurements have been blamed on poor alignment of the liquid crystals due to flow and surface effects.

The viscosities of cholesteric and smectic phases are more difficult to measure than those of nematics.^{8,9b,15-17} Smectics and cholesterics have been reported to be ca. 10 times more viscous than nematics. Viscosity measurements of smectics and cholesterics are complicated by the fact that the shear rates used dramatically influence the measured viscosities. Slight changes in shear rates can result in viscosity measurements differing by orders of magnitude. This has been explained to be the result of non-Newtonian behaviour of the mesophases. In short, high shear rates perturb solvent order and consequently the measured viscosities are abnormally large. For a comprehensive review of the theory and measurement of viscosities of liquid crystalline phases, the reader should consult the cited references.

A property that is closely related to viscosity is the rate of binary or self diffusion. Diffusion in liquid crystals has been studied by several techniques yielding some very interesting results.²⁰⁻²⁵

Diffusion in liquid crystals is, as expected, anisotropic. For nematics, the ratio of diffusion parallel to the molecular long axis to that perpendicular to the molecular axis (D_{\parallel}/D_{\perp}) is around 1.6.²⁰⁻²² In smectic phases the results are more dramatic.²²⁻²⁵ Due to the layer packing, the diffusion anisotropy is, as expected, larger than that for nematic phases. However, diffusion perpendicular to the direction of orientation is consistently faster. Doane *et al* looked at the diffusion of small molecules in the smectic A phase of 4-n-butoxy-benzilidene-4'-n-octylaniline and found a ratio (D_{\perp}/D_{\parallel}) of approximately 10.²⁵ The reported explanation is that diffusion can proceed through the more fluid like interlayer regions perpendicular to the long axes of the molecules more efficiently than through the layers themselves.

The diffusion rates of methane and chloroform in the isotropic, nematic and smectic phases of a number of liquid crystalline phases have been examined.²² The results show that diffusion of small molecules is slower in smectic phases than in nematic phases by at least one order of magnitude. The diffusion rates in liquid crystals vary considerably depending on both solvent structure and solute size.

1.3. Organic Reactions in Liquid Crystals

1.3.1. General

It is known that solutes dissolved in liquid crystalline phases become oriented to a degree that depends on the structural similarity between guest and host.^{9b,9c,26-34} Reactants that are similar to the solvent in shape, size and structure are incorporated into the mesophase matrix with little disruption of orientational order while reactants of a dissimilar shape and size are more disruptive to liquid crystalline order. For well-oriented reactants, conformational and translational order will no longer be random. Reactivity which requires disruption of this order might then be energetically less favourable than it would be in an isotropic environment.

A number of factors may influence the degree to which solvent orientational order can influence reactivity;

1, The structural similarity between solute and solvent;

The degree to which a solute disrupts mesogenic order depends on the structural similarity between the solute and the solvent^{9b,c,26-34}. A reactant that fits unobtrusively into the mesogen may be more likely to show an order induced influence on chemical reactivity than a reactant that is more disruptive to the ordered matrix.

2, The ordered nature of the liquid crystal;

Phases which are inherently more fluid-like may not be able to constrain reactants as well as more ordered mesogens.³⁵ However, more ordered phases may be less accommodating to solute molecules and as a result, the reactants may reside in a local environment that is less restrictive than the mesophase itself.³⁶⁻⁴⁰

3, The steric requirements of the reactive process;

The largest effects of liquid crystalline order are expected to be seen with

reactions that involve conformational changes that are grossly incompatible with solvent order. Reactions involving more subtle shape changes may not be influenced as dramatically by mesophase order.

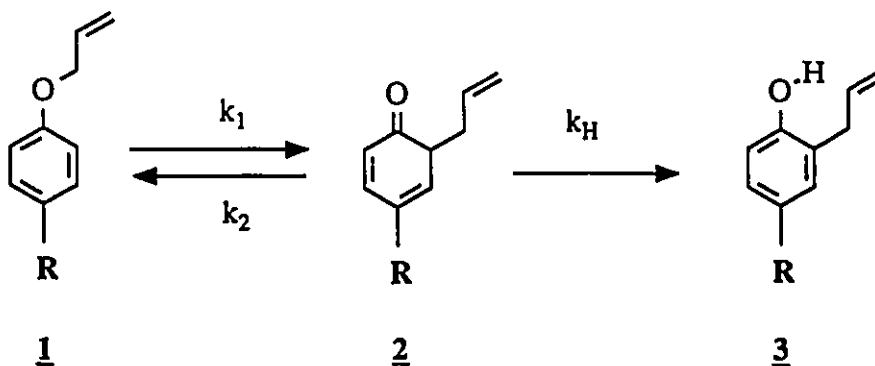
A survey of the literature reveals that many of the earlier attempts to control chemical reactivity were unsuccessful. More recent attempts, with better engineered systems have shown that control of reactivity can be significant (*vide infra*). The rather discouraging results of many of the earlier studies may be attributed to neglecting one or more of the above factors. By recognizing the problems associated with the earlier studies, it is hoped that a better insight can be gained into the factors which influence the control of reactivity in liquid crystals. The ultimate goal is to be able to predict how liquid crystalline media might influence a given reaction.

A critical review of the current literature will now be presented. Examples will be discussed in terms of the factors previously mentioned which may have influenced the success or failure of each study. While not exhaustive, this review is representative of the progression of knowledge in this area of research. The relevance of our work will then be discussed in light of these results.

1.3.2. Unimolecular Reactions in Liquid Crystalline Solvents

There have been a number of studies performed investigating the effect of liquid crystalline solvents on various unimolecular processes.⁴¹⁻⁶³ The premise behind these investigations has been that a reactive solute will be oriented in a conformation that is compatible with the liquid crystalline solvent. Unimolecular reactions involving shape changes disruptive to solvent order may be impeded, as reflected in the activation parameters for the reaction.

Several years ago, Bacon and Brown studied the Claisen rearrangement of some para-substituted allyl phenyl ethers in isotropic and nematic solvents.⁵⁰



Where R = CH₃, Cl, CN, and NO₂

Scheme 1.1. Claisen rearrangement of allyl phenyl ethers.

The kinetics of the Claisen reaction have been well studied.^{64,65} The rate determining step in isotropic solvents is the cyclization step, k_1 .

The authors anticipated that in the nematic phase, the reactants would be in an extended conformation. Consequently, the Claisen rearrangement would require large conformational changes of the allyl substituent which may be incompatible with the nematic solvent order.

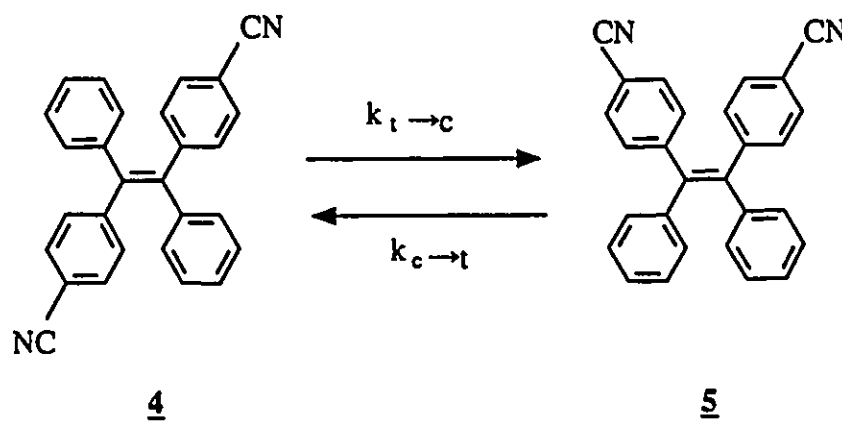
The rearrangement was studied at several temperatures in both the nematic and isotropic phases of the solvent. They found that nematic solvent order had no influence on the rate of this Claisen rearrangement. The Arrhenius plot showed no discontinuity at the phase transition temperature.

In a related study, Dewar and Nahlovsky studied the Claisen rearrangement of a cinnamyl phenyl ether in nematic solvents and also determined that solvent order did not influence the reaction.⁵¹ When performed in an inclusion compound however, they found that the rearrangement was strongly inhibited. Dewar's conclusion was that it seems unlikely that the rates of any unimolecular reactions could be altered

significantly using nematic solvents.

What these workers did not address was the possibility that the reactant may cause a large disruption of the nematic order. Others have found that the cinnamyl phenyl ether used by Dewar *et al* causes significant transition temperature depression in some nematic solvents.⁸ This suggests that local disruption of the solvation shell of the reactant may well be responsible for the lack of effect.

In another thermal unimolecular reaction, Leigh and co-workers looked at the isomerization of *trans*-1,2-di-(4-cyanophenyl)-1,2-diphenylethylene (**4**) in a number of model isotropic and cholesteric solvents⁵² (Scheme 1.2).



Scheme 1.2. Cis-trans isomerization of a bulky olefin.

The isomerization was performed over a 70°C temperature range and the Arrhenius parameters were determined. The results show that, in cholesteric solvents, the activation energy is 1-1.5 kcal/mol higher and the entropy of activation is slightly more positive than those found in the model isotropic solvents.

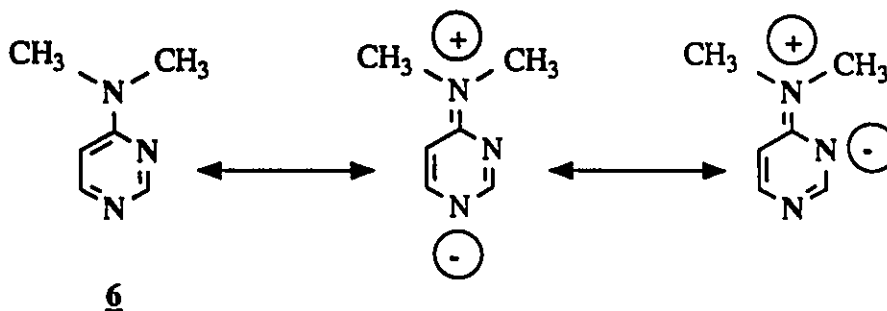
While there is a trend toward slower thermal isomerization in the cholesteric phases, the origin of this effect is uncertain. The reactant is rather bulky and has large effects on the Ch-I phase transition temperatures of the mesogens even at low (0.5

wt%) solute concentrations. Disruption of solvent order by the bulky reactant may truncate any potential orientational effect on the isomerization. The results could be interpreted as being an effect of viscous drag rather than solvent order.

The two examples discussed thus far have served to illustrate the importance of selecting a well-engineered system. The rather bulky reactants used may be expected to cause a large disruption of liquid crystalline order and consequently they may not be well-oriented within the mesophases. The poor solvation of such reactants may have reduced the potential for the successful control of reactivity.

A number of investigations have been reported which use dynamic N.M.R. techniques to investigate the conformational mobility of solutes in liquid crystals⁵³⁻⁵⁸. Many of these investigations, such as the ring inversion of cyclohexane or p-dioxane have shown no effect of liquid crystalline order. This is not surprising in light of the very subtle shape changes associated with such isomerizations.⁵⁸ Fung *et al* demonstrated that liquid crystalline solvents can influence conformational motions when the shape changes are more significant.

Using natural abundance ¹³C N.M.R., Fung *et al* showed that a nematic phase could inhibit the hindered rotation of the dimethylamino group in 4-(dimethylamino) pyrimidine.⁵⁸ The most stable rotamer is very nearly planar and has two important charge separated resonance contributors (Scheme 1.3.).



Scheme 1.3. Hindered rotation of dimethylamino group.

In isotropic solvents, the barrier to rotation is highly dependent on solvent polarity. Polar solvents stabilize the zwitterionic resonance structures of the ground state, increasing the barrier to rotation as shown in Table 1.1.^{66,67}

TABLE 1.1. Activation parameters for hindered rotation of dimethylamino group^{a,b,c}.

SOLVENT	ΔH^\ddagger (KJmol ⁻¹)	ΔS^\ddagger (J mol ⁻¹ K ⁻¹)
CD ₃ OD ^a	52±1	-8±4
CHCl ₃ ^b	45±2	-21±4
CD ₂ Cl ₂ ^c	35±1	-39±3
ZLI 2142 ^c (nematic)	53±1	+20±6

^a Reference 67,

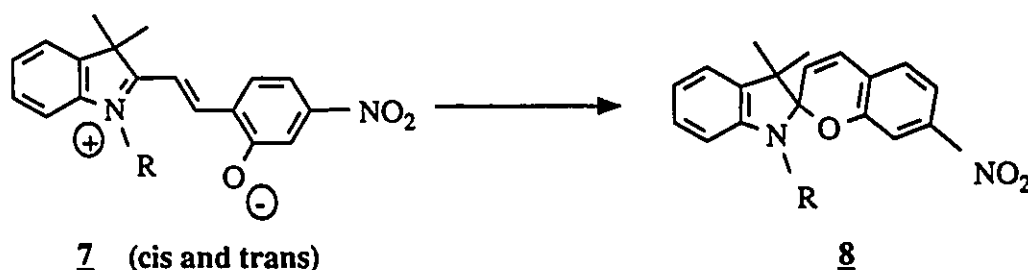
^b Reference 66,

^c Reference 58.

The nematic solvent, a ternary mixture of *trans*-4-alkylcyclohexyl compounds has a very low overall polarity yet the barrier to rotation in this solvent is much higher than that in methylene chloride and equal to that in the very polar deuteriomethanol. Fung rationalized that the non-planar transition state to rotation is sufficiently disruptive to nematic order to result in an observable impediment to rotation. This result is very encouraging. While the shape change associated with this rotation is relatively small, nematic order does appear to hinder the rotation. Presumably the reactant is solvated very efficiently in the nematic phase in order for this effect to be perceptible.

In an effort to maximize the effect of liquid crystalline order on unimolecular

reactivity, Weiss and Otruba chose to study a reaction which requires a large shape change in a highly ordered smectic B liquid crystal. They were in fact successful in altering the rate of isomerization of a photochromic merocyanine to indolinospiropyran using a liquid crystalline solvent (Scheme 1.4.).⁵⁹



Scheme 1.4. Isomerization of photochromic merocyanine.

Dye **7** has a planar ground state which, on thermal reversion to **8** goes through a transition state where the phenyl moieties are twisted by 90°. Weiss found that the rate of this isomerization was dramatically affected by solvent order. In isotropic n-butyl stearate (**BS**) the activation energy for isomerization was found to be 17±1 kcal/mol and the entropy of activation was -9±2 e.u.. In the smectic phase, of the same solvent, the activation energy increased by more than a factor of 2 and the entropy of activation was 64 entropy units more positive.

While the effect is clearly very large, it should be pointed out that the rate of this isomerization is highly dependent on solvent polarity. Some of the effect may in fact be due to polarity differences in the two phases caused by solvation effects. Weiss pointed out that the nature of the solubilization of **7** in smectic **BS** is only speculative. The dissimilar shapes of the solute and solvent suggest that a large disruption of liquid crystalline order is possible. Weiss speculated that the solute molecules may be incorporated either within the solvent layers or in the more fluid interlayer region.

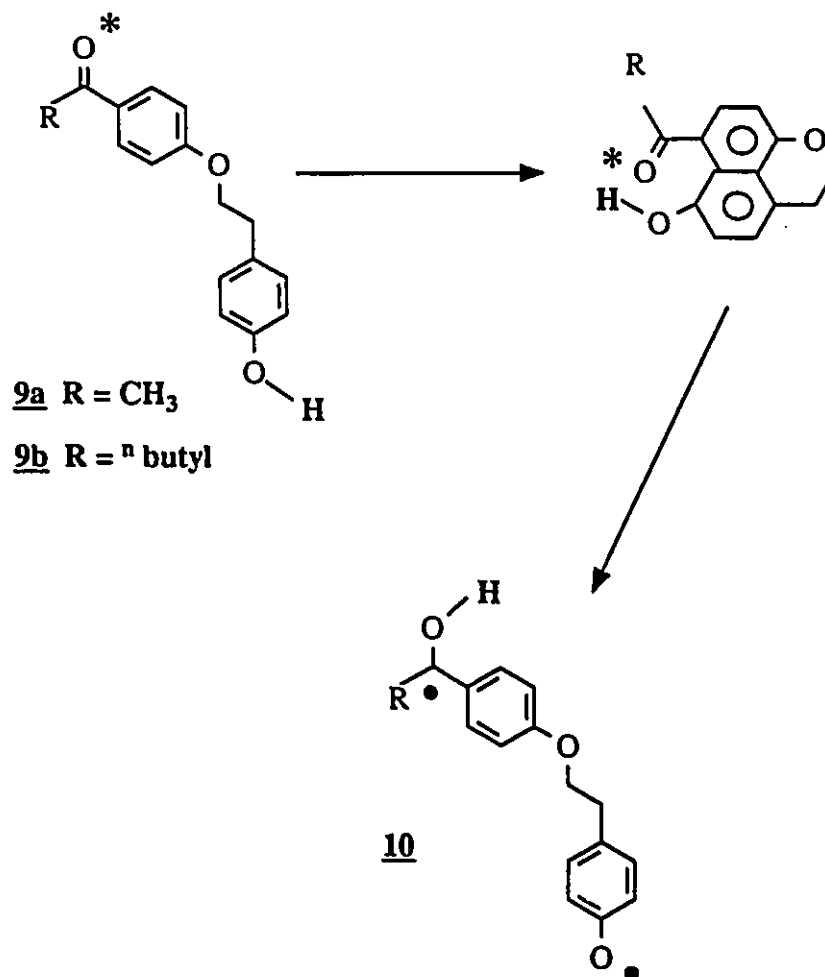
A number of important points can be gleaned from the first few examples. In

general, little control of reactivity is found for reactants which are disruptive to solvent order. Most of the unsuccessful studies have used disruptive solutes in less ordered types of mesogens such as cholesterics. By looking at reactions involving larger shape changes and using more ordered smectic mesophases, some control of reactivity has been observed. However, a more systematic approach is required to better understand the complex solute/solvent interactions. A better approach may be to take well understood reactions, where solvent orientational effects should be quite dramatic, and probe various liquid crystalline solvents. In this way, structure/compatibility relationships and solvation requirements may be more effectively delineated.

Ketone photochemistry is a prime candidate as reactivity is often intimately dependent on conformational factors.⁶⁸ Ketones can also be structurally modified easily to probe solubility requirements. The liquid crystalline solvents used are obviously limited to those that do not contain absorbing chromophores.

The first example investigates intramolecular quenching of linked phenolic ketones where large conformational changes are required to attain the necessary quenching geometry.⁶⁰

Investigations into the photochemistry of some remote phenolic ketones (Scheme 1.5.) have shown that their lack of reactivity and short triplet lifetime (15ns in CH₃CN 25°C) are due to efficient triplet quenching *via* phenolic hydrogen abstraction in an end-to-end conformation.^{69,70} A large deuterium isotope effect indicates that the rate determining step in triplet quenching is hydrogen transfer *via* a sandwich-like quenching geometry, as shown in Scheme 1.5..



Scheme 1.5. Remote hydrogen abstraction in linked phenolic ketones.

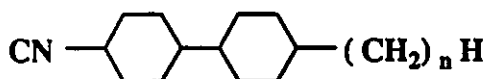
The premise behind studying this reaction in ordered media is simply that solvent order may impose conformational restrictions on the ketone which would inhibit formation of the quenching geometry. As a result, the triplet lifetime would increase and photoreactivity associated with the carbonyl group may be observed. In view of the large conformational changes associated with triplet quenching, one would expect that a large influence of liquid crystalline order on triplet lifetimes is possible.

When R is methyl, the ketones are not photoreactive and were monitored by

triplet decay. In liquid crystalline solvents, an impediment to obtaining the quenching geometry will be reflected by longer triplet lifetimes.

When R is butyl, the ketones are photoreactive and the efficiency of intramolecular quenching can be monitored by the quantum yield for Norrish II reactivity. Slower intramolecular quenching will be reflected in more efficient formation of the Norrish II products

The reactivity of these linked phenolic ketones was studied in two smectic mesogens;



n = 2	<u>CCH- 2</u>	n = 4	<u>CCH- 4</u>
	K-Sm 28 ⁰ C		K-Sm 29 ⁰ C
	Sm-N 44 ⁰ C		Sm-N 54 ⁰ C
	N-I 48 ⁰ C		N-I 79 ⁰ C

Figure 1.3. CCH-n liquid crystals.

The triplet lifetimes for the methyl substituted ketone were measured at 30°C in acetonitrile, a nematic mixture of **CCH-2/CCH-4**, and smectic **CCH-4**. The triplet lifetime in the isotropic solvent is very short (15ns). In the nematic mixture the lifetime increases to 275 ns while in smectic **CCH-4** the triplet lifetime increases to 3800 ns. Formation of the quenching conformation appears to be largely suppressed in ordered media, resulting in the dramatic increases in triplet lifetime.

For the butyl-substituted ketones, the relative quantum yields for Norrish II reactivity at 30°C show interesting results. In acetonitrile, essentially no Norrish II reactivity is detectable owing to the short triplet lifetime. In a viscous model isotropic

solvent, some photochemistry is observed, due presumably to viscous drag decreasing the rate of intramolecular quenching. In the nematic phase, as well as in smectic CCH-4, Norrish II reactivity is largely enhanced. However, it is enhanced to the same degree in both the nematic and smectic phases. This indicates that in smectic CCH-4, the ketone experiences an environment which is similar in nature to that of the bulk nematic phase. In smectic CCH-2, Norrish II reactivity is comparable to that in isotropic media. These results illustrate a very sensitive structure/solubility relationship. In spite of the fact that CCH-2 has a more ordered smectic phase than CCH-4, the slightly shorter length of the alkyl chain has caused a local isotropization of the ketone environment.

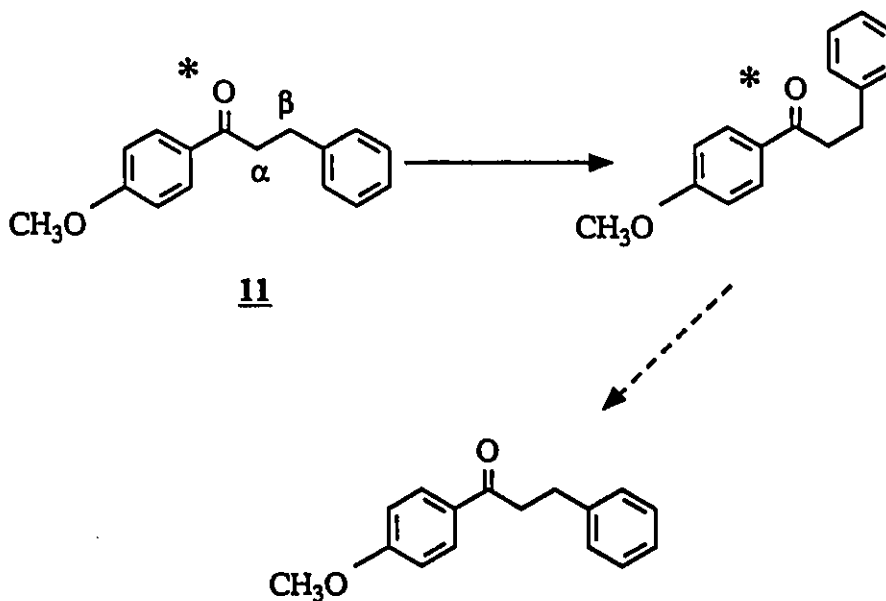
To help understand the photochemical results, the solute/solvent mixtures were examined by thermal microscopy. Thermal microscopy indicates that the methyl substituted ketones are homogeneously soluble in smectic CCH-4. This is consistent with the increasing triplet lifetime on going from isotropic to nematic to smectic solvents. Increasing the order of the medium results in a greater impediment to attaining the quenching geometry and consequently longer triplet lifetimes result. The larger butyl substituted ketones however cause a more significant disruption of local solvent order. On annealing the smectic samples for several days at room temperature, two phase behaviour is evident. The samples are mainly smectic with a small amount of a phase-separated nematic region. Apparently, the butyl substituted ketones are less soluble in the smectic phase and in fact reside in a ketone rich nematic phase in equilibrium with the bulk smectic phase. This is also consistent with the photoreactivity of these ketones where the enhancement of the Norrish II process is the same in the smectic and nematic solvents. Evidently, the ketone is experiencing a nematic-like environment in both solvents.

In summary, it is obvious from this study that structure compatibility

requirements are very important. The smaller ketones appear to be incorporated homogeneously into smectic CCH-4 and consequently the control of reactivity was greater than that in the nematic solvents. The larger ketones were more disruptive to smectic order and caused phase separation to give the ketones a much more isotropic-like environment.

Some other interesting results concerning structure/compatibility relationships in unimolecular photochemical reactions have recently been reported.⁶¹⁻⁶³

The very short triplet lifetimes (ca. 1 ns) of β -phenyl ketones is due to intramolecular exciplex formation via C_{α} - C_{β} bond rotation (Scheme 1.6).⁷¹



Scheme 1.6. Intermolecular exciplex formation in β -phenyl ketones.

In ordered solvents, the inhibition to attaining the quenching geometry should be reflected in longer triplet lifetimes.⁶¹

Initially, Arrhenius plots were constructed for a 1 mol% sample of 11 in CCH-4. However, using ²H N.M.R., it has been found that, at 1 mol%, 11 exists in a

biphasic environment over the entire smectic temperature range. That is, **11** resides in both smectic **CCH-4** and a more fluid-like (nematic or isotropic) phase. Consequently, the Arrhenius parameters calculated represent composite values for the ketone in two environments.

At lower concentrations (0.25 mol%), ^2H N.M.R. shows that **11** is homogeneously solubilized in the smectic phase of **CCH-4** with no phase separation. Arrhenius data for this sample shows that in the smectic environment, the triplet lifetime is more than double that in the nematic phase.

These examples illustrate how important it is to consider the nature of the solubilization of the reactants. Solutes **9** and **11** both have very low solubility limits (< 1 mol%) in **CCH-4**. At concentrations greater than the solubility limit, the ketones exist in a biphasic environment. We cannot assume a homogeneous solubilization of reactants even if the samples appear homogeneous by microscopy. At such low solute concentrations, it is very difficult to see biphasic behaviour by optical methods. Deuterium N.M.R. is proving to be very useful in determining how solutes are incorporated into smectic liquid crystalline solvents.

1.3.3. Summary: Unimolecular Reactions in Liquid Crystalline Solvents

The insight into controlling unimolecular processes using liquid crystalline solvents has grown remarkably. Earlier studies utilized the more fluid-like nematic and cholesteric mesophases to probe the reactivity of solutes that may be very disruptive to mesophase order. Consequently, many of these studies failed to show any influence of mesogenic order on reactivity. By probing systems with larger shape changes and using more highly ordered (smectic) mesophases, a larger degree of orientational control was realized. More systematic studies of unimolecular reactivity

in mesophases have recently given us initial information into the complicated nature of the solubilization of reactants in liquid crystalline solvents. From these results, some feeling into the requirements needed to control reactivity more reliably have been developed.

A major disadvantage of using unimolecular reactivity is the difficulty in delineating between effects due to microviscosity and effects related to the average orientational order induced by the solvent. This is particularly true for nematic or cholesteric solvents. In many cases the observed effects are so small that the contribution due to viscous drag can not be ruled out as an important factor in altering the activation parameters.

1.3.4. Bimolecular Reactivity in Liquid Crystalline Solvents

The influence of liquid crystalline order on solute orientation has also been shown to affect bimolecular reactivity. As we have seen, solute molecules dissolved within a liquid crystalline matrix may experience an average orientation similar to that of the mesogen itself. As a result, bimolecular collisions between these solute molecules may be biased towards those where they are oriented, on average, parallel to each other.

For diffusion controlled bimolecular reactions, the solute orientation on first contact will dictate the mode of reactivity. Reaction products resulting from this type of collision orientation may be formed preferentially. As well, because binary diffusion in liquid crystals has been found to be both anisotropic and slower than that in isotropic media, the rate of diffusion controlled processes may be altered.

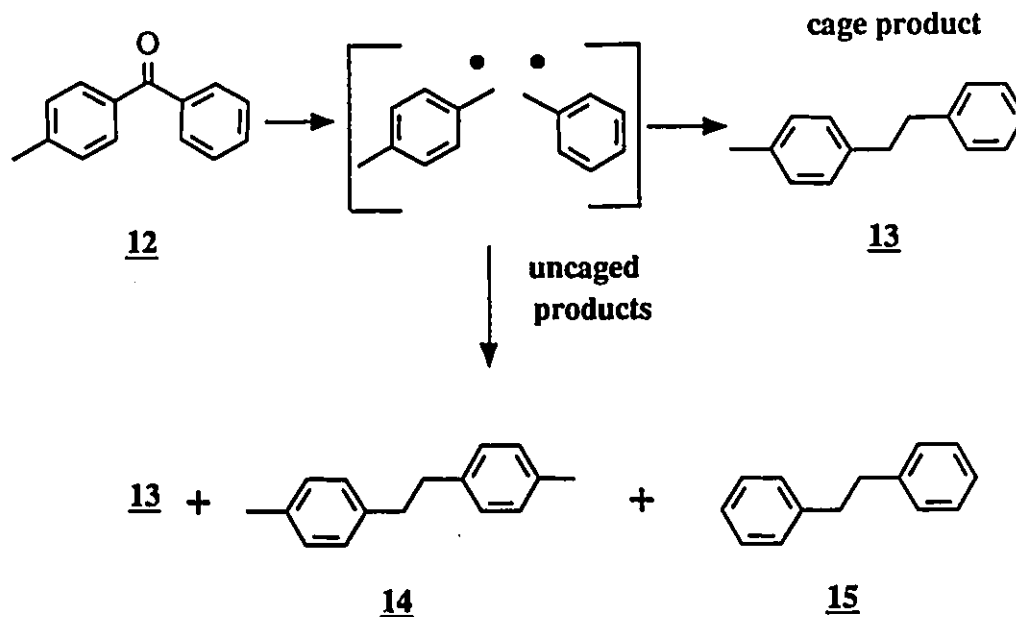
For bimolecular reactions which are not diffusion controlled, size or shape factors may alter reactivity. The formation of transition states that are compatible with

mesophase order are expected to be energetically favoured over those which are more disruptive to the solvent order. For example, in a competitive bimolecular reaction, products that result from a parallel orientation of the reactants might be preferred over those which are more disruptive to liquid crystalline order.

The problems associated with this scenario are identical to those we have encountered with unimolecular reactivity. It is important to consider both the nature of the probe reaction and the disruptive influence that the reactant molecules might have on liquid crystalline order. As we have seen, many unsuccessful attempts to control reactivity using liquid crystalline solvents have been explained in terms of disruptive solutes causing an isotropization of the local solvation shell. The largest influence of liquid crystalline order is to be expected from tightly solvated reactants that undergo substantial shape changes on reaction.

A number of studies have been reported that investigate the possibility of controlling bimolecular reactivity using liquid crystalline solvents.^{35,72-81,83-84}

Weiss *et al* presented an interesting study that investigated how the slower diffusion rates in liquid crystalline solvents alter the reactivity of photogenerated benzyl radicals.⁷²(Scheme 1.7.)



Scheme 1.7. The fate of photogenerated benzyl radicals.

The only product that can be formed from the solvent caged pair is 13. On escape from the cage, 13, 14 and 15 are formed in a ratio of 2:1:1. The fraction of 13 formed inside the initial solvent cage is given by Equation 1.1..

$$F_c = \frac{2 \cdot 13}{2 \cdot 13 + 14 + 15} \quad (\text{Eq. 1.1.})$$

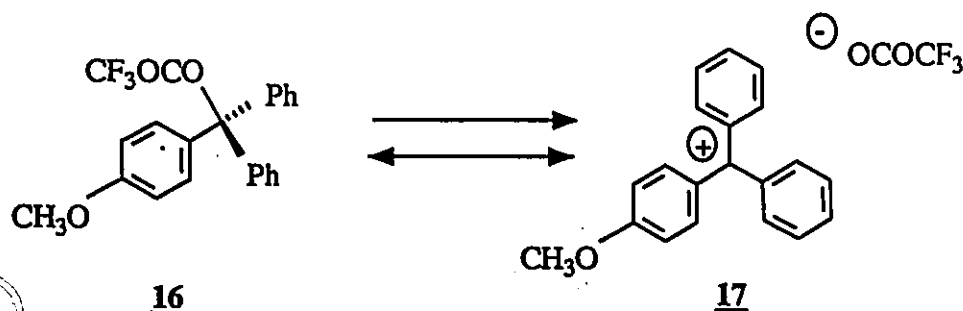
The premise behind this investigation was that in liquid crystalline media, slower diffusion rates may result in a higher proportion of 13 than would be found in isotropic media.

The photolysis of 12 was carried out in a number of isotropic, nematic and smectic phases. The effect of solvent order was found to be very small in most cases. The only possible exception was found using the isotropic, nematic and smectic phases

of n-butyl stearate where F_c increases slightly with increasing solvent order. In general, the lack of mesophase influence may be due to local disruption of solvent order by the rather large reactant.

The majority of the investigations of bimolecular reactivity in liquid crystalline solvents have been aimed at exploring the effects of reactant orientation or solvation. A couple of examples have been reported where bimolecular equilibria are influenced by liquid crystalline order. The idea is that the ordered environment may shift equilibria in favour of product(s) which are more compatible with solvent orientation.

An example of this was recently reported by Dickert *et al.*⁷³



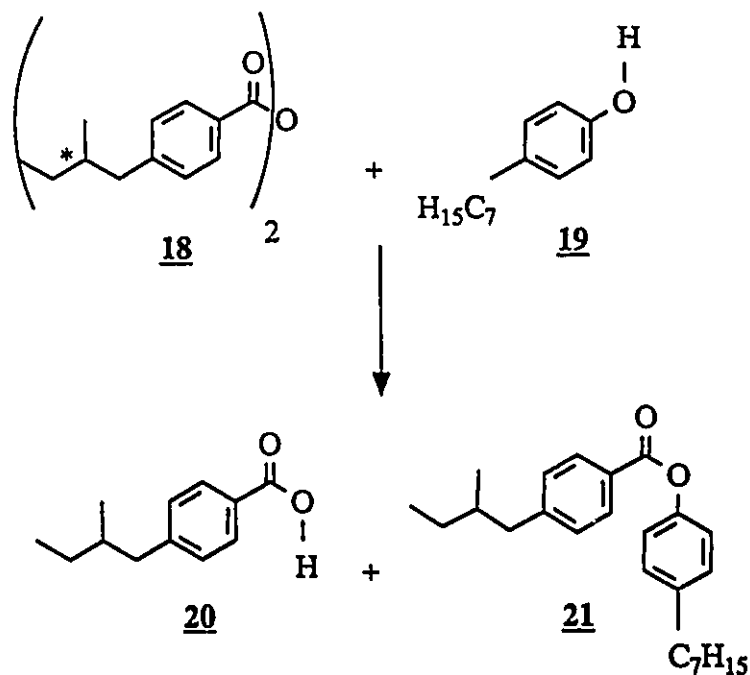
Scheme 1.8. Dissociation equilibrium of 4-methoxytriphenyltrifluoroacetate.

It was found that, on cooling from the isotropic to the nematic phase of a mesogenic solvent, the 16/17 equilibrium shifted (albeit slightly) to the right. This was explained in terms of the relative ability of the nematic phase to solvate 16 and 17. The planar trityl cation 17 was proposed to be less disruptive to nematic liquid crystalline order than the tetrahedral species 16.

In a similar study, Sergeev and co-workers found that the equilibrium between 2-methyl-2-nitrosopropane and its dimer was shifted greatly toward the dimer in nematic solvents.⁷⁴ This was explained in terms of preferential solvation of the

dimer (relative to the monomer) in nematic solvents.

In one of the earlier studies of bimolecular reactivity in liquid crystals, Labes and co-workers tried to minimize the disruptive influence of the reactants by carefully matching the solute and solvent. They chose to use a binary cholesteric solvent (40% cholesteryl nonanoate in 2-chloro-4-(p-pentyl-benzoyloxy)benzoate) to study the esterification of a chiral anhydride with p-(n-heptyloxy) phenol.⁷⁵



Scheme 1.9. Esterification of a chiral anhydride.

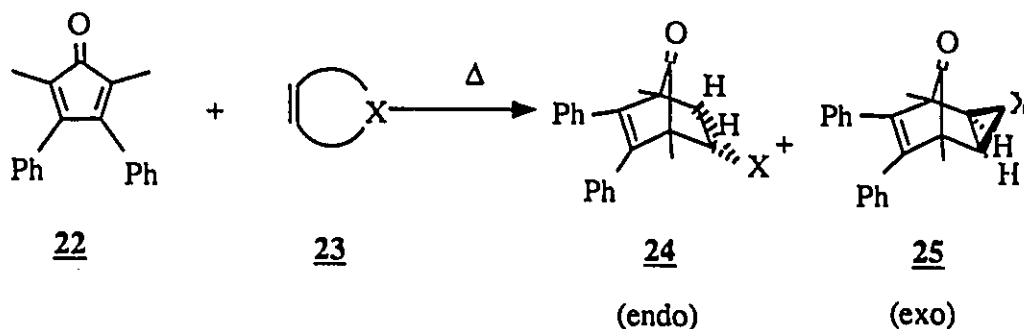
This chiral reactant was chosen because it shows a high helical twisting propensity and consequently it may be adopted unobtrusively into the cholesteric medium.

In spite of the laborious search for a solute system which may be compatible with the cholesteric solvent, Labes found no effect of cholesteric order on the reaction rate compared to that in isotropic phases. This may not be surprising since the reaction does not appear to have any significant steric requirements which might be influenced

by cholesteric order. Other systems with much greater steric demands than this one have been studied in cholesteric media (*vide supra*) and have shown little or no influence of orientational order on reactivity.

A far better approach in general, would be to look at competing bimolecular reactions. Simple Arrhenius calculations show that even small changes in the activation parameters will be reflected by perceptible changes in product ratios. As well, by investigating relative reactivity, the influences of microviscosity or diffusion rates are eliminated.

Leigh took this approach in investigating the stereochemical control of a Diels-Alder reaction.⁷⁶ The cycloaddition of 2,5-dimethyl-3,4-diphenyl-cyclopentadienone with several dienophiles was performed in a number of model isotropic, cholesteric and smectic solvents (Scheme 1.10.).



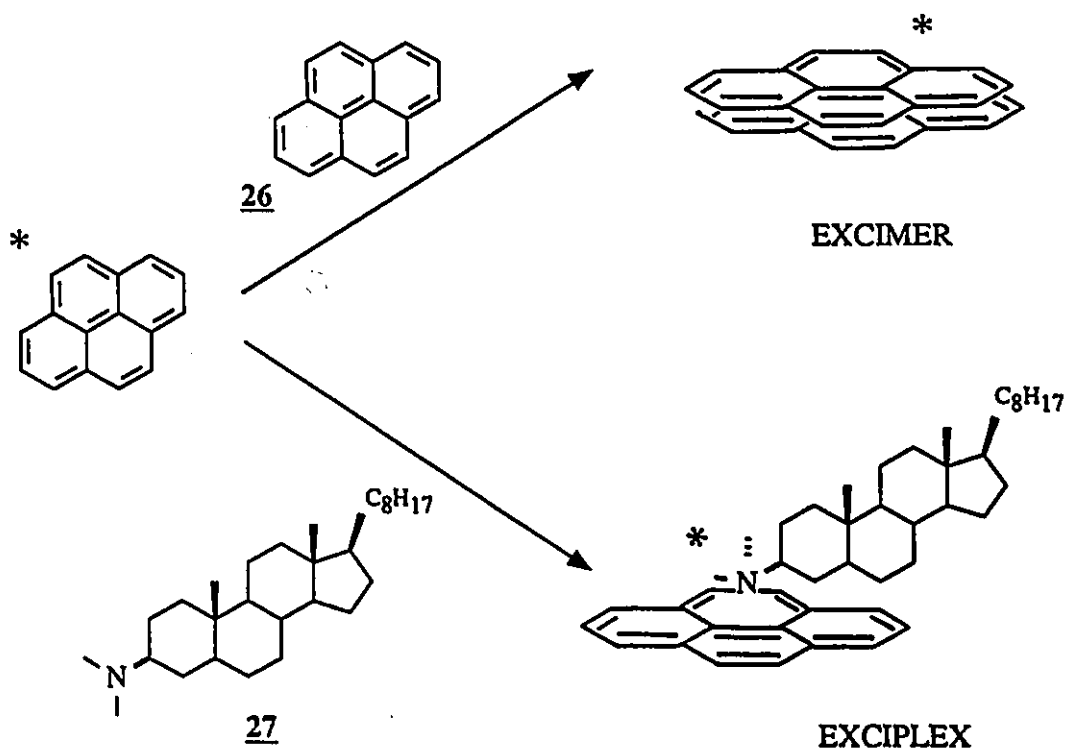
Scheme 1.10. Diels-Alder reaction of substituted cyclopentadienone with various dienophiles.

The transition state to 24 endo has a very globular shape while 25 exo has a more planar or plate-like transition state. In spite of these rather specific geometric requirements, the product ratio for each dienophile is identical in all the solvents investigated.

Most likely, solute disruption of the ordered solvents has caused a local isotropization of the reactant environment. The diene is a large molecule with

non-planar phenyl groups and a structure that is very different from the steroidal solvents used. The phase transition temperatures of the solvents are affected greatly by even small amounts (0.4 - 0.8 % wt) of 22. Solubilization of the reactants must be very poor and this could account for the lack of stereochemical control.

Anderson, Craig and Weiss investigated the bimolecular quenching of the pyrene singlet state by the formation of both the pyrene¹/pyrene excimer and the pyrene¹/5 α -cholesta-3 β yl-dimethylamine exciplex in cholesteric phases^{77,78} (Scheme 1.11.).

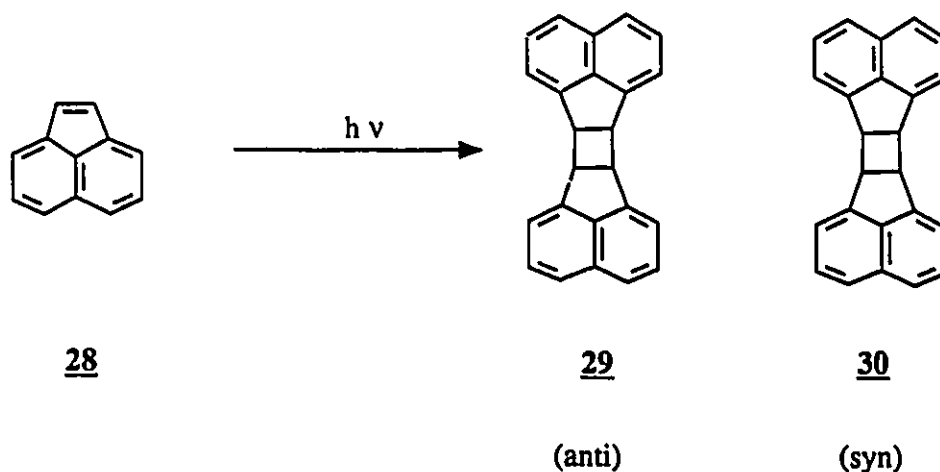


Scheme 1.11. Competitive excimer/exciplex formation.

The pyrene excimer occurs *via* a sandwich-like overlap of the moieties while the amine/pyrene exciplex is formed by a perpendicular approach of the nitrogen lone

pair with the pi system of the singlet pyrene. While the activation energies for both pathways were greater in cholesteric phases than in isotropic phases, the increase was larger (by 2 fold) for exciplex formation than for excimer formation. As well, $\Delta\Delta S^\ddagger$ is 8 e.u. more positive for exciplex formation. The differences in the activation parameters are consistent with the fact that the exciplex geometry would be much more disruptive to the mesophase order than would be the excimer geometry.

In another photochemical study, Weiss and Nerbonne looked at the effects of liquid crystalline solvents on the photodimerization of acenaphthalene.^{79,80}



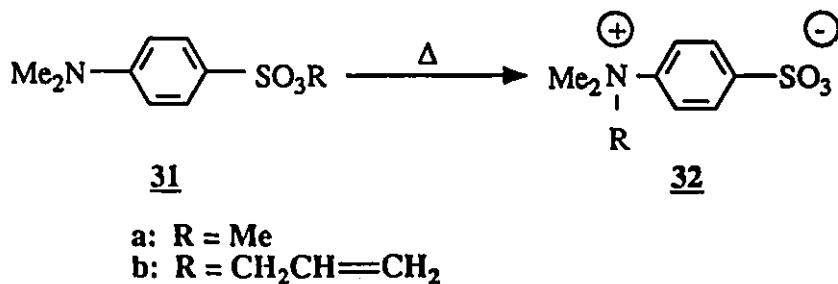
Scheme 1.12. Photodimerization of acenaphthalene

While the ordered media did not influence the syn/anti product ratio, Weiss did find that the quantum efficiency of the dimerization was much higher in cholesteric phases than in isotropic phases. Weiss reasoned that the dimerization was made more efficient by orienting the reactant molecules with their long axes parallel and consequently increasing the number of solute collisions with the correct geometry for reaction.

He also found that the quantum yield for dimer formation in cholesteric solvents *increased* as the concentration of acenaphthalene was decreased. Weiss

explained this in terms of the factors which influence the efficiency of the process. The quantum yield for photodimerization will depend on the excited state lifetime, the number of bimolecular collisions within that lifetime and the proportion of these collisions that leads to product formation. As the concentration of acenaphthalene is decreased, the number of reactant collisions will decrease. However, the orientational constraints imposed by the solvent will be greater leading to a disproportionate number of successful reactant collisions.

Samori proposed that the control of bimolecular reactivity should be greatest using highly ordered smectic liquid crystals. He demonstrated this by studying a rather novel bimolecular rearrangement^{35,81} (Scheme 1.13.). The rearrangement of methyl benzenesulfonate (**31a**) to its zwitterionic species (**32a**) occurs only in the crystalline state.⁸² It is thought that this intermolecular rearrangement occurs by methyl migration to an adjacent molecule in the solid lattice and requires a very specific stacking of the reactant molecules. The rearrangement of a similar compound, (**31b**), is not known to occur even in the solid phase, presumably due to unfavourable lattice packing.⁸²



Scheme 1.13. Isomerization of benzene sulfonate esters.

Samori performed the rearrangements in the highly ordered smectic B phases of three liquid crystalline solvents (Figure 1.4.).

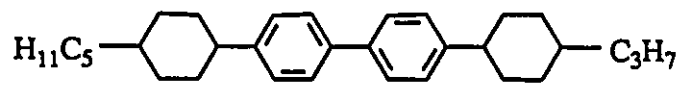
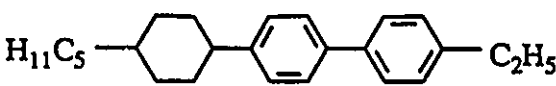
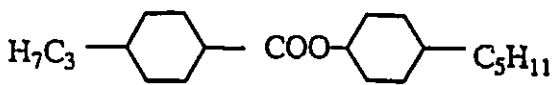
SOLVENT	TRANSITION TEMPERATURES
 <p>(S1544)</p>	K-SmB 54°C SmB-SmA 232°C SmA-N 251°C N-I 312°C
 <p>(S1409)</p>	K-SmB 34°C SmB-N 146°C N-I 165°C
 <p>(OS35)</p>	K-SmB 24°C SmB-N 52°C N-I 54°C

Figure 1.4. Smectic B liquid crystalline solvents used by Samori *et al.*

The rearrangements of 31a and 31b were both found to proceed easily in each of the smectic phases. This very important result shows that smectic order can catalyze reactions that otherwise would not occur. To eliminate the possibility that the rearrangement occurs *via* microcrystallization of the reactant, the reaction of 31a was performed at temperatures above and below its melting point. The rate increased at the higher temperature indicating that aggregation was not responsible for the formation of 32a. Increasing the concentration of 31a above 6.8×10^{-2} M caused a reduction of the reaction rate presumably due to perturbation of the smectic order.

Some very interesting results were found for the investigation of the kinetics of the rearrangement of 31b in the smectic phase of OS-35. Samori found that the rate

of the isomerization was dramatically influenced by reactant concentration. With increasing reactant concentration, the rate of the reaction was found to decrease.

Using differential scanning calorimetry and optical microscopy, Samori found that samples with a solute concentration greater than ca. $2.8 \times 10^{-2} \text{M}$, exhibited heterogeneous phase behaviour. The bulk smectic phase co-existed in equilibrium with isotropic droplets, probably due to incomplete dissolution of the reactant within the smectic mesogen. This type of phase separation behaviour is very similar to that found for the previously discussed ketone/CCH-4 studies performed by Leigh *et al.*⁶⁰⁻⁶²

1.3.5. Summary: Bimolecular Reactivity in Liquid Crystalline Solvents

The research done to date in this area indicates that there is potential to significantly influence bimolecular reactivity using liquid crystalline solvents. A number of studies have shown changes in chemical reactivity that are difficult to attribute to anything but the orientational order of the mesogenic solvents. However, many studies have reported negligible effects. What is lacking in this area are more systematic approaches to the question of reactivity in liquid crystals. We need to use probe reactions where control of reactivity in ordered media has been established in order to investigate how solvent order and reactant structure influence the observed effects. Examples of this type of approach have been reported for the unimolecular photoreactivity of ketones (*vide supra*) and, because of this, some very interesting reactant solubilization phenomena have been discovered. For bimolecular reactivity, no such systematic investigation has yet been reported. It is important that a better fundamental understanding of reactant solubilization be gained in order to help define the potential of liquid crystalline solvents to alter chemical reactivity.

1.3.6. Purpose of our Study.

The major purpose of our work is to design and carry out a more systematic study of the hypothesis that the regiochemistry of a thermal bimolecular reaction can be altered by using liquid crystalline solvents.

Our goals are;

- 1, To establish an order induced effect of liquid crystalline solvents on bimolecular reactivity.
- 2, To probe how the type of solvent used and the structure of the reactants may influence any observed regiochemical control of reactivity.

To accomplish these goals, we have chosen to investigate the bimolecular cycloaddition reactions of rigid, rod-like enophiles with a steroidal diene. The reaction yields a number of ene and Diels-Alder products. The selection of the reaction itself and the techniques used to identify the products are discussed in detail in Chapter 2.

The premise is simply that by orienting the solutes in liquid crystalline solvents, reactivity should be altered. Reactive pathways which require reactant orientations similar to that of the liquid crystalline solvent itself should be favoured over reactive pathways which require a large disruption of matrix order (Figures 1.5. and 1.6.).

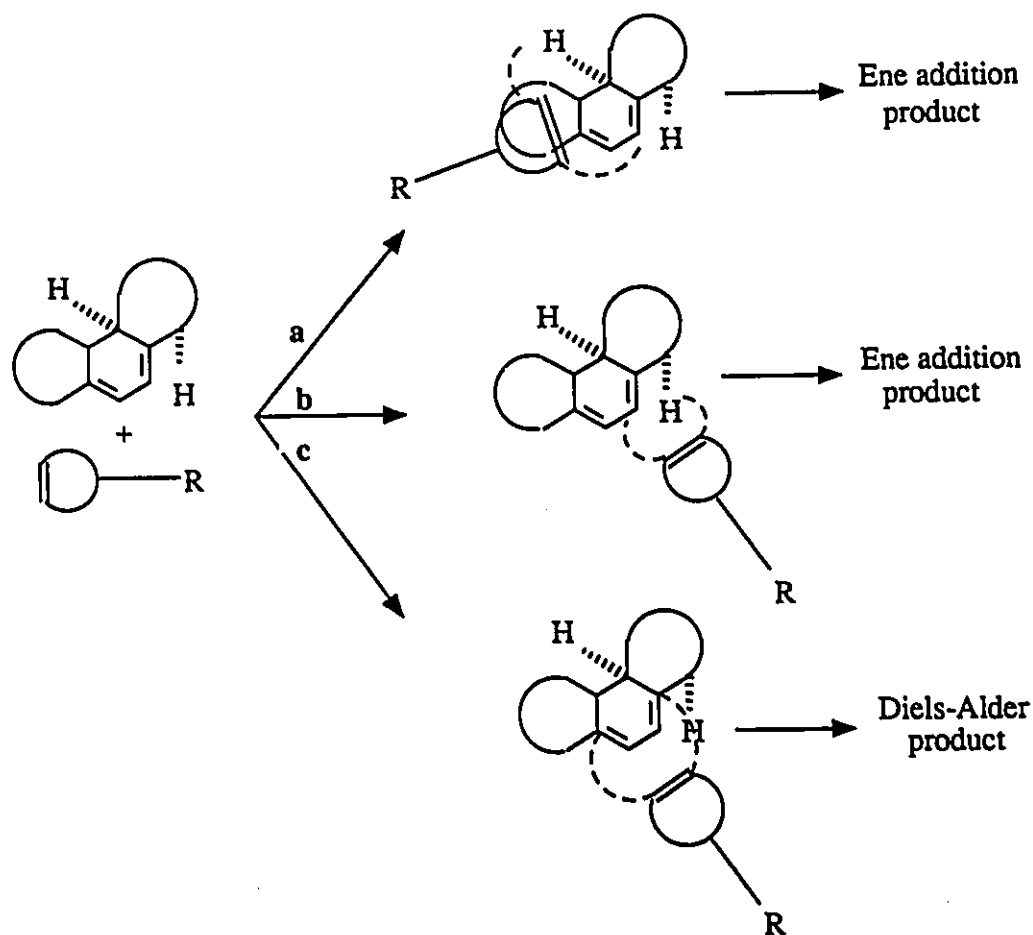


Figure 1.5. Cycloaddition reactions of a rod-like enophile with a steroidal diene.

The transition state for pathway a requires the reactants to be oriented in a manner which would cause little disruption to the order within the liquid crystalline matrix while pathways b and c require reactant orientations that must result in a severe disruption of orientational order (Figure 1.6.).

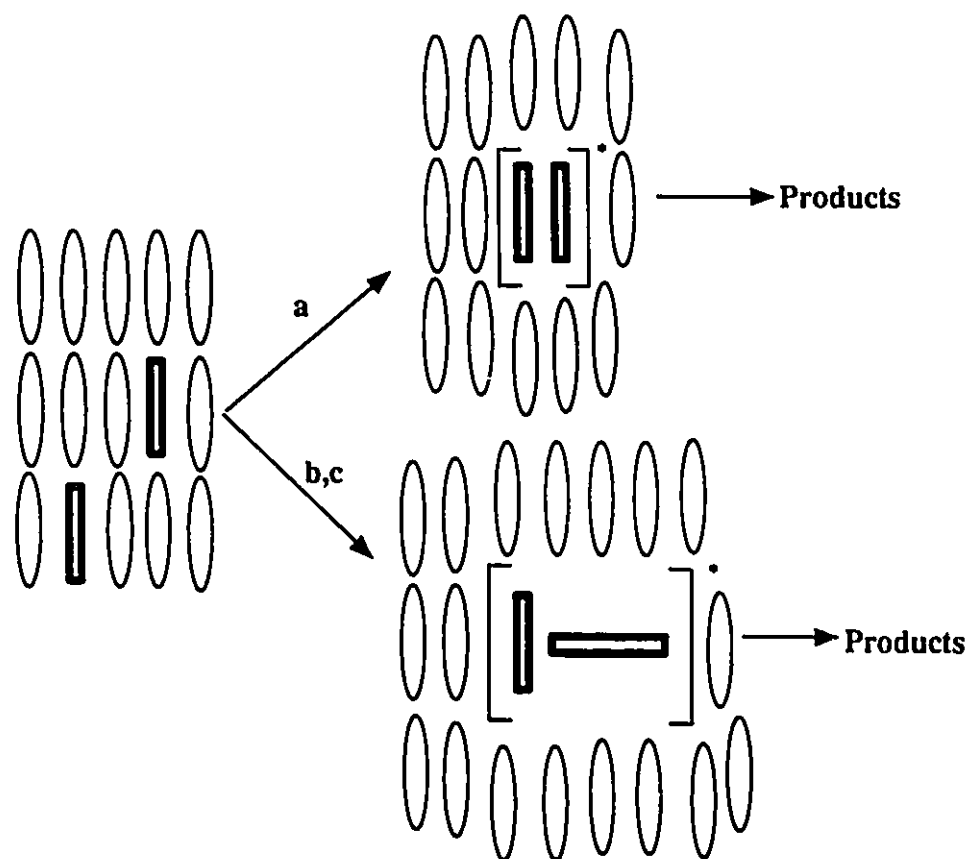


Figure 1.6. Reactant orientations in liquid crystalline solvents.

Pathway a should be favoured energetically in a liquid crystalline solvent and, as a result, the relative proportion of the product formed *via* pathway a should increase (relative to that found in isotropic solvents).

Through this study, we hope to provide a better understanding of how solute structure and liquid crystalline order influence the control of chemical reactivity. It may eventually be possible to predict under what circumstances and to what degree liquid crystalline order can be expected to influence chemical reactivity.

CHAPTER 2: REACTION OF N-ARYLMALEIMIDES WITH CHOLESTA-5,7-DIEN-3 β -YL ACETATE

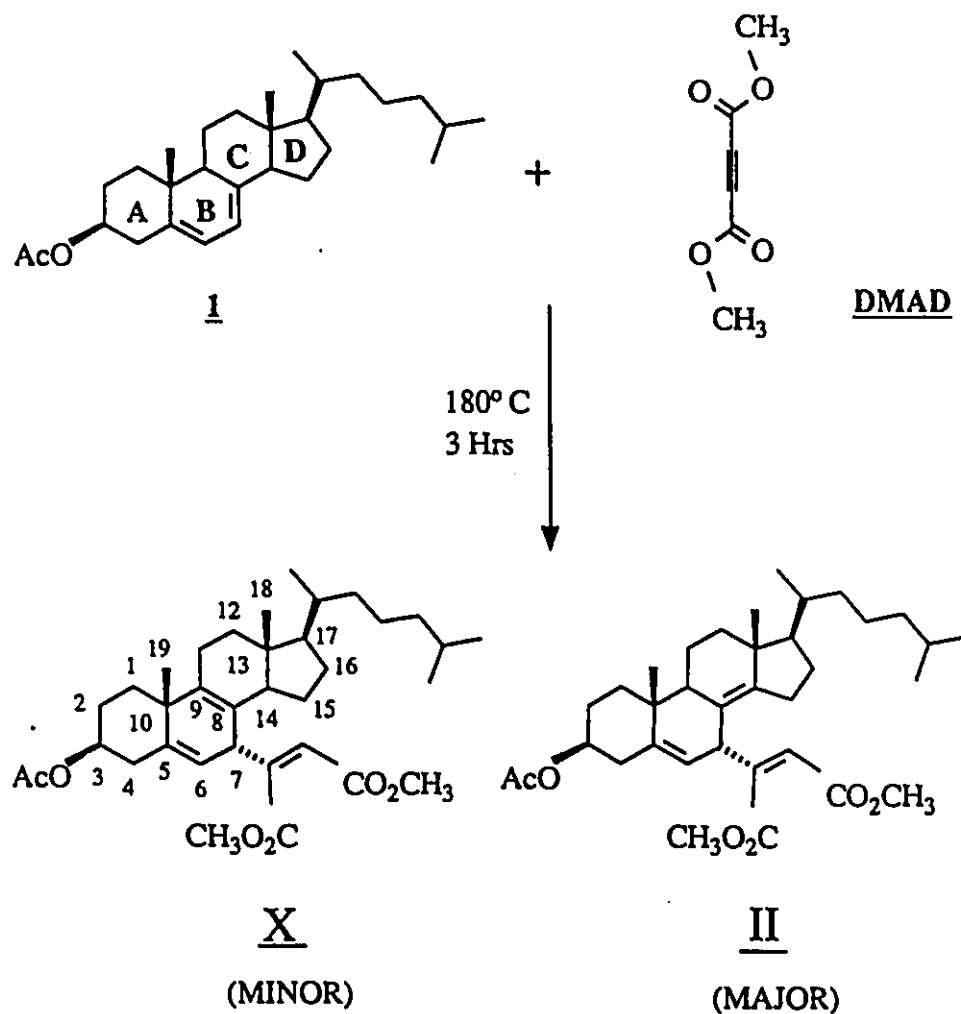
2.1. Introduction

The selection of a suitable bimolecular reaction and identification of the reaction products will now be discussed. This chapter begins with an account of why the cycloaddition of cholesta-5,7-dien-3 β -yl acetate (**1**) with various rigid enophiles was chosen to probe the effects of liquid crystalline order on the regiochemical control of bimolecular reactivity. The structural assignments of the adducts using one and two dimensional ^1H and ^{13}C N.M.R. spectroscopy will then be discussed. Using 2-D N.M.R. techniques, the adduct structures have been unambiguously assigned.

2.2. Selection of a Suitable Bimolecular Reaction

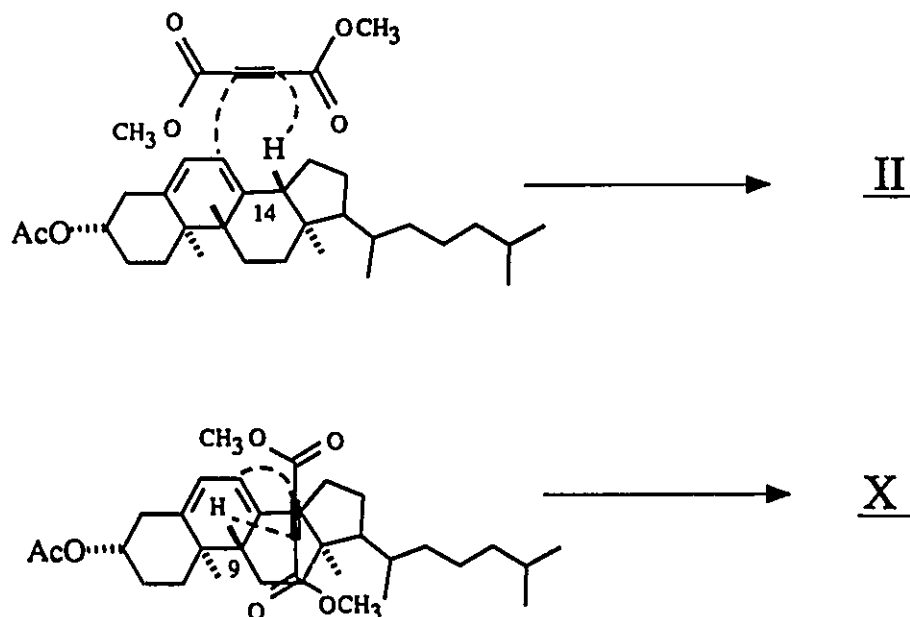
2.2.1. The Reaction of **1 with Dimethyl Acetylenedicarboxylate**

Previous work involving bimolecular reactions in ordered media has been performed in our laboratory using the cycloaddition reaction of cholesta-5,7-dien-3 β -yl acetate (**1**) with dimethyl and di- n -pentyl acetylenedicarboxylate (**DMAD** and **DPAD**). This reaction, originally reported by Huisman *et. al.* yields only the ene addition products to the exclusion of Diels-Alder adducts⁸⁵ (Scheme 2.1.).



Scheme 2.1. Reaction of **1** with dimethyl acetylenedicarboxylate (**DMAD**).

This reaction was chosen for study due to the rather specific transition states required for formation of the two products (Scheme 2.2.).



Scheme 2.2. Transition states to 1/DMAD products.

The transition states leading to the two products have very different steric requirements. While both products result from ene cycloadditions at C₇, the migrating hydrogens are different. The transition state to adduct II involves abstraction of the hydrogen at C₁₄. To accomplish this, the reactive centres must approach in a geometry where the reactants are in a parallel alignment. This contrasts the transition state to X where a perpendicular orientation of the reactive species is required for abstraction of the hydrogen at C₉.

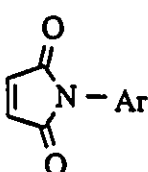
The reaction to form II involves a transition state which should be much less disruptive to liquid crystalline solvent order than would be the transition state to X. Any change in the activation parameters for formation of the two products should be reflected in the relative product yields as compared to those in isotropic media.

This system is particularly appealing because the diene is a steroidal ester

and should be incorporated relatively well in the cholesteric liquid crystalline phases of steroidal mesogens. The amount of solvent order disruption (by the diene) should be minimal. To probe the effect of structure/compatibility relationships on the degree of regiochemical control, the alkyl groups on the enophile can easily be altered. As well, concerted cycloadditions should show no influence of solvent polarity on reaction rates.

There is however a problem with this system. While the transition states appear to be quite specific in terms of orientational requirements, the enophiles are very flexible due to rotation about the carboxylate groups. Consequently, the steric requirements and geometric specificities of the transition states may not be maintained. Space filling models indicate that the bulk shapes of the transition states are very similar. Initial work indeed showed that thermolyses in a number of isotropic, and mesogenic phases yield identical product ratios in all cases.

By using an enophile which is not conformationally labile, the various transition state geometries should be more effectively maintained. We chose to use N-arylmaleimides as the enophiles because of their rod-like shape, rigid skeleton and because enophile length can be easily altered by varying the N-aryl substituent. Each of three enophiles has been used; N-phenylmaleimide (**NPMI**), N-biphenylmaleimide (**BPMI**) and N-terphenylmaleimide (**TPMI**) (Figure 2.1.).



Ar = Phenyl (**NPMI**)

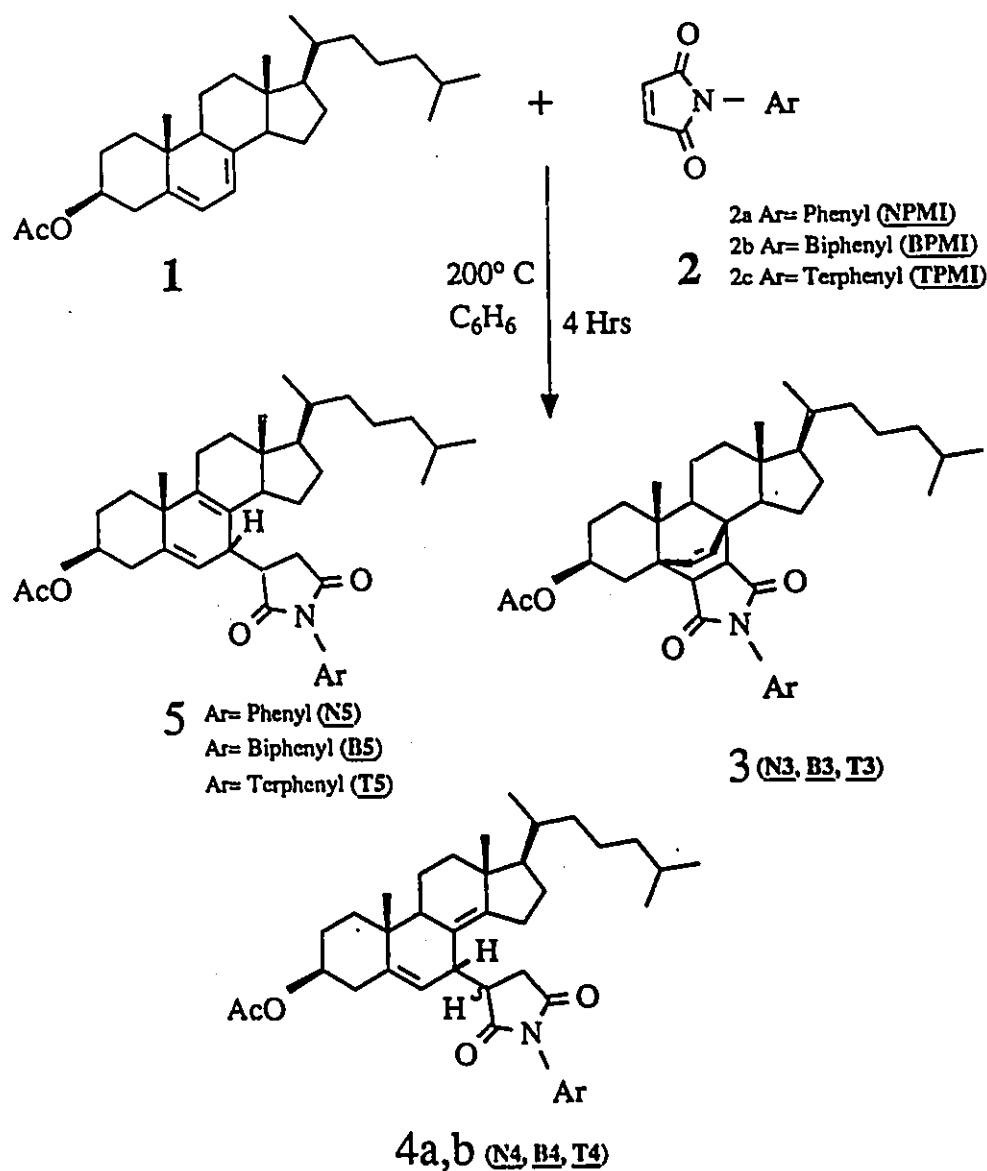
Biphenyl (**BPMI**)

Terphenyl (**TPMI**)

Figure 2.1. Structures of rigid enophiles used in this work.

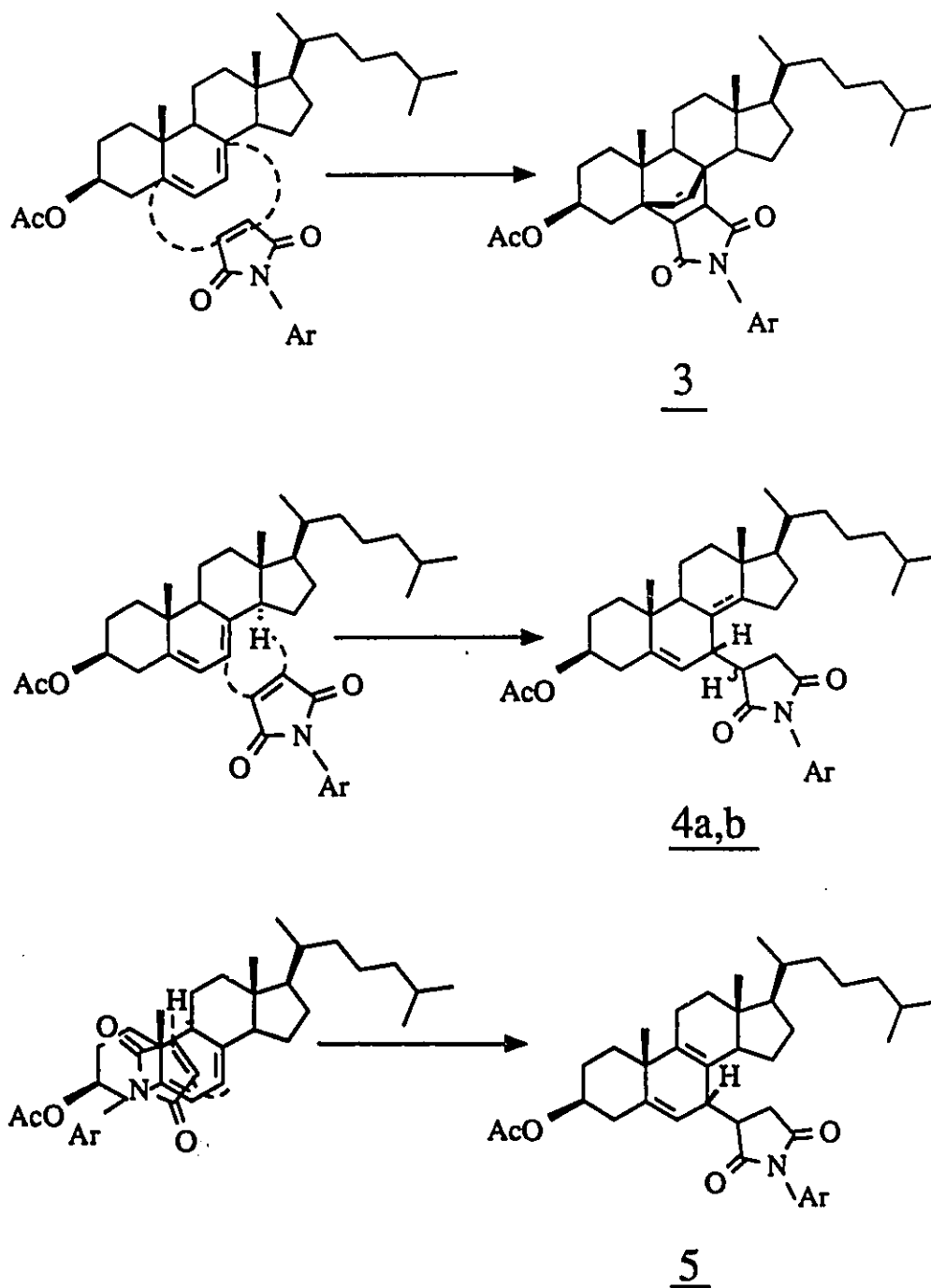
2.2.2. Reaction of **1** with N-Arylmaleimides

The thermal reaction of **1** with each of the three N-arylmaleimides yields three ene adducts, one Diels-Alder adduct, and one or two additional minor product(s).



Scheme 2.3. Reaction of **1** with N-arylmaleimides

The transition states to these products have very different bulk shapes;



Scheme 2.4. Transition States to 1/*N*-arylmaleimide products.

It is clear that the transition state to 5 should be much less disruptive to liquid crystalline order than would be the transition states to the other adducts. Using these more rigid enophiles, the bulk shapes of the transition states should be maintained. Consequently, this system is a good candidate to show some influence of mesogenic order on chemical reactivity.

2.3 Structural Identification of Cycloaddition Adducts:

2.3.1. Introduction

The reaction of 1 with N-arylmaleimides has not been previously reported, and the cycloaddition adducts obtained were all new compounds. The products have been identified by I.R., mass and N.M.R. spectroscopy. N.M.R. techniques have been particularly important in the assignment of the product structures. The remainder of this chapter will deal with how the products have been identified using N.M.R. spectroscopy.

Similarities between the ^1H N.M.R. spectra for X and II, reported by Huisman, and those of our products were important in the initial identifications. Consequently, some time will first be spent explaining the rationale by which Huisman identified X and II and discussing the ^{13}C and ^1H N.M.R. spectra of these adducts. The identification of the 1/BPMI adducts will then be discussed by first comparing the ^1H and ^{13}C spectra to those of X and II and then by assigning all carbon and hydrogen resonances using one and two dimensional N.M.R. techniques.

2.3.2 Structural Assignments; Adducts of I with DMAD

Huisman *et. al.* assigned the structures of X and II based on the ^1H N.M.R. spectra of the adducts and by chemical degradation techniques.

i, Proton N.M.R. Spectra; Adducts X and II

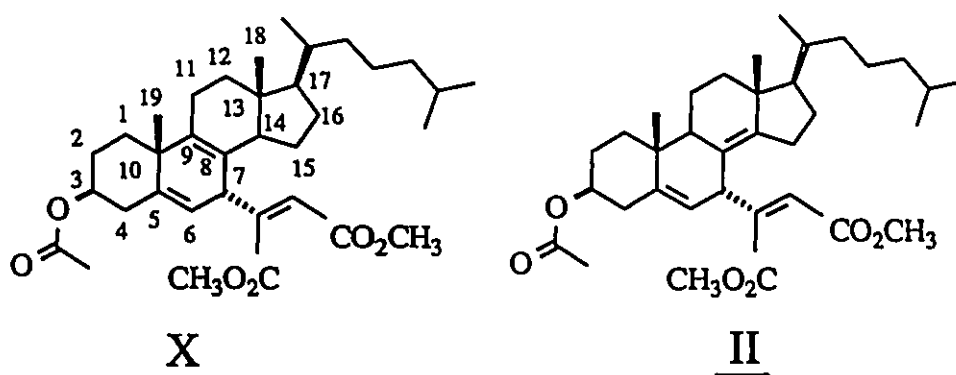


Figure 2.2. Structures of adducts X and II.

Huisman found that the low field regions of the proton spectra of each adduct show two vinyl proton signals between 5 and 6 ppm. These vinyl resonances consist of a singlet and a doublet. This precludes the possibility that they are Diels-Alder products which would give a characteristic doublet of doublets in the vinyl region.

Catalytic hydrogenation of the ester activated double bond resulted in loss of the vinyl singlet, indicating that only one vinyl proton existed on the steroidal skeletons. This is consistent with ene addition at C_6 or C_7 . However, addition at C_6 can be excluded because the resulting adducts would contain 3 vinyl protons. This indicates that X and II are the result of ene addition at C_7 .

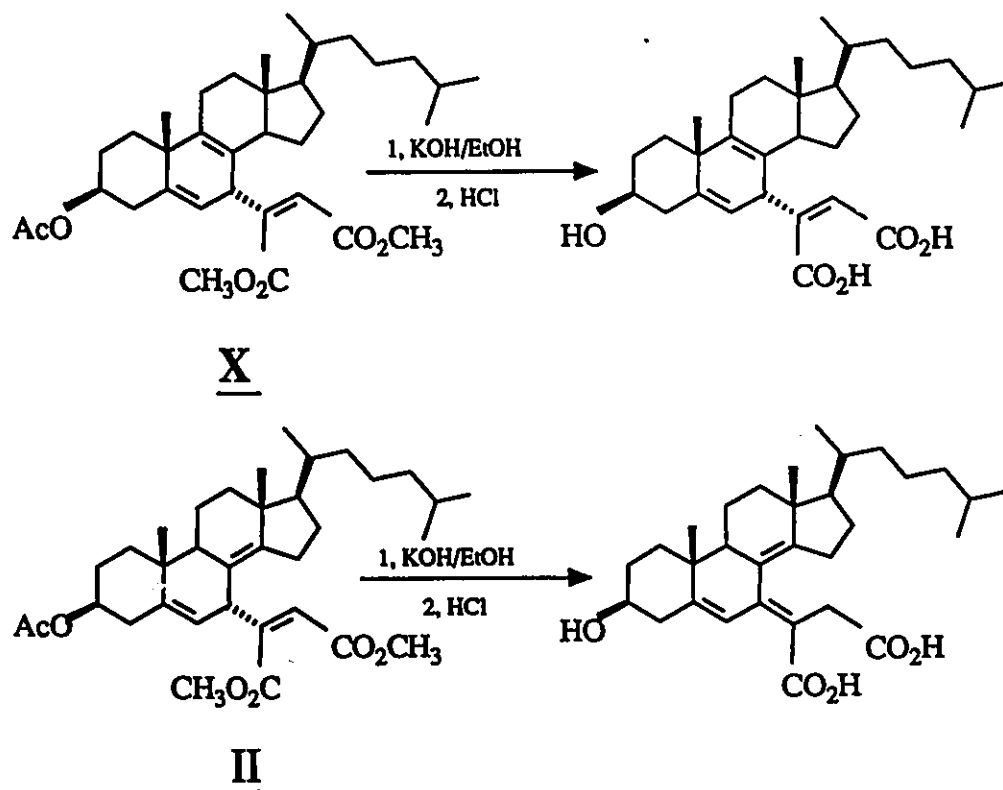
Huisman also reported ^1H N.M.R. evidence for the assignments of the sites of unsaturation within the rings. Adduct X has distinct singlet resonances for methyl

groups 18 and 19 at $\delta = 0.65$ and 1.2 ppm, respectively, while adduct **II** has only a single peak at $\delta = 0.90$ ppm for these two resonances. Huisman rationalized that for adduct **X**, the C₁₈ methyl group lies in the shielding cone of the C₈(C₉) double bond causing the observed upfield shift while the C₁₉ methyl is slightly deshielded by the double bond. This contrasts the single resonance for these two groups in adduct **II** where no C₈(C₉) unsaturation exists.

ii, Chemical Degradation Studies

Hydrolysis of the adducts (Scheme 2.5.) gave very interesting results.

Hydrolysis of **X** yielded the corresponding hydroxy-dicarboxylic acid. Hydrolysis of **II** however resulted in the formation of a new cross-conjugated rearrangement product.



Scheme 2.5. Hydrolysis of **II** and **X**.

Huisman explained the fact that only II rearranged in terms of steric factors. He reasoned on the basis of models that the transition state to the rearranged product produces significant steric interaction between the ester function and the C₁₅ methylene group. It was also evident that adduct X had a much larger steric interaction between these groups initially than did II. Consequently, the activation energy for rearrangement of II should be higher than that for X and therefore X would show a greater tendency for rearrangement. On the basis of the proton N.M.R. and the hydrolysis work, Huisman assigned the structures of X and II as shown above.

iii, Carbon-13 N.M.R. Analysis

In the present work ¹³C N.M.R. has been used to add further evidence to support the structural assignments of the adducts. The ¹³C N.M.R. spectra of authentic samples⁸⁶ of adducts X and II are shown in Appendix 2a. Resonances on the steroid skeleton were assigned by analogy to the ¹³C spectrum of the starting diene 1.⁸⁷⁻⁸⁸

One factor that distinguishes the two isomers are the resonances of carbons 9 and 14. In the starting material (1), C₉ and C₁₄ are allylic, resonating at 46.02 and 54.42 ppm, respectively.⁸⁸ In adducts X and II one of these resonances is missing in each case. In adduct X, methyne carbon C₁₄ is assigned at 50.2 ppm while no signal for C₉ is evident in the allylic region. A signal at 124.9 ppm is assigned as the signal for the new vinyl carbon C₉. This illustrates that the unsaturation is in the C₈(C₉) bond. For adduct II, a new signal appears at 34.2 ppm which is assigned to C₉ while the C₁₄ signal now resonates at 121.8 ppm, indicating that the unsaturation in this molecule is, as expected, at the 8(14) bond. These observations have been extended to the adducts derived from the reaction of 1 with N-arylmaleimides to help provide initial indications

as to the locations of the unsaturation in these adducts.

2.3.3. Structural Assignments; Adducts of 1 with Biphenylmaleimide

Product Identification

Structure assignments were made based on ^{13}C and ^1H N.M.R. data. The N.M.R. spectra of X and II were of great help in the initial assignments of the adducts. In particular, the unique chemical shifts of methyls 18 and 19 and carbons 9 and 14 seen in adducts X and II were also seen in the 1/BPMI adducts allowing preliminary assignment of the isomeric identities of each adduct.

After using spectral comparison to tentatively identify the adduct structures, 2-D N.M.R. was used to completely assign the ^1H and ^{13}C resonances. All of the aromatic, vinylic and allylic regions were assigned by following the correlations between coupled nuclei. The higher field regions of the 2-D N.M.R. spectra were very congested and correlations were sometimes difficult to assign. To help with these assignments, similarities with the known ^1H and ^{13}C spectra of the starting material (1) were used.⁸⁶⁻⁸⁸ All assignments made initially using one-dimensional methods were verified later in the COSY and shift correlated spectra for the 1/BPMI adducts. Structural assignments of the adducts formed using NPMI or TPMI as the enophile, were accomplished by comparisons of the ^1H and ^{13}C spectra to those of the 1/BPMI adducts.

The complete carbon and proton assignments for all the 1/BPMI adducts and for 1 are tabulated in Appendix 1. Representative N.M.R. spectra of the 1/BPMI adducts are collected in Appendix 2. The ^1H and ^{13}C chemical shift assignments of all the 1/NPMI and 1/TPMI adducts are collected in Appendix 3.

2.3.4. Product Identification; Adduct **B5**

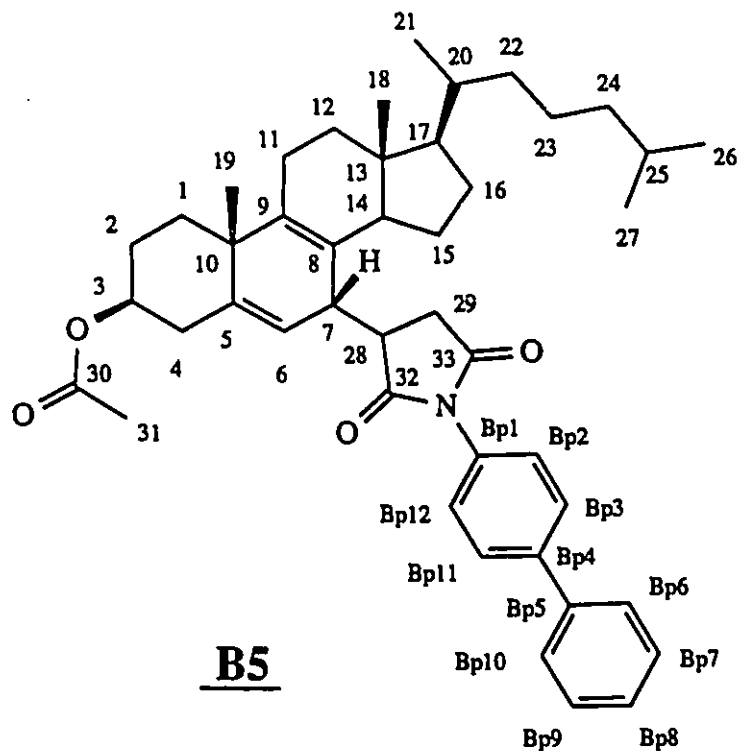


Figure 2.3. Adduct **B5**.

i, Spectral Comparison of Adduct **B5** to the 1/DMAD Adducts

The ^1H NMR spectrum of **B5** is shown in Appendix 2b. Adduct **B5** shows a single vinyl resonance at $\delta = 5.17$ ppm indicating that the product is not a Diels-Alder adduct. The methyl groups resonate at 0.65 and 1.20 ppm which is consistent with the shielding effect of 8(9) unsaturation seen in adduct **X**.

This tentative assignment is substantiated by comparison of the ^{13}C spectra. The ^{13}C spectrum shows a resonance at 50.65 ppm which has been assigned as C_{14} (cf. 54.42 ppm for C_{14} in **1**) while the C_9 resonance is now downfield in the region of 120-130 ppm. This is consistent with unsaturation of the 8(9) bond in adduct **B5**. For a complete treatment, the shift-correlated and COSY spectra have been used along with analogy to **1** to completely assign the ^{13}C and ^1H spectra of adduct **B5**.

ii, Complete Assignment; Adduct B5

The purpose of this section is to lead the reader through the ^1H - ^1H COSY and ^1H - ^{13}C shift-correlated spectra and assign all the carbon and hydrogen resonances. The reader is referred to the numbered structure of adduct B5 on the previous page and to the N.M.R. spectra collected in Appendix 2b.

Adduct B5, Ring A;

Ring A has seven protons on three methylene carbons (1,2,4) and one methyne (3). Proton 3α ($\delta= 4.55$) is the best starting place for the assignment of this ring as it has correlations to 4α and 4β at $\delta= 2.36$ and 2.34 respectively and a weak correlation to 2α ($\delta= 1.93$) ppm. While no correlation to 2β can be seen, the shift correlated spectrum clearly shows 2β at $\delta=1.67$ ppm. There is also a strong $2\alpha/2\beta$ correlation. Methylene protons on carbon 1 are assigned from correlations to 2α and 2β as summarized in the table below. From the shift-correlated spectrum, 1α and 1β can be more easily assigned at $\delta=1.32$ and 1.98 ppm respectively. The assignment of these seven protons are also consistent with the known spectrum of the steroidal starting material⁸⁸ (see Appendix 1).

The three methylene carbons (1,2,4) and the methyne carbon (3) are easily assigned from the shift correlated spectrum. The chemical shifts are listed in the table below. The vinyl quaternary carbon 5 resonates in the region of a number of other carbons between 125 and 147 ppm. By comparison with the spectra of the other adducts, carbon 5 has been assigned at $\delta= 126.86$ ppm. Quaternary carbon 10 has been assigned by analogy to 1 to resonate at 38.99 ppm.

Table 2.1. ^1H and ^{13}C chemical shifts (ppm) and important ^1H - ^1H correlations; ring A, adduct **B5**.

Carbon Number	^{13}C	^1H	Important ^1H - ^1H Correlations
1 α	37.12	1.32	1 β , 2 α , 2 β
1 β		1.98	1 α , 2 α
2 α	28.34	1.93	2 β , 1 α , 1 β , 3 α
2 β		1.67	2 α , 1 α
3 α	74.67	4.55	4 α , 4 β , 2 α
4 α	38.89	2.36	4 β , 3 α
4 β		2.34	4 α , 3 α
5	126.86		
10	38.99		

Adduct B5, Ring B;

Ring B protons are easily identified as the vinyl signal for H₆ ($\delta = 5.17$ ppm) shows a strong correlation to H₇ ($\delta = 3.53$ ppm). Carbons 6 and 7 are easily assigned at 118.11 and 39.62 ppm respectively based on the shift correlations to the respective protons. Quaternary carbons 8 and 9 are assigned by comparison to the I/NPMI adducts to resonate at 143.79 and 147.14 ppm respectively.

Table 2.2. ^1H and ^{13}C chemical shifts (ppm) and important ^1H - ^1H correlations; ring B, adduct **B5**.

Carbon Number	^{13}C	^1H	Important ^1H - ^1H Correlations
6	118.11	5.17	7
7	39.62	3.53	6, 28
8	143.79		
9	137.14		

Adduct B5, Ring C;

Ring C has three allylic protons (11 α 11 β , 14) and one methylene group (12). The allylic methylene protons, 11 α and 11 β appear at 2.20 and 2.10 ppm, respectively,

and show a strong geminal correlation to each other in the COSY spectrum. Correlations between 11 α and the two protons at 12 are also very strong and assignments of 12 α (δ =1.30) and 12 β (2.00) are consistent with both the shift-correlated spectrum and with the similarities to the starting material (**1**). The allylic methyne proton 14 can be easily assigned at 1.90 ppm based on the shift-correlated spectrum. The correlations of proton 14 to the protons at 15 are shown on the COSY spectrum. They are however convoluted with other signals and are consequently somewhat speculative. The carbons on this ring are assigned from the shift-correlated spectrum (Table 2.3). Quaternary carbon 13 is assigned by analogy to (**1**) to resonate at 42.91 ppm.

Table 2.3. ^1H and ^{13}C chemical shifts (ppm) and important ^1H - ^1H correlations; ring C, adduct **B5**.

Carbon Number	^{13}C	^1H	Important ^1H - ^1H Correlations
11 α	23.27	2.20	11 β , 12 β , 12 α
11 β		2.10	11 α , 12 α
12 α	36.71	1.30	11 α , 11 β , 12 β
12 β		1.98	11 α , 12 α
13	42.91		
14	50.65	1.85	15 α , 15 β

Adduct **B5, Ring D;**

Ring D has two methylene protons (15,16) and a methyne proton (17).

Carbon 17 is easily identifiable by analogy to the spectrum of **1** and by correlation to the methyne proton that has been identified as H₂₀. Carbon 17 appears at 54.80 ppm and proton 17 resonates at 1.10 ppm as confirmed by the shift-correlated spectrum.

Initial assignments of the methylene protons at 15 and 16 were based on analogy to the starting material and were confirmed by correlations between protons 16 and 17 as well as correlations of protons 15 α and 15 β to protons 16 α and 16 β . The

only correlation that cannot be seen explicitly is that of protons 15 β to 16 α because of overlapping resonances.

Protons 15 α and 15 β should show correlations to proton 14. Assigning these correlations is speculative due to overlap with correlations of protons 15 and 16. The important correlations are shown on the COSY and shift-correlated spectra in Appendix 2b.

Table 2.4. ^1H and ^{13}C chemical shifts (ppm) and important ^1H - ^1H correlations; ring D, adduct **B5**.

Carbon Number	^{13}C	^1H	Important ^1H - ^1H Correlations
15 α	24.01	1.81	15 β , 16 α , 16 β
15 β		1.37	15 α , 16 β
16 α	29.31	1.35	16 β , 15 α
16 β		1.89	16 α , 15 α , 15 β
17	54.80	1.10	16 α , 16 β , 20

Adduct B5, Succinimide Portion and Carbonyls;

The biphenyl succinimide portion has 2 methylene protons (29), a methyne proton (28) as well as 9 aromatic protons. Proton 28 is easily identified by a strong correlation to proton 7 and in turn, both protons at position 29 show a strong correlation to proton 28. From the shift-correlated spectrum, carbons 28 and 29 were assigned. The aromatic resonances and carbonyls have been assigned as shown in the table below. The carbonyl carbons (30, 32 and 33) are easily assigned as the three lowest field resonances in the molecule (Table 2.5).

Table 2.5. ^1H and ^{13}C chemical shifts (ppm) and important ^1H - ^1H correlations; succinimide portion and carbonyls, adduct **B5**.

Carbon Number	^{13}C	^1H	Important ^1H - ^1H Correlations
28	43.53	3.27	7, 29(2)
29	30.81	2.55	29, 28
		2.52	29, 28
30 ^a	170.63		
32 ^a	176.40		
33 ^a	178.75		
Bp1	131.63		
Bp4	142.14	Aromatic protons multiplet $\delta = 7.0\text{-}7.7$ ppm	
Bp5	140.86		
Bp8	128.16		
Bp2/Bp12	129.40		
Bp3/Bp11	128.59		
Bp6/Bp10	127.89		
Bp7/Bp9	127.43		

^acarbonyl carbon assignments for all 1/N-arylmaleimide adducts may be interchanged.

Adduct **B5**, Alkyl Chain and Methyl Groups;

The alkyl chain attached to carbon 17 contains two methyne groups (20 and 25) and the three methylene groups (22, 23 and 24). The methynes are easily assigned by looking at the correlations to methyls 21, 26 and 27. Proton 20 resonates at 1.33 ppm and shows a strong correlation with the methyl protons on carbon 21. Similarly, proton 25 resonates at 1.46 ppm and is strongly coupled to its vicinal methyl neighbours (26 and 27). The corresponding carbon resonances were assigned from the shift-correlated spectrum. Methylene carbons 22, 23 and 24 should not vary greatly from the resonances in the starting diene. By analogy these resonances were tentatively assigned at 36.80, 24.46 and 40.10, respectively. The shift-correlated spectrum supports these assignments as all three are indeed methylene groups with proton chemical shifts which are consistent with these assignments. The COSY spectrum is fairly congested in this region. In spite of this, several of the correlations between these groups were assigned. These assignments are believed to be correct as supported

by the shift-correlated spectrum and analogies to the starting material.

The methyl groups in this adduct appear as 3 proton doublet patterns (21, 25, 26) and three singlets (31, 18, 19). Methyls 26 and 27 are doublets at 0.80 and 0.82 ppm coupled to proton 25 while 21 resonates at 0.89 ppm and is coupled to methyne proton 20. The methyl proton singlets corresponding to carbons 31, 19 and 18 were assigned from the shift correlated spectrum (*vide infra*) and are all consistent with the known assignments of the starting material (**1**) (see Appendix 1).

Table 2.6. ^1H and ^{13}C chemical shifts (ppm) and important ^1H - ^1H correlations; alkyl chain and methyl groups, adduct **B5**.

Carbon Number	^{13}C	^1H	Important ^1H - ^1H Correlations
18	12.20	0.65	
19	24.23	1.20	
31	21.90	1.96	
20	36.72	1.33	17, 21,
21	19.36	0.89	20
22	36.80	0.95	23(2),
		1.33	23(2)
23	24.46	1.29	22, 23, 24
		1.15	22, 23, 24
24	40.10	1.08	(2)23,
25	28.63	1.46	26, 27
26	23.40	0.82	25
27	23.15	0.80	25

2.3.5. Product Identification; Adducts B4a and B4b

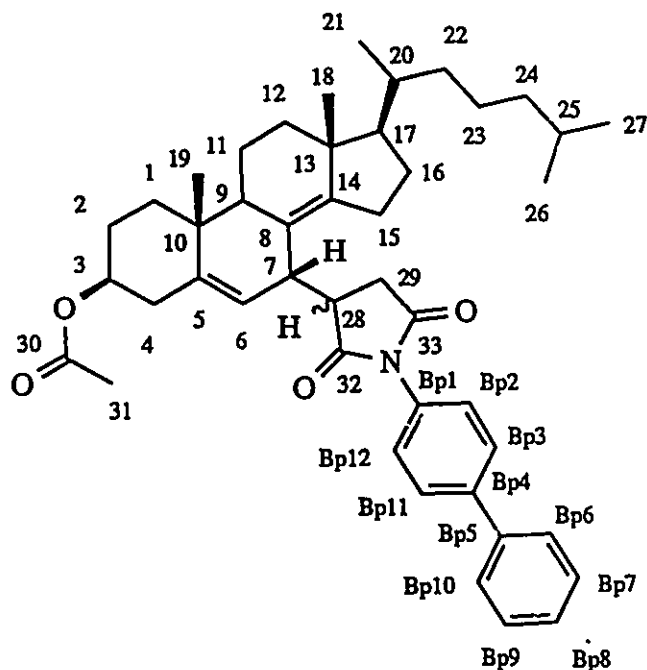


Figure 2.4. Adducts B4a and B4b

i, Spectral Comparison to 1/DMAD Adducts

Adducts B4a and B4b are isomers which are epimeric at position 28 and are analogous to adduct II of the 1/DMAD reaction. Structural speculation based on similarities to the N.M.R. spectra of the DMAD adducts will be followed by complete assignments of each isomer.

The vinyl and allylic regions of these two isomers are similar to that for B5 and the DMAD adducts indicating that they are definitely ene addition products. The methyl resonances (18 and 19) appear almost coincidentally at 0.90 ppm. This indicates that, in accord with Huisman's results, no diamagnetic shielding effects are

observed and consequently, the unsaturation in these molecules cannot be in the 8(9) bond.

The ^{13}C spectra of B4a and B4b show that C_{14} resonates in the vinyl region while C_9 appears, (c.f. 1), around 45 ppm. This indicates that the unsaturation in these adducts must be at the 8(14) bond which is in complete agreement with the results found by Huisman. The complete assignment of the B4 adducts confirm these initial results.

ii, Complete Assignment; Adduct B4b

The complete assignment of adduct B4b can be followed in a similar route to that of adduct B5. The reader is referred to the numbered structure of adduct B4b on the previous page and to the N.M.R. spectra collected in Appendix 2c.

Adduct B4b, Ring A;

Ring A consists of three methylene sites (1,2,4), one methyne site (3), and two quaternary sites (5,10). Proton 3α ($\delta=4.61$) shows correlations to 2α ($\delta = 1.84$) and 2β ($\delta=1.42$) as well as to 4α ($\delta = 2.45$) and 4β ($\delta = 2.34$). The protons on site 2 show strong correlations to the 1α and 1β protons ($\delta = 1.24$ and 1.78 respectively). The corresponding carbons were assigned from the shift-correlated spectrum (Appendix 2c). The quaternary sites assigned, by comparison with the other adducts, to the resonances at 131.67 and 39.62 ppm (C_5 and C_{10} , respectively).

Table 2.7. ^1H and ^{13}C chemical shifts(ppm) and important ^1H - ^1H correlations; ring A, adduct **B4b**.

Carbon Number	^{13}C	^1H	Important ^1H - ^1H Correlations
1 α	36.60	1.24	1 β , 2 α , 2 β
1 β		1.78	1 α , 2 α , 2 β
2 α	28.32	1.87	2 β , 1 α , 1 β
2 β		1.55	2 α , 1 α , 1 β
3 α	73.75	4.61	2 α , 2 β , 4 α , 4 β
4 α	38.38	2.45	4 β
4 β		2.34	4 α , 6
5	125.89		
10	39.26		

Adduct **B4b**, Ring B;

Ring B consists of three methyne sites (6,7,9) and one quaternary site (8).

The assignments of the methyne groups are relatively easy. Proton 6 ($\delta = 5.51$) shows a strong correlation to proton 7 ($\delta = 3.16$) as well as a weak allylic coupling to 4 β .

Proton 9 was initially assigned based on the shift-correlated spectrum and substantiated by strong correlations to protons 11 α and 11 β . From the shift-correlated spectrum the corresponding carbon chemical shifts were assigned as shown in the table below.

Quaternary carbon 8 was assigned on the basis of analogies with the other adducts.

Table 2.8. ^1H and ^{13}C chemical shifts (ppm) and important ^1H - ^1H correlations; ring B, adduct **B4b**.

Carbon Number	^{13}C	^1H	Important ^1H - ^1H Correlations
6	121.96	5.51	7, 4 β
7	40.47	3.16	28
8	148.23		
9	44.51	2.25	11 α , 11 β

Adduct B4b, Ring C;

Ring C has four protons on two methylene groups, 11 and 12. The starting point is to find the correlations between the previously assigned proton 9 with the 11 protons. These correlations are strong and are shown on the COSY spectrum (Appendix 2c). Strong correlations of 11 α and 11 β to 12 α and 12 β are clearly visible. The corresponding carbons have been assigned from the shift-correlated spectrum. Quaternary carbons 13 and 14 been assigned by comparison to the ^{13}C spectra of the starting material and the 1/ NPMI adducts.

Table 2.9. ^1H and ^{13}C chemical shifts(ppm) and important ^1H - ^1H correlations; ring C, adduct B4b.

Carbon Number	^{13}C	^1H	Important ^1H - ^1H Correlations
11 α	19.69	1.64	9, 11 β , 12 β , 12 α
11 β		1.54	9, 11 α , 12 α , 12 β
12 α	37.67	1.16	12 β , 11 α , 11 β
12 β		2.01	12 α , 11 α , 11 β
13	44.11		
14	144.02		

Adduct B4b, Ring D;

Ring D has 5 protons on two methylene carbons and one methyne carbon. The methyne group (17) has been assigned to a carbon chemical shift of 58.28 ppm and a proton resonance at 1.15 ppm based on correlations to proton 20 and on the shift-correlated spectrum. Protons 16 α and 16 β were assigned by correlations to proton 17 and in turn correlations of protons 16 were used to assign protons 15 α and 15 β .

Table 2.10. ^1H and ^{13}C chemical shifts(ppm) and important ^1H - ^1H correlations; ring D, adduct **B4b**.

Carbon Number	^{13}C	^1H	Important ^1H - ^1H Correlations
15 α	26.70	2.27	15 β , 16 α , 16 β
15 β		2.17	15 α , 16 α , 16 β
16 α	27.31	1.42	16 β , 15 α , 15 β
16 β		1.84	16 α , 15 α , 15 β
17	58.28	1.15	16 α , 16 β

Adduct B4b, Succinimide Portion and Carbonyls;

The biphenyl succinimide ring has 2 methylene protons (29), a methyne proton (28) and 9 aromatic protons. Proton 28 shows strong correlations to protons 7 and 29(2). The corresponding carbons were assigned from the shift-correlated spectrum. The 9 aromatic protons appear as a multiplet, between 7.0 and 7.7 ppm. The 12 aromatic carbon signals are assigned to the 8 resonances in the aromatic region while the three lowest field carbon signals are assigned as the carbonyls (Table 2.11).

Table 2.11. ^1H and ^{13}C chemical shifts (ppm) and important ^1H - ^1H correlations; succinimide portion and carbonyls, adduct **B4b**.

Carbon Number	^{13}C	^1H	Important ^1H - ^1H Correlations
28	46.17	3.09	7, 29(2)
29	34.40	2.93, 2.70	29, 28
30	170.94		
32	176.22		
33	178.90		
Bp1	131.67		
Bp4	142.25		
Bp5	140.96		
Bp8	128.20		
Bp2/Bp12	129.40		
Bp3/Bp11	128.65		
Bp6/Bp10	127.89		
Bp7/Bp9	127.38		

Aromatic protons multiplet
 $\delta = 7.0-7.7$ ppm

Adduct B4b, Alkyl Chain and Methyl Groups;

The alkyl chain can be assigned in a similar manner to that used for adduct B5. Methyne protons 20 and 25 are easily distinguished by their correlations to neighbouring methyl groups 21, 26 and 27. Correlations between protons 20 and 17 are also clearly visible and labelled on the COSY spectrum. Methylene groups 22, 23 and 24 were all initially assigned from analogies to 1. These assignments were confirmed from the shift correlated spectrum as well as from the geminal and vicinal correlations between these groups which were all assignable in the high field region. These correlations are all fairly convoluted and have not been explicitly labelled on the COSY spectrum.

The only methyl groups yet to be assigned are methyl groups 31, 18 and 19. All three of these can be easily assigned by analogy to the proton spectrum of the 1/DMAD adducts and from the spectrum of 1 itself (see Table 2.12.).

Table 2.12. ^1H and ^{13}C chemical shifts (ppm) and important ^1H - ^1H correlations; alkyl chain and methyl groups, adduct B4b.

Carbon Number	^{13}C	^1H	Important ^1H - ^1H Correlations
18	18.16	0.90	
19	19.81	0.89	
20	35.21	1.45	17, 21, 22
21	19.95	0.93	20
22	36.53	1.03	20, 23
		1.26	
23	24.60	1.36	23, 22, 24
		1.12	23, 22, 24
24	40.10	1.10(2)	23(2), 25
25	28.59	1.51	24, 26, 27
26	23.41	0.84	25
27	23.14	0.85	25
31	21.96	1.98	

Complete Assignment; Adduct B4a

As mentioned previously, adducts B4a and B4b are isomers which are epimeric at position 28. The assignment of adduct B4a is very similar to that of B4b. The reader is referred to the structure of this adduct (Figure 2.2.) and to the N.M.R. spectra collected in Appendix 2c.

B4a, Ring A;

Proton 3 α shows correlations to each of protons 2 α,β and 4 α,β . Protons 1 α and 1 β were assigned from correlations to 2 α and 2 β . The corresponding carbons were assigned from the shift correlated spectrum. Quaternary resonances show no correlations on the shift correlated spectrum and were assigned based on comparison with the ^{13}C spectrum of the starting material and with the other adducts.

Table 2.13. ^1H and ^{13}C chemical shifts(ppm) and important ^1H - ^1H correlations; ring A, adduct B4a.

Carbon Number	^{13}C	^1H	Important ^1H - ^1H Correlations
1 α	36.60	1.23	1 β , 2 α , 2 β
1 β		1.82	1 α , 2 α , 2 β
2 α	28.24	1.99	2 β , 1 α , 1 β , 3 α
2 β		1.61	2 α , 1 α , 1 β , 3 α
3 α	73.72	4.66	4 α , 4 β , 2 α , 2 β
4 α	38.12	2.44	4 β , 3 α
4 β		2.30	4 α , 3 α
5	125.86		
10	39.05		

Adduct B4a, Ring B;

Vinyl proton 6, shows correlations to proton 7 and an allylic coupling to proton 4 β . Proton 9 is assigned from its characteristic allylic chemical shift and shows strong correlations to 11 α,β . Quaternary carbon 8 was assigned from the ^{13}C spectrum

and comparison with the spectra of the other adducts.

Table 2.14. ^1H and ^{13}C chemical shifts(ppm) and important ^1H - ^1H correlations; ring B, adduct **B4a**.

Carbon Number	^{13}C	^1H	Important ^1H - ^1H Correlations
6	119.86	5.05	7, 4 α (weak allylic coupling)
7	37.97	3.64	6, 28
8	147.18		
9	45.66	1.95	11 α , 11 β

Adduct B4a, Ring C;

Methylene groups 11 and 12 were initially assigned from the shift-correlated spectrum and are substantiated by correlations between protons 9 and 11(2) and correlations of protons 11(2) with 12(2). The corresponding carbons were assigned from the shift-correlated spectrum. Quaternary carbons 13 and 14 were assigned from analogies to the starting material and the other adducts.

Table 2.15. ^1H and ^{13}C chemical shifts (ppm) and important ^1H - ^1H correlations; ring C, adduct **B4a**.

Carbon Number	^{13}C	^1H	Important ^1H - ^1H Correlations
11 α	19.73	1.63	9, 11 β , 12 β , 12 α
11 β		1.54	9, 11 α
12 α	37.84	1.09	12 β , 11 α , 11 β
12 β		1.97	12 α , 11 α , 11 β
13	43.81		
14	146.55		

B4a, Ring D;

Methyne proton (17) was assigned from correlations to proton 20.

Correlations to proton 17 were used to assign protons 16 α , β and in turn protons 15 α

and 15 β were assigned from correlations to the protons at 16.

Table 2.16. ^1H and ^{13}C chemical shifts(ppm) and important ^1H - ^1H correlations; ring D, adduct **B4a**.

Carbon Number	^{13}C	^1H	Important ^1H - ^1H Correlations
15 α	25.79	2.38	15 β , 16 α , 16 β
15 β		2.35	15 α , 16 α , 16 β
16 α	27.39	1.43	16 β , 15 α , 15 β
16 β		1.88	16 α , 15 α , 15 β
17	57.97	1.11	16 α , 16 β

Adduct **B4a, Succinimide Portion and Carbonyls;**

Proton 28 shows strong correlations to protons 7 and 29 (2). The corresponding carbons were identified from the shift-correlated spectrum.

Table 2.17. ^1H and ^{13}C chemical shifts(ppm) and important ^1H - ^1H correlations; succinimide portion and carbonyls, adduct **B4a**.

Carbon Number	^{13}C	^1H	Important ^1H - ^1H Correlations
28	45.02	3.17	7, 29(2)
29	32.17	2.93	29, 28
		2.75	29, 28
30	178.39		
32	176.29		
33	171.00		
Bp1	131.66		
Bp4	142.07		
Bp5	141.00		
Bp8	128.20		
Bp2/Bp12	129.40		
Bp3/Bp11	128.44		
Bp6/Bp10	127.83		
Bp7/Bp9	127.18		

Aromatic protons multiplet
 $\delta = 7.0-7.7$ ppm

Adduct B4a, Alkyl Chain and Methyl Groups;

The alkyl chain was assigned in a method similar to that for adduct B4b.

Proton 20 shows correlations with the previously assigned proton 17 and, from correlations to 20, the protons at site 21 were assigned. Similarly, methyne proton 25 was easily assigned from correlations with protons 26 and 27. Methylene groups 22, 23 and 24 as well as the remaining methyl groups (18, 19 and 31) were all assigned in the same manner as in adduct B4B. (*vide supra*).

Table 2.18. ^1H and ^{13}C chemical shifts (ppm) and important ^1H - ^1H correlations; alkyl chain and methyl groups, adduct B4a.

Carbon Number	^{13}C	^1H	Important ^1H - ^1H Correlations
18	18.36	0.90	
19	19.66	0.91	
20	35.05	1.49	17,21, 22
21	19.81	0.93	
22	36.52	1.08	20, 23
		1.49	
23	24.38	1.36	23, 22, 24
		1.10	23, 22, 24
24	40.10	1.11(2)	23(2), 25
25	28.61	1.50	24, 26, 27
31	21.93	2.02	

2.3.6. Product Identification; Adduct B3.

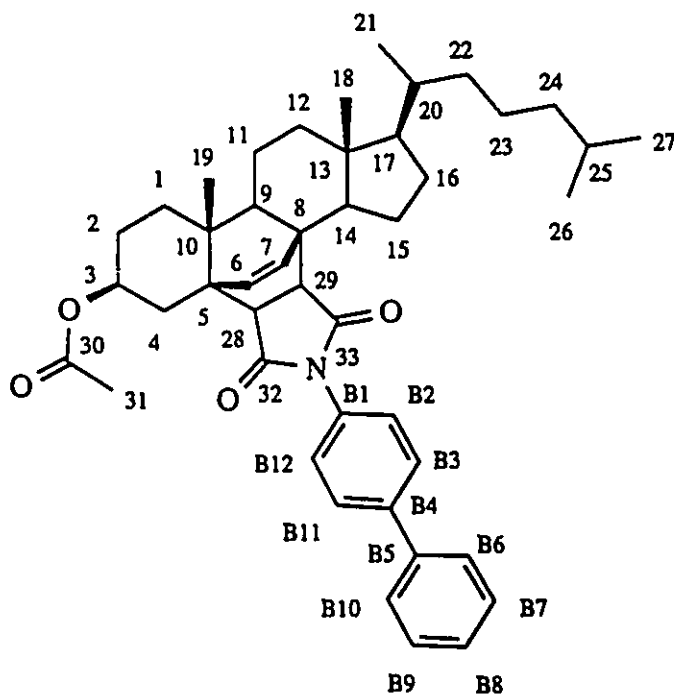


Figure 2.5. Adduct B3

Initial structural speculation can be obtained by comparison of the proton spectrum of B3 with those for the other cycloaddition adducts. The most noticeable difference is the presence of a doublet of doublets in the vinyl region of the ^1H N.M.R. spectrum. This indicates that the adduct is not an ene adduct and is probably a Diels-Alder product. Further evidence for the Diels-Alder assignment is that the proton signal at $\delta = 3.66$ is absent, indicating that H_7 is no longer allylic. As well, the signals from protons 28 and 29, which were three protons in the ene adducts, now show only two signals coupled only to each other in a doublet of doublets which is consistent with the Diels-Alder product.

The ^{13}C spectrum of adduct B3 shows some noteworthy differences from the

spectra of the ene adducts. The most obvious of these is that the signal for carbon 7, an allylic methyne group in the ene adducts, has moved downfield and now appears in the vinylic region along with its vicinal neighbour carbon 6. As well, carbons 9 and 14, which appear in the ene adducts as a methyne and a vinyl (depending on the unsaturation), now appear together as a pair of methyne signals. From these initial observations, it is certain that this adduct is in fact the Diels-Alder adduct which Huisman did not observe in the cycloaddition of **1** with **DMAD**.

Complete Assignment; Adduct B3

The purpose of this section is to lead the reader through the total assignment of the proton and carbon spectra of adduct **B3**. Initial assignments were determined by comparison of the ^{13}C resonances of **B3** to those of the other adducts. The spectra are very similar in many cases and these initial assignments were made by analogy. To confirm these initial assignments, the shift-correlated spectrum was used to show that the carbons as assigned do indeed carry the correct number of hydrogens and that the proton chemical shifts are consistent with those that would be expected. Finally, the COSY spectrum was used to assign the important correlations. In a couple of cases, weaker correlations are missing. In spite of this, the strong correlations present can be used to assign the signals. The assignments are consistent with the other adducts and with the shift correlated spectrum.

Adduct B3, Ring A;

The 3α proton at $\delta=5.33$ shows correlations to protons 4α , 4β , 2α and 2β . The correlations are weak but clearly visible and are shown on the COSY spectrum. From this, as well as the shift correlated-spectrum, these protons and corresponding carbons have been assigned.

Assignment of carbon 1 was more tricky as correlations to carbon 2 were convoluted with a number of other signals. From comparison of the shift-correlated spectrum of **B3** with the spectra of the other ene adducts, it can be seen that the resonances for carbons 1, 12, and 22 are very close together. In **B3** they are separated but the identity of each is not clear. Carbon 22 was assigned as shown on the spectra because it should resonate at the same chemical shift in all the adducts since it is on the remote alkyl chain. The problem is to assign carbons 1 and 12 correctly. By comparing the proton shifts of these sites to those of the other adducts, 12 and 1 were assigned. From the COSY spectrum, the following proton correlations have been assigned; $1\alpha/1\beta$, $12\alpha/12\beta$, $12\beta/11\beta$ and $1\beta/2\alpha$ (under $2\alpha/2\beta$ correlation). There are four quaternary carbons in the molecule (5,8,10,13) which are easily assigned from the ^{13}C and shift-correlated spectra to be the four resonances between 40 and 47 ppm. Quaternary sites 5 and 8 were assigned by comparison to the other adducts. The assignments of carbons 10 and 13 are not definitive and they may be reversed.

Table 2.19. ^1H and ^{13}C chemical shifts (ppm) and important ^1H - ^1H correlations; ring A, adduct **B3**.

Carbon Number	^{13}C	^1H	Important ^1H - ^1H Correlations
1α	31.95	1.58	1β
1β		1.78	$1\alpha, 2\alpha$
2α	27.27	2.06	$2\beta, 3\alpha$
2β		1.65	$2\alpha, 3\beta$
3α	70.07	5.33	$4\alpha, 4\beta, 2\alpha, 2\beta$
4α	35.07	2.85	$4\beta, 3\alpha$
4β		2.06	$4\alpha, 3\alpha$
10	44.21		

Adduct **B3, Ring B;**

Ring B consists of two vinylic sites (6,7), three methyne sites (9, 28, 29) and

two quaternary carbons (5, 8). The vinylic protons, 6 and 7 are coupled to form a doublet of doublets at $\delta = 6.24$ and 5.83 . The corresponding carbon resonances were assigned based on the shift-correlated spectrum. Protons 28 and 29 give a strongly coupled doublet of doublets at somewhat higher field (table 2.20). Methyne group 9 was initially assigned from the shift-correlated spectrum. This is confirmed by the strong couplings to protons 11α and 11β . Quaternary carbons 5 and 8 were assigned based on comparison to the other adducts to be the two higher field quaternary sites at $\delta = 46.41$ and 45.50 .

Table 2.20. ^1H and ^{13}C chemical shifts (ppm) and important ^1H - ^1H correlations; ring B, adduct **B3**.

Carbon Number	^{13}C	^1H	Important ^1H - ^1H Correlations
5	46.41		
6	136.27	6.24	7
7	131.06	5.83	6
8	45.50		
9	55.40	1.71	11α , 11β
28	42.95	3.40	29
29	57.21	2.77	28

Adduct **B3**, Ring C;

Ring C consists of two methylene groups (11,12), a methyne site (14) and a quaternary carbon (13). Carbon 11 can be assigned initially based on comparisons of the shift-correlated spectrum to those of the other adducts. This speculation is confirmed by the COSY spectrum as couplings between proton 9 and the two 11 protons are evident. Carbon 12, as previously mentioned, was first assigned from the shift-correlated spectrum by comparison to the other adducts. The problem was to discern between methylenes 1 and 12 which were overlapped in the ene adducts but separated in the Diels-Alder product. They were tentatively identified based on the

proton chemical shifts. From the COSY spectrum, the proton correlations are weak and consequently the only supporting evidence here are weak correlations that have been assigned as $12\beta/11\beta$ and perhaps $1\beta/2\alpha$ underneath the $2\alpha/2\beta$ correlation. While distinguishing between carbons 12 and 1 is somewhat tenuous, the available evidence is consistent with the assignments listed in Table 2.21. below. Methyne 14 was initially assigned from the shift-correlated spectrum and from comparisons to the spectra of the other ene adducts and 1. This assignment was further substantiated by correlations in the COSY spectrum that have been assigned to correlations between protons 14 and $15\alpha,\beta$. Quaternary carbon 13 has been assigned at $\delta = 42.91$ ppm.

Table 2.21. ^1H and ^{13}C chemical shifts (ppm) and important ^1H - ^1H correlations; ring C, adduct B3.

Carbon Number	^{13}C	^1H	Important ^1H - ^1H Correlations
11 α	23.71	2.57	9, 11 β
11 β		1.43	9, 11 α , 12 β
12 α	39.49	1.11	12 β
12 β		2.03	12 α , 11 β
13	41.36		
14	55.69	1.12	

Adduct B3, Ring D;

Ring D consists of methyne carbon (17) and two methylene carbons, (15, 16). Carbon 17 is easily assigned based on several factors; its characteristic carbon chemical shift, its correlation to proton 20 and the shift-correlated spectrum. Unfortunately, correlations between 17 and methylene carbon 16 are not seen and consequently, initial assignments of both 15 and 16 were based on analogies of the shift correlated spectrum to those of the other adducts. Carbon 16 has been assigned by analogy to the ^{13}C and shift-correlated spectra of the other adducts and the

corresponding protons are assigned at $\delta = 1.35$ and 1.89 (16α and 16β respectively). Carbon 15 has been assigned at $\delta = 23.45$ with proton signals at $\delta = 1.43$. While these assignments cannot be confirmed from the COSY spectrum, they are consistent with the ^{13}C and shift correlated spectra of the other adducts.

Table 2.22. ^1H and ^{13}C chemical shifts (ppm) and important ^1H - ^1H correlations; ring D, adduct **B3**.

Carbon Number	^{13}C	^1H	Important ^1H - ^1H Correlations
15 α	23.45	1.39	15 β
15 β		1.39	15 α
16 α	28.27	1.31	16 β
16 β		1.90	16 α
17	54.03	1.07	20

Adduct **B3**, Succinimide Portion and Carbonyls;

The succinimide portion and the carbonyls were assigned as they were in the ene adducts and are listed in Table 2.23 below.

Table 2.23. ^1H and ^{13}C chemical shifts (ppm) and important ^1H - ^1H correlations; succinimide portion and carbonyls, adduct **B3**.

Carbon Number	^{13}C	^1H	Important ^1H - ^1H Correlations
30	170.87		
32	176.71		
33	176.90		
31	21.91	2.02	
B1	131.76		
B2/B12	129.39		Aromatic proton resonances appear between 7.2 and 7.7 ppm
B3/B11	128.32		
B4	140.98		
B5	142.04		
B6/B10	127.81		
B7/E.9	127.36		
B8	128.16		

Adduct **B3**, Alkyl Chain and Methyl Groups;

Methyl proton signals 21, 26 and 27 are all doublets and are easily assigned from their correlations to their methyne neighbours (20 and 25). The methylene protons (22, 23, 24) are all assigned initially by analogy to the other adducts and confirmed from the shift-correlated spectrum. All corresponding carbon resonances were also confirmed using the shift-correlated spectrum (Table 2.24).

Table 2.24. ^1H and ^{13}C chemical shifts (ppm) and important ^1H - ^1H correlations; alkyl chain and methyl groups, adduct **B3**.

Carbon Number	^{13}C	^1H	Important ^1H - ^1H Correlations
18	19.22	0.96	
19	13.04	0.74	
20	35.95	1.39	21
21	19.66	0.92	20
22	36.58	1.03	22
		1.36	
23	24.43	1.34	23, 24
		1.15	
24	40.09	1.11(2)	23
25	28.61	1.51	26, 27
26	23.14	0.86	25
27	23.39	0.85	25

2.4 Summary; Chapter 2

In this chapter, the probe reaction of N-arylmaleimides with cholesta-5,7-dien-3 β -yl acetate (**1**) has been introduced. The reaction products for the cycloaddition of **1** with **BPMI** have been described and identified using N.M.R. techniques. These results are tabulated in Appendix 1 while representative N.M.R. spectra are collected in Appendix 2. The products found for the other enophiles were

identical to those described above. These were identified by comparison of the N.M.R. spectra to those of the 1/BPMI adducts. The assignments of these adducts are tabulated in Appendix 3.

**CHAPTER 3: ORIENTATIONAL CONTROL OF REACTIVITY IN LIQUID
CRYSTALLINE SOLVENTS; THE REACTION OF
CHOLESTA-5,7-DIEN-3 β -YL ACETATE WITH N-ARYLMALEIMIDES.**

3.1. Introduction

The objectives of this study were to first establish that regiochemical control of our probe reaction could be accomplished using liquid crystalline solvents and then to investigate the influence of solvent order and solute structure on the observed effect. Our results show in fact that both the type of liquid crystalline phase and the structure of the solutes do have a great influence on the degree of regiochemical control observed.

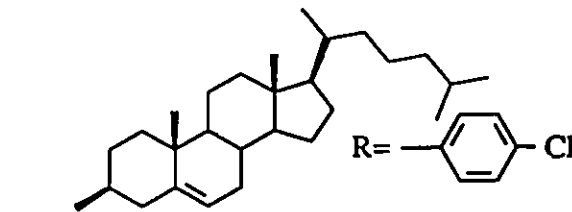
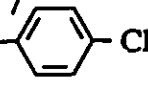
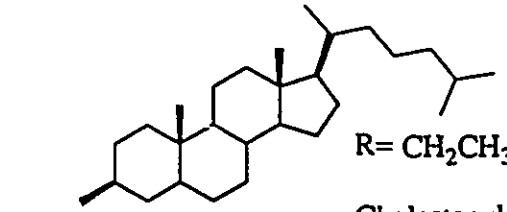
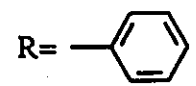
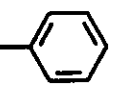
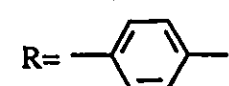
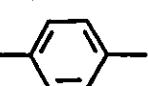
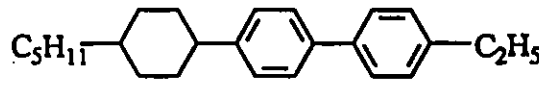
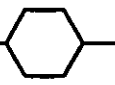
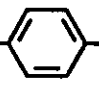
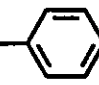
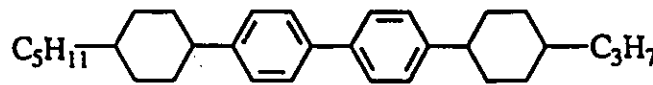
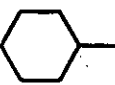
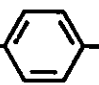
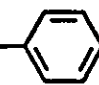
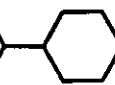
In this chapter, the results of our investigations into the regiochemical control of chemical reactivity will be presented followed by a discussion of how the ordered nature of the solvent and the structure of the reactants have influenced the observed effects. The discussion will first describe qualitatively how liquid crystalline order may be expected to influence bimolecular reaction energetics and then, using the physical theories of liquid crystals, we will try to estimate how much of an effect may be expected. Our results concerning the influence of solvent type and solute structure will be explained in terms of how these factors influence the energy of orientation associated with liquid crystalline compounds.

3.2. Results

3.2.1. Solvent Selection and Transition Temperatures

The cycloaddition reaction of **1** with each of the three enophiles has been performed in a number of cholesteric and model isotropic solvents as well as in a highly ordered smectic B phase. We chose to use the cholesteric liquid crystalline phases formed by steroidal esters because they are very similar in structure to the reactive diene (**1**). As well, these mesogens are easily synthesized and are available over a wide temperature range.^{89,90} Several steroidal esters are cholesteric over our required temperature range (180-240°C) while a number of others are isotropic liquids and can serve as model isotropic solvents at these temperatures. The smectic solvent used was the commercially available compound 4-(*trans*-4-*n*-pentylcyclohexyl)-4'--(*trans*-4-*n*-propyl-cyclohexyl)biphenyl (**S1544**), chosen primarily because it forms a highly ordered smectic B phase over a broad temperature range (54-232°C).^{35,81} While this mesogen is not an ideal structural match with the reactants, such highly ordered phases may provide the greatest potential to orient reactive species. Consequently, it may be interesting to compare the degree of regiochemical control imposed by the smectic mesogen with that imposed by the more fluid like cholesteric phases. It should be recognized however that problems may arise due to the possibility of heterogeneous reactant solubilization. Recent studies have shown that even low (< 1mol%) solute concentrations can result in heterogeneous solubilization phenomena (*vide supra*). The solvents used in this study, are shown in Table 3.1.

Table 3.1. Molecular structures of liquid crystalline solvents.

SOLVENT		PHASE AT 200°C
 <p>RCO₂</p> <p>R=  Cl</p>	Cholesteryl-4-chlorobenzoate (CCB)	Cholesteric
 <p>RCO₂</p> <p>R= CH₂CH₃</p>	Cholestanyl Propionate (CP)	Isotropic Liquid
 <p>R= </p>	Cholestanyl Benzoate (CB)	Isotropic Liquid
 <p>R= </p>	Cholestanyl Toluate (CT)	Cholesteric
 <p>C₅H₁₁————C₂H₅</p>	(S1409)	Isotropic Liquid
 <p>C₅H₁₁—————C₃H₇</p>	(S1544)	Smectic B

The reactant/solvent samples were prepared by evaporation of methylene chloride solutions of the appropriate mixtures to ensure complete mixing of the components. The transition temperatures for the neat and solute doped cholesteric solvents are collected in Table 3.2. Thermal microscopy shows that, while the doped samples do have broader transition temperature ranges, than the neat mesogens, they all appear to remain homogeneous over their respective cholesteric temperature ranges. It is a little surprising that the transition temperatures for the doped samples do not vary much as a function of the enophile used. Transition temperature depression, has generally been used as an indication of the degree of solute-induced disruption of liquid crystalline order.⁸

To investigate this, transition temperatures were measured for 0.5 mol% samples of each enophile in C.C.B. (see Table 3.2.). For each of these samples, the transition temperatures are very similar. It was expected that the degree of transition temperature depression would increase with enophile length as the longer solutes may be more disruptive to cholesteric order. This will be considered further in the discussion section.

Transition temperatures and thermal microscopy of the smectic mesogen (S1544) and model isotropic solvent (S1409) will be discussed in the final section of this chapter.

Table 3.2. Transition temperatures for neat and solute doped cholesteric and model isotropic solvents.^a

SAMPLE	TRANSITION TEMPERATURE(°C)	
	K-Ch	Ch-I
Cholestanyl Propionate (C.P.)	(K-I)	125.5-126.5
(C.P.) + 1.5wt% (NPMI+I)		122.5-126.5
(C.P.) + 1.6wt% (BPMI+I)		122.0-126.5
(C.P.) + 1.76wt% (TPMI+I)		122.5-126.5
Cholestanyl Benzoate (C.B.)	135.5-136.5	156.5-157.0
(C.B.) + 1.5wt% (NPMI+I)	132.5-136.5	155.6-156.5
(C.B.) + 1.6wt% (BPMI+I)	132.0-135.5	152.0-154.0
(C.B.) + 1.76wt% (TPMI+I)	131.5-135.0	152.0-155.0
Cholestanyl Toluate (C.T.)	172.3-173.0	229.0-230.0
(C.T.) + 1.5wt% (NPMI+I)	168.0-173.0	227.0-229.0
(C.T.) + 1.6wt% (BPMI+I)	167.5-173.5	226.5-228.5
(C.T.) + 1.76wt% (TPMI+I)	168.0-172.3	226.2-227.5
Cholesteryl-4-Chlorobenzoate	166.0-168.0	250.0-253.0
(C.C.B.) + 1.5wt% (NPMI+I)	165.0-168.0	242.0-250.0
(C.C.B.) + 1.6wt% (BPMI+I)	164.0-168.0	242.0-250.0
(C.C.B.) + 1.76wt% (TPMI+I)	164.5-168.0	241.0-249.5
(C.C.B.) + 0.5mol% NPMI	164.5-169.0	244.0-252.5
(C.C.B.) + 0.5mol% BPMI	164.0-168.0	243.0-250.0
(C.C.B.) + 0.5mol% TPMI	164.0-168.5	243.5-251.0

^a measured by thermal microscopy; K=crystal, Ch=cholesteric and I=Isotropic

3.2.2. Cycloaddition Reaction of **1** with N-Arylmaleimides in Liquid Crystalline Solvents

The reaction conditions for the cycloaddition were determined by monitoring the course of the reaction of equimolar amounts of N-phenylmaleimide with cholesta-5,7-dien-3 β -yl acetate (**1**) in benzene (1.5% total weight of reactants) by ¹H N.M.R. and H.P.L.C.. The reaction appears to proceed to ca. 70% completion in 4 hours at 200°C and yields four product peaks by analytical H.P.L.C. (2%

CH₃CN/CH₂Cl₂ as eluant).

The reaction was then performed under identical conditions in the various liquid crystalline and model isotropic solvents. Samples were prepared by doping the liquid crystal with 1 wt% of 1 and an equimolar amount of the enophile. The samples were dissolved in methylene chloride which was then removed by evaporation to ensure complete mixing of all the components. This procedure was used for the preparation of all analytical samples.

The reaction appears to proceed at approximately the same rate in each of the solvents with the possible exception of the smectic mesogen where the reaction appears to be somewhat slower. This may be a reflection of the slower rates of binary diffusion in smectic liquid crystals. Reaction times of two or four hours were used for all the reactions performed at 200°C with the exception of the reactions of N-terphenylmaleimide with 1 in S1544 where reaction times of six and twelve hours were required to obtain approximately the same conversions.

The relative product yields were determined by analytical H.P.L.C. analysis of the crude reaction mixtures. The products were identical to those found in benzene and no new products were observed. Many of the thermolyses were performed for both two and four hours and in all cases, the relative product yields were independent of heating time. Isolated samples of the BPMI/1 adducts were found to be stable at 200°C for extended periods of time (ca. 10 hours).

The relative product yields for the reaction of each enophile with (1) in the various solvents are collected in Tables 3.3.-3.5. (*vide infra*).

Table 3.3.^{a,b,c} Product yields (%); thermolysis of **1** with N-phenylmaleimide.

SOLVENT (PHASE)	ADDUCT				
	N5	N4a	N4b	N3	?
Benzene (isot.)	12.7	36.3	25.3	19.4	6.3
C.B. (isot.)	16.1	32.6	22.9	21.1	7.3
C.P. (isot.)	15.6	34.4	23.8	19.4	6.8
S1409 (isot.)	14.9	33.7	23.9	20.8	6.7
C.C.B. (choles.)	19.5	34.2	19.5	17.9	8.9
C.T. (choles.)	19.7	32.7	21.9	18.2	8.5
S1544 (smectic)	27.8	30.9	17.3	16.7	7.3

^a all reactions were performed at 200°C.

^b all product ratios are the average of 2-4 trials.

^c error in all numbers is $\pm 0.6\%$ (abs. 95% con. lim. see appendix 4)

Table 3.4.^{a,b,c} Product yields (%); thermolysis of 1 with N-biphenylmaleimide.

SOLVENT (PHASE)	ADDUCT			
	B5	B4a	B4b+B3	?
Benzene (isot.)	13.4	32.0	47.5	7.1
C.B. (isot.)	16.9	31.2	42.6	9.4
C.P. (isot.)	15.8	32.2	41.8	10.2
S1409 (isot.)	16.8	31.0	44.1	8.1
C.C.B. (isot.) + 15% chlorobenzne	14.4	30.5	47.7	7.4
C.T. (isot.) + 15% toluene	15.9	30.6	45.1	8.4
C.C.B. (choles.)	32.8	25.1	28.8	13.3
C.T. (choles.)	29.0	26.7	32.2	12.1
S1544 (smectic)	38.4	23.0	29.5	9.1

^a all reactions were performed at 200°C.

^b all product ratios are the average of 2-4 trials

^c error in all numbers is $\pm 0.6\%$ (abs. 95% con. lim. see appendix 4)

Table 3.5.^{a,b,c} Product yields (%); thermolysis of **1** with N-terphenylmaleimide.

SOLVENT (PHASE)	ADDUCT			
	T5	T4a	T4b+T3	?
Benzene (isot.)	14.7	31.5	46.7	7.1
C.B. (isot.)	18.4	27.3	44.7	9.6
C.P. (isot.)	17.3	30.3	44.9	7.5
SI409 (isot.)	18.4	29.6	44.1	7.9
C.C.B. (choles.)	40.3	20.9	23.2	15.6
C.T. (choles.)	36.2	24.3	26.3	13.2
SI544 (smectic)	49.1	13.4	26.4	11.1

^a all reactions were performed at 200°C.

^b all product ratios are the average of 2-4 trials.

^c error in all numbers is $\pm 0.6\%$ (abs. 95% con. lim. see appendix 4)

3.2.3. Relative Activation Parameters for the Reaction of 1 with TPMI in Liquid Crystalline Solvents

The cycloaddition reaction of N-terphenylmaleimide with cholesta-5,7-dien-3 β -yl-acetate was also performed at a number of temperatures between 180°C and 240°C in a cholesteric phase, a smectic phase and two model isotropic liquids. The reaction was performed at six temperatures with at least duplicate runs for each temperature in each of the solvents. The product yields, shown in tables 3.6-3.9, are the average values of these trials. Because the products for the reaction have been found not to interconvert at 200°C and because the relative product yields are unaffected by heating time, we can conclude that the reaction is under kinetic control.

Using these data, treated according to Eyring, plots were constructed as shown in Figures 3.1 and 3.2.. The differences in the activation parameters for the formation of adducts T5 and T4a were compared in a cholesteric solvent (C.C.B.), a smectic solvent (S1544) and two model isotropic solvents (C.B. and S1409).

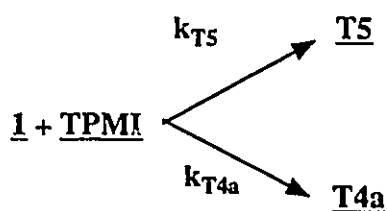
Eyring Equation;

The Eyring equation (Eq. 3.1) was developed from transition state theory in order to describe the relationship between the rate of a reaction and the activation parameters.

$$k = kT/h (c^\ominus)^{\Delta V} \exp(-\Delta H^*/RT) \exp(\Delta S^*/R) \quad (\text{Eq. 3.1.})$$

Where k is the rate constant, k is the Boltzman constant, h is Planck's constant, T is the Kelvin temperature, c° is the standard concentration (1 mol/L) and Δv is the net increase in the stoichiometric coefficients of the reaction. (for the bimolecular reactions studied, $\Delta v = -1$)

For the competing bimolecular reactions to form T5 and T4a,



the respective Eyring equations are;

$$k_{T5} = kT/h \exp(-\Delta H^*_{T5}/RT) \exp(\Delta S^*_{T5}/R) \text{ (M}^{-1}\text{s}^{-1}\text{)} \quad (\text{Eq. 3.2.})$$

$$k_{T4a} = kT/h \exp(-\Delta H^*_{T4a}/RT) \exp(\Delta S^*_{T4a}/R) \text{ (M}^{-1}\text{s}^{-1}\text{)} \quad (\text{Eq. 3.3.})$$

dividing Eq. 3.2. by Eq. 3.3.;

$$\ln(k_{T5}/k_{T4a}) = (\Delta\Delta H^*)/RT + (\Delta\Delta S^*)/R \quad (\text{Eq. 3.4.})$$

In spite of the fact that the regiochemical control of reactivity is apparently larger in the smectic solvent than in the cholesteric solvents, (Tables 3.3-3.5), the change in the activation parameters is larger in the latter. This will be considered in some detail in the discussion.

Tables 3.6., 3.7.^{a,b} Product yields (%); reaction of 1 with N-terphenylmaleimide at various temperatures between 180 and 240 °C.

Solvent; Cholestanyl Benzoate (C.B.); Isotropic Liquid;

TEMPERATURE (°C)	ADDUCT			
	T5	T4a	T4b+T3	?
180	19.3	27.3	44.3	9.0
200	18.4	27.3	44.7	9.6
210	20.3	29.3	41.2	9.2
220	20.4	29.5	39.9	10.2
230	21.5	31.5	35.4	11.6
240	22.0	31.3	34.3	12.4

Solvent; Cholesteryl-4-chlorobenzoate (C.C.B.); Cholesteric Liquid Crystal

TEMPERATURE (°C)	ADDUCT			
	T5	T4a	T4b+T3	?
180	47.1	19.0	20.2	13.6
200	40.3	20.9	23.3	15.5
210	39.7	20.6	26.1	13.6
220	37.3	23.0	24.4	15.3
230	35.8	24.8	24.0	15.4
240	29.6	25.6	32.1	12.7

^a all product ratios are the average of several trials

^b error in all numbers is $\pm 0.6\%$ (abs. 95% con. lim. see Appendix 4)

Tables 3.8., 3.9.^{a,b} Product yields (%); reaction of 1 with N-terphenylmaleimide at various temperatures between 180 and 240 °C.

Solvent; S1409; Isotropic Liquid

TEMPERATURE (°C)	ADDUCT			
	T5	T4a	T4b+T3	?
180	18.8	28.7	44.8	7.7
200	18.4	29.6	44.1	7.9
210	19.0	30.2	42.1	8.7
220	20.2	31.2	39.4	9.2
230	20.0	31.5	37.3	11.2
240	19.5	32.6	37.3	10.6

Solvent; S1544; Smectic Liquid Crystal

TEMPERATURE (°C)	ADDUCT			
	T5	T4a	T4b+T3	?
180	47.0	11.7	28.2	13.1
200	49.1	13.4	26.4	11.1
210	50.6	15.3	22.5	11.6
220	51.1	14.9	17.3	16.7
230	56.2	15.7	12.0	16.1
240	53.9	17.2	11.6	17.3

^a all product ratios are the average of several trials

^b error in all numbers is $\pm 0.6\%$ (abs. 95% con. lim. see Appendix 4)

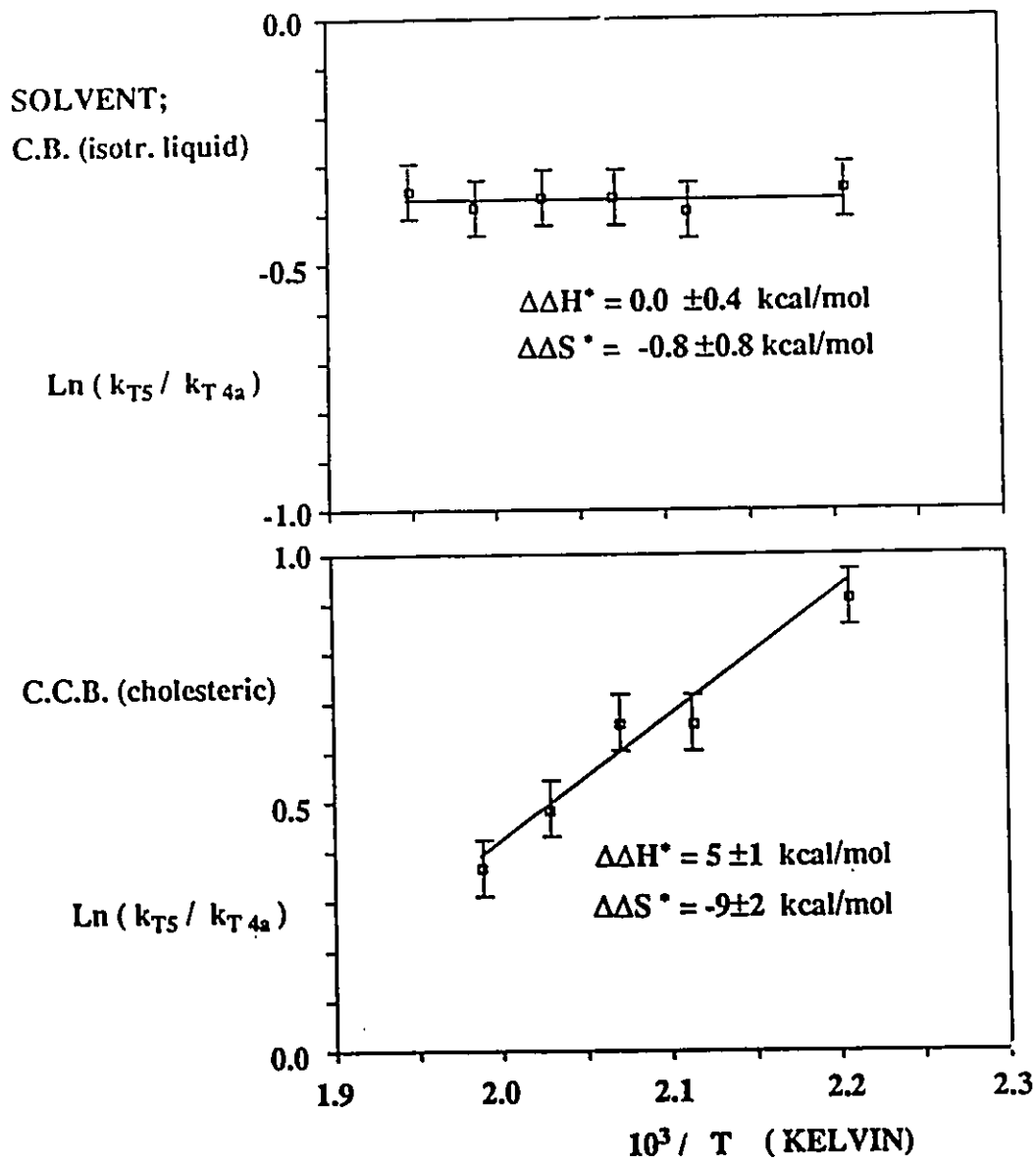


FIGURE 3.1. Eyring Plot^{a,b}; reaction of 1 with TPMI in C.B. and C.C.B.

^a the ratios of k_{T5}/k_{T4a} were determined using the product ratios at each temperature from Tables 3.6-3.9.

^b see Appendix 4 for error analysis

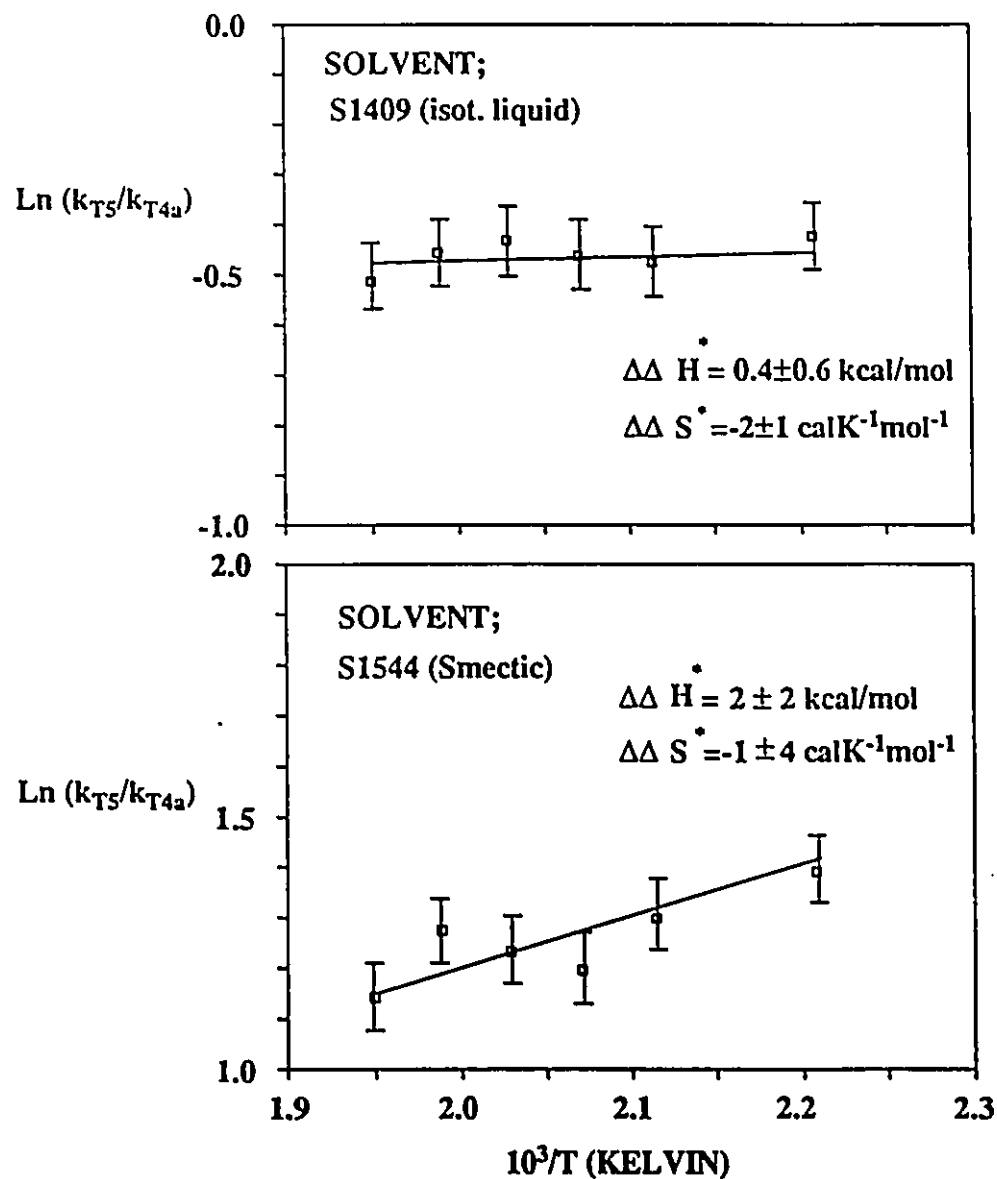


FIGURE 3.2. Eyring Plot^{a,b}; reaction of 1 with TPMI in S1409 and S1544

^a the ratios of k_{T5}/k_{T4a} were determined using the product ratios at each temperature from Tables 3.6-3.9.

^b see Appendix 4 for error analysis

3.3. Discussion: Reaction of 1 with N-Arylmaleimides in Liquid Crystalline Solvents

The remainder of this chapter deals with a discussion of our results. Most studies using liquid crystalline solvents have been aimed at better defining the extent to which chemical reactivity may be altered. It would be a good idea to also have some concept as to how large an effect may be expected. Consequently this section begins with a qualitative discussion of how the orientational ordering of the reactants may influence chemical reactivity, followed by an outline of the theoretical work available that may help us estimate how large the influence of liquid crystalline order might be on reaction energetics. The results for our work using cholesteric phases will then be rationalized in terms of how much of an effect may be expected and how this is influenced by enophile structure. A discussion of the regiochemical control of reactivity using the smectic mesogen will complete the chapter.

3.3.1. General; The Influence of Orientational Order on Chemical Reactivity - How Much Can We Expect?

Let us first consider, in a qualitative manner, how liquid crystalline order might be expected to influence a bimolecular reaction. In a system where the reactants are well oriented within the solvent matrix, intermolecular collisions will be biased towards those where the reactive moieties are parallel to one another. For a diffusion controlled reaction, the influence of liquid crystalline order will depend strictly on orientational factors. The orientation of the reactants on first collision will dictate the mode of reaction. Products favoured by solute orientations similar to those in the ordered medium should be favoured. For a reaction that is not diffusion controlled,

product formation will only occur after many reactant collisions within the solvent cage. Only when reactant orientation is correct and the energy of the collision exceeds the activation energy will reaction occur. Reactant orientations that are not compatible with the orientational order of the liquid crystalline solvents will require additional energy to disrupt the local solvation shell. In this case, the ordered medium will influence reactivity by altering the energetics of the possible reactive pathways.

The free energy of activation (ΔG^*) for a reaction in an ordered solvent will be influenced by both enthalpic and entropic factors ($\Delta G^* = \Delta H^* - T\Delta S^*$). A reaction that is grossly incompatible with liquid crystalline order will have a correspondingly higher enthalpy of activation (compared to that in an isotropic medium) due to the additional energy required to disrupt solvent order on transition state formation. The entropy term however would be expected to favour the increased disorder in the system. In contrast, a reaction requiring a parallel orientation of the reactants in the transition state may in fact be stabilized by the oriented environment, lowering the enthalpy of activation. Entropy factors would however impede such a pathway.

Most of the investigations involving chemical reactivity in liquid crystals have been reported in terms of how orientational order may influence reaction energetics. However, there has been little speculation as to what the maximum influence of liquid crystalline order on reaction energetics might be.

Theoretical treatments of the liquid crystalline phase are being developed using statistical mechanical models.^{9a,b,91} These models, describing the interactions between molecules in a liquid crystalline lattice, may be helpful in understanding how liquid crystalline solvents may influence the reaction energetics of dissolved solutes.

The molecular-statistical theory that describes liquid crystals, known as the continuum theory was introduced almost 70 years ago by C.W. Oseen.^{9b,91} This theory treats the liquid crystalline state as an anisotropic, elastic medium with unique

symmetry, viscosity and elastic properties. The most comprehensive review of this theory and of the physics of liquid crystals is that of de Gennes.⁹¹ The physical theories of liquid crystals are very complicated and by no means complete. Exact solutions to even the very simple models have not yet been worked out. The theories do however provide mathematical expressions describing the interactions between mesogenic molecules. These equations may in fact be helpful in explaining our results.

The most complete mathematical descriptions have been developed for the nematic and cholesteric phases. The only difference between these models is that recent investigators have introduced higher order terms in hopes of describing the macroscopic pitch associated with cholesteric solvents.^{91,9b} For our intents and purposes, the mathematical descriptions for the nematic phase, developed by Maier and Saupe can be applied to our cholesteric solvents.

Maier and Saupe used the continuum theory to consider the interactive forces between liquid crystalline molecules. They ultimately developed the concept of an "energy of order", E_o (Equation 3.5.).^{9b,92-95}

$$E_o = -A/V^2 [1/2(3\cos^2\Theta_L - 1)][1/2(3\cos^2\Theta_S - 1)] \quad (\text{Eq. 3.5.})$$

What this equation describes is the order-induced interaction energy, E_o , for a molecule "L" within a nematic environment, where A is a lattice constant describing the dipolar interaction between the solvent molecules, V is the molar volume of the solvent and the $[1/2(3\cos^2\Theta - 1)]$ terms are the order parameters for "central molecule", L and for the solvent molecules, S respectively.

The first term ($-A/V^2$) is actually a simplification of a double sum describing the order induced Coulombic interaction between the central molecule L and its environment. The second and third terms are order parameters which are used as a

description of the degree of parallelism within a given system.^{9,92-94,96,97} The angle Θ is defined as the angle between the long axis of a molecule and the orientational direction of the environment. An order parameter of 1 corresponds to perfect alignment within a system while an order parameter of 0 describes an isotropic environment. For solutes dissolved in liquid crystalline phases, order parameter measurements provide an indication of the average orientation within the system. For a well oriented solute, the order parameter will be similar to that of the solvent itself while for a poorly oriented sample the order parameter may approach 0. Experimental techniques used to calculate the order parameters for solutes dissolved in liquid crystalline solvents include N.M.R,⁹⁷⁻⁹⁹ E.S.R,¹⁰⁰ absorption dichroism¹⁰¹ and fluorescence depolarization.^{102,103}

The energy of order can be used to describe the orientational energy associated with a solute molecule L in a nematic liquid crystal. That is, it represents the energy required by molecule L to completely disrupt its orientation within the nematic environment. To our knowledge, solutions to this equation have not yet been calculated, although de Gennes has estimated that the typical interaction energy of a nematic molecule with its neighbours should be ca. 2-3 kcal/mol.⁹¹ Assuming that this is correct, it is expected that the influence of nematic or cholesteric order on the activation energy for a given reaction should not exceed ca. 2-3 kcal/mol.

While quantitative solutions to the energy of order equation do not exist, it does illustrate that the energy of order for a solute molecule will be proportional to its order parameter. If a solute has an order parameter similar to that of the liquid crystal, the energy of order would then be close to that of the solvent itself. Solute molecules which are less well-oriented will have an energy of order that is correspondingly less than that for the mesogen.

For a transition state that is particularly disruptive to matrix order, energy

would be required to rotate the reactant(s) into the required geometry. Relative to the reaction in an isotropic liquid, an increase in the enthalpy of activation would be expected, the magnitude of which would depend on the degree of solvent disruption required to form the transition state. The maximum increase in the activation barrier will occur when the orientational order must be completely disrupted on transition state formation. This energy should correspond to the energy of order (E_o) for the solute. If, on the other hand, the reaction involves a transition state that is favourably oriented with respect to the mesogenic solvent, the transition state may be energetically more favourable than in an isotropic medium. The result would be an order induced enhancement of the rate of reaction. While, in principle, this activation energy decrease should have a maximum value corresponding to the energy of order, the actual effect will depend on the degree of interaction between the transition state and the solvent.

Theory concerning the entropy effect of reactions in liquid crystalline solvents is somewhat less well-defined. The differences in the entropy of activation, for a reaction in a liquid crystalline phase compared to an isotropic phase can be described by Equation 3.6,^{91,104} where S^*_I , S^*_N , S^A_I , S^A_N , S^B_I , and S^B_N are the entropies for the transition state, reactant A and reactant B in the isotropic and nematic phases respectively.

$$\Delta S^*_I - \Delta S^*_N = (S^*_I - S^*_N) - (S^A_I - S^A_N) - (S^B_I - S^B_N) \quad (\text{Eq. 3.6.})$$

From the continuum theory, equation 3.6 transforms into equation 3.7¹⁰⁴ where $f^*(\Theta)$, $f^A(\Theta)$, $f^B(\Theta)$ are the angular distribution functions for the long axes of each species and each integral describes the probability of finding a molecule within a

small solid angle, $d\Omega$.

$$\Delta S^*_T - \Delta S^*_N = R \int f^*(\Theta) \ln(4\pi f^*(\Theta)) d\Omega - R \int f^A(\Theta) \ln(4\pi f^A(\Theta)) d\Omega - R \int f^B(\Theta) \ln(4\pi f^B(\Theta)) d\Omega \quad (\text{Eq. 3.7.})$$

The point of this description is to illustrate that because $f(\Theta)$ is directly related to the order parameter,⁹¹ the entropy change on reaction is related to how well each of the species are oriented within the liquid crystalline solvent. However, this description is not of any quantitative use when describing entropy changes associated with chemical reactions in liquid crystals. While this equation accounts for the entropies of all the reactive species, it does not account for the entropic influences associated with solvent disruption on chemical reaction. It has been pointed out by Sergeev that the entropic influence of the solvent may in fact be larger than the entropy effects of the reaction itself and as a result, the overall increase or decrease in entropy in an ordered medium will depend on the interactions between both the solute and the solvent.¹⁰⁴ To our knowledge, no other theoretical work has been carried out to quantify how liquid crystalline order might influence entropies of activation for the chemical reactions of solutes.

The molecular statistical theory of liquid crystalline behaviour may be very useful in discussing the results of our work. While the quantitative aspects of the energy of order have not been utilized greatly, the mathematical equations can be used to describe how the order parameter for the solutes may influence the energetics of reactions in mesogenic solvents.

In the remainder of this chapter, the results of our work will be discussed. The first point that will be addressed is the Eyring data for the reaction of N-terphenylmaleimide (TPMI) with 1 in cholesteric solvents. The differences in the

activation parameters for two of the reaction products have been compared in a cholesteric and an isotropic solvent. The results will be discussed in terms of how the reaction energetics may be influenced by the average orientation of the reactants and their environment. The results for the three enophiles will then be compared and rationalized in terms of how the orientational constraints imposed on each may influence regiochemical control. A discussion of the results found using smectic solvents will conclude this chapter.

3.3.2. Reaction of 1 with N-Arylmaleimides in Cholesteric Solvents

Comparing the relative yields of the reaction products in isotropic and cholesteric liquid crystalline solvents, (Figure 3.3.) it can be seen that in ordered media, the percentage yield of adduct 5 increases at the expense of the other cycloadducts. We explain this result in terms of how the liquid crystalline solvent influences the free energy of activation (ΔG^\ddagger). Because the products for the reaction have been found not to interconvert at 200°C and because the relative product yields are unaffected by heating time, we can conclude that the reaction is under kinetic control. Consequently, the relative product yields will be proportional to the free energies of activation for the respective pathways. In cholesteric solvents, the free energy of activation for product 5 is stabilized relative to those for the other cycloaddition products.

This result indicates that the influence of ordered solvents on the relative yields of products is dominated by the enthalpy factor. The enhanced adduct, 5 requires a parallel orientation of the reactants in the transition state while the other three adducts require a more perpendicular reactant orientation. From our earlier discussion it is obvious that in ordered media, enthalpic factors would favour the formation of the transition state to adduct 5 while entropic factors would favour the

products that are more disruptive to solvent order. For this reason, we will discuss our

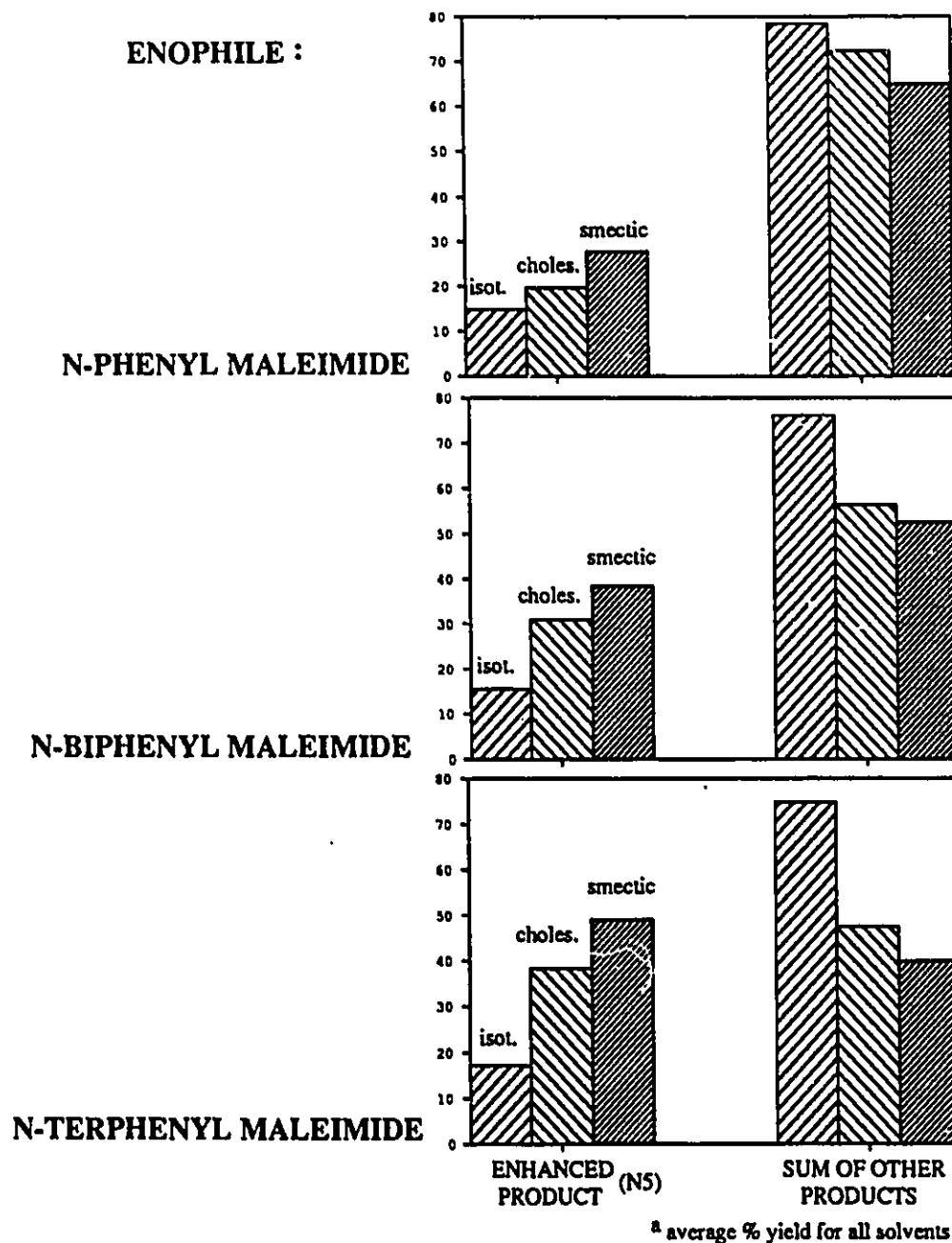


FIGURE 3.3. Percent yield of products for each enophile in isotropic, cholesteric and smectic solvents

results in terms of how the enthalpy of activation for the possible reactive pathways will be influenced by the average orientation of the reactants. The entropic term will be treated as an influence that may truncate the degree of regiochemical control.

3.3.3. Relative Activation Parameters for the Reaction of **1** with **TPMI** in Cholesteric Liquid Crystalline Solvents

While it is true that in cholesteric solvents, the formation of adduct **5** is enhanced relative to the other products, this result tells us nothing about the magnitudes to which ΔH^* and ΔS^* are influenced. In fact, because these parameters will have a counteractive effect on the free energy term, very large changes in both the enthalpic and entropic terms may only result in small overall changes in ΔG^* .

In order to delineate how the ordered solvent actually influences the activation parameters, temperature studies were used to construct the Eyring plots shown previously. We chose to investigate the reaction of N-terphenylmaleimide with **1** because this system showed the largest influence of ordered media on the relative product yields (Table 3.5). In cholesteric solvents, the yield of the enhanced adduct (**T5**) is over twice that found in the model isotropic medium. The differences in the activation parameters for the formation of adducts **T5** and **T4a** were compared in cholesteric (**C.C.B.**) and isotropic (**C.B.**) solvents (Fig. 3.1.).

In the model isotropic solvent, $\Delta\Delta H^*$ ($\Delta H^*_{T4a} - \Delta H^*_{T5}$) is negligible (0.0 ± 0.4 kcal/mol). In the cholesteric phase, $\Delta\Delta H^*$ increases to 5 ± 1 kcal/mol. We attribute this change in $\Delta\Delta H^*$ in the cholesteric solvent to be a result of the orientational order destabilizing the pathway to adduct **T4a** while stabilizing the pathway to **T5**.

The change in $\Delta\Delta H^*$ between these two solvents is very large. The

maximum influence of cholesteric order on a given reaction should be dictated by the energy of order, E_o as defined by Maier and Saupe. For solute molecules, the energy of order will depend on its order parameter. The largest energy of order expected for a solute will be around 2-3 kcal/mol which corresponds to a situation where the solute is oriented as well as a solvent molecule.

Let us consider this reaction in terms of the energy of order concept.

Because the steroidal diene used is very similar in structure to the cholesteric solvents, we expect it to be incorporated relatively well within the cholesteric mesophases. The differences in the enthalpies of reaction for the reactive pathways can therefore be approximated in terms of how much energy is required to rotate the enophile into the reactive orientation. To form adduct **T4a**, the enophile must adopt a conformation that is approximately perpendicular to the steroidal diene. Such an orientation would be grossly disruptive to the average orientation of the solvation shell and as a result, the energy of order associated with the enophile must be severely affected. To form adduct **T5**, the reactive moieties must approach in an orientation that is much more compatible with solvent order. If the reactive geometry is favourable, the transition state may be enhanced relative to that in isotropic media. The magnitude of this stabilization will depend on the interaction between the transition state and the solvent.

The larger $\Delta\Delta H^*$ value in **C.C.B.** represents the sum of the energy increase required to form the transition state to **T4a** and the energy decrease caused by the stabilization of the transition state to form **T5**. For a difference in the $\Delta\Delta H^*$ values of ca. 5 kcal/mol, the pathway to **T4a** must be destabilized by close to 2-3 kcal/mol while the transition state to **T5** must be stabilized by about the same amount. These changes in the activation enthalpies are close to the energies of order expected for the neat liquid crystal samples themselves. Consequently, it appears that N-terphenylmaleimide must be oriented very well within the cholesteric matrix.

From this result it is clear that the order parameter for TPMI in C.C.B. must be very similar to that of the mesogen itself and that the transition state orientations required for the respective pathways must represent the extremes in compatibility with the average orientation of the system. While the order parameter of C.C.B. itself has not been published, those for many other cholesteric liquid crystals have; they are all remarkably similar and have about the same temperature dependence.¹⁰⁷ Order parameters for cholesteric phases vary non-linearly with temperature from ca. 0.5 at the lower end of the temperature range to about 0.3 close to the Ch-I transition temperature. Because C.C.B. is in the lower end of its cholesteric temperature range at 200°C, an order parameter of ca. 0.45-0.50 should be a good estimate. In light of the large influence of cholesteric order on the enthalpies of activation, the order parameter of TPMI in the cholesteric phase must be very similar to that of C.C.B.

In general, the criterion for choosing a solute that should be well oriented within a liquid crystal has been to match the molecular structures as closely as possible.^{9b,9c,26-34} While this has been shown to be a very important factor in solute/solvent compatibility, our results suggest that TPMI experiences an average orientation in C.C.B. that is similar to that of a solvent molecule itself in spite of their rather dissimilar shapes. The reason that the average orientation of this enophile is very close to that of the mesogen itself may be a consequence of the fluid-like nature of the cholesteric phase. It is possible that the more fluid mesogens (cholesterics and nematics) may be better able to conform to solutes with structures which are not strictly similar to the mesogen itself. While the N-terphenylmaleimide molecule is not a structural mimic of the steroids, it has a rod-like shape which is apparently well oriented within the cholesteric solvent.

The large enthalpy effect indicates that the reactants are oriented very well within the solvent and the reactive pathways must represent extremes in transition state

compatibility. Consequently, the entropy effects must also be about as large as can be expected. In C.C.B., $\Delta\Delta S^*$ ($\Delta S_5^* - \Delta S_4^*$) is ca. 9 entropy units more negative than in C.B.. This illustrates that in the cholesteric phase, the transition state to T4a is more disruptive to solvent order than is the transition state to adduct T5.

While the influence of liquid crystalline order on the activation parameters appears very large, the overall influence this has on $\Delta\Delta G^*$ is relatively small. At 200°C, the entropy term has a significant effect on the differences in the free energies of activation for the two pathways ($\Delta\Delta G^* = \Delta\Delta H^* - T\Delta\Delta S^*$). While the difference between $\Delta\Delta H^*$ in the cholesteric and the isotropic phases is 5 ± 1 kcal/mol, the entropy change (9 ± 2 e.u.) reduces the difference in $\Delta\Delta G^*$ to 1 ± 1 kcal/mol. Although the activation parameters are greatly affected by the cholesteric solvent, the differences in the product yields only reflect the much smaller change in the free energies of activation.

3.3.4. Structural Studies: The Influence of Enophile Length on the Control of Chemical Reactivity Cholesteric Solvents

We have seen above that reaction energetics are influenced dramatically for the reaction of 1 with TPMI and from these results we have concluded that the order parameter for this enophile in the cholesteric phase must be very close to that of the mesogen itself.

Comparing the results for each maleimide, it can be seen that the number of phenyl groups on the enophile dramatically influences the control of reactivity. Figure 3.4 shows the percentage yield ratios of adduct 5 to adduct 4a as a function of the number of phenyl groups in the two liquid crystalline solvents and a model isotropic solvent (C.B.). (thermolyses at 200°C) The results found using the smectic solvents

will be discussed later.

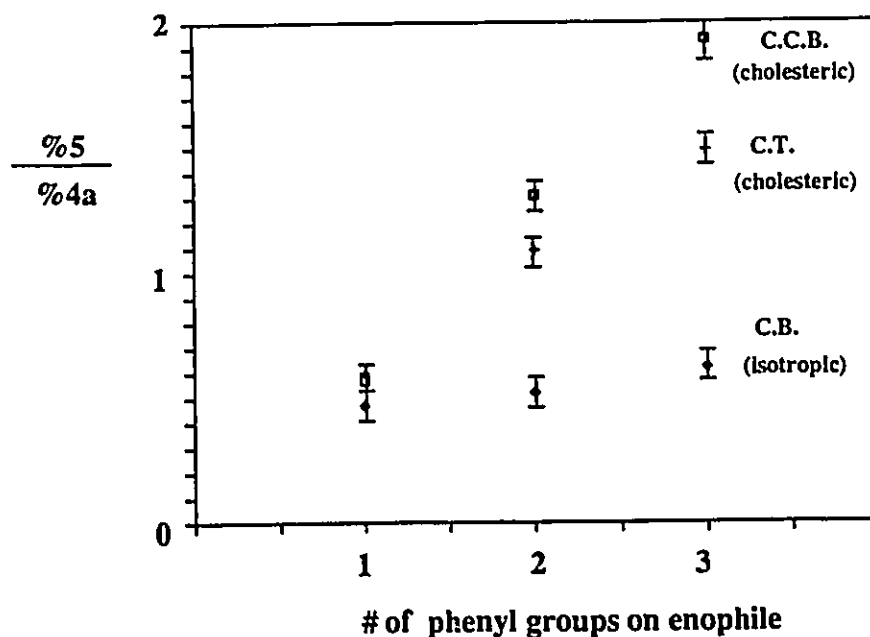


Figure 3.4. Ratio of %5/%4a in cholesteric and isotropic solvents vs number of phenyl groups on enophile

Before discussing the effect of the solvents themselves we will consider how in general the length of the enophile influences the degree of regiochemical control. From the product yields given above, it is obvious that the control of reactivity decreases as the length of the enophile decreases. We will discuss these results in terms of how well-oriented we expect each of the enophiles to be in the cholesteric solvents and how this will influence the activation parameters in each case.

Under kinetic control, the relative product yields will reflect the differences in the free energies of activation for each pathway. From the product ratios in Tables 3.3, 3.4 and 3.5, $\Delta\Delta G^*$ values have been calculated for each enophile in C.C.B. and C.B. using the equation $\ln(k_{T5}/k_{T4a}) = \Delta\Delta G^*/RT$ (Table 3.10.). The purpose for doing this is to give us some idea of how enophile length influences the energetics of the reaction.

TABLE 3.10. ($\Delta G^*_{4a} - \Delta G^*_5$ (kcal/mol)) for the reaction of **1** with each enophile in **C.C.B.** and **C.B.**

	Solvent		
	<u>C.C.B.</u>	<u>C.B.</u>	Difference
N-phenylmaleimide	-0.53±0.04	-0.67±0.04	0.1±0.1
N-biphenylmaleimide	0.25±0.03	-0.58±0.04	0.8±0.1
N-terphenylmaleimide	0.62±0.03	-0.40±0.04	1.0±0.1

For the reaction of **1** with **TPMI**, we see that the difference in the free energy change between the isotropic and the cholesteric phases is 1 ± 0.1 kcal/mol. In contrast, the difference in the free energy change for the reaction with **NPMI** as the enophile is only 0.1 ± 0.1 kcal/mol. It is obvious that with the shorter enophile the influence of cholesteric order on reactivity is substantially reduced. We attribute this effect to be the result of a much smaller order parameter for N-phenylmaleimide in the cholesteric phase. From the differences in the free energies of activation it is estimated that the order parameter for **NPMI** in **C.C.B.** is less than 0.2, (i.e. less than 1/2 that for **TPMI** in **C.C.B.**).

While the order parameter for N-phenylmaleimide in cholesteric **C.C.B.** has not been determined, an order parameter of 0.15 has been published for N-phenylmaleimide in nematic p-methoxybenzylidene-p-n-butylaniline (**MBBA**)¹⁰⁸. It is reasonable to expect that **NPMI** may be better oriented in **MBBA** than in a steroidal solvent and consequently, we estimate that the order parameter of **NPMI** in **C.C.B.** will be roughly 0.10-0.15. This value is about 1/5 of that which was estimated for **TPMI** in **C.C.B.** (ca. 0.45-0.50). Qualitatively it is easy to see that because N-phenylmaleimide is much less well oriented, the influence of liquid crystalline order is dramatically less. While it is rather tenuous to make any quantitative conclusions based on these estimates, we can say that based on the approximate order parameters, the energy of order (E_o) of N-phenylmaleimide in **C.C.B.** will be about 1/5 of that for

N-Terphenylmaleimide. If we assume that the entropy effect will be truncated by a similar amount, then we can speculate that for N-phenylmaleimide, the influence of cholesteric order on the free energy difference should be about 5 times smaller than that for N-terphenylmaleimide. Comparing the differences in the $\Delta\Delta G^*$ values for NPMI and TPMI, (0.1 ± 0.1 and 1.0 ± 0.1 kcal/mol respectively), we can at least say that the results are consistent with the order parameter approximations.

The results for the intermediate length enophile, BPMI are quite interesting. It is evident from figure 3.4 and from table 3.10 that the regiochemical control found using this reactant is much closer to that of TPMI than that of NPMI. The estimated difference in $\Delta\Delta G^*$ between the cholesteric and isotropic solvents for the reaction of N-biphenylmaleimide with 1 (0.8 ± 0.2 kcal/mol) is not remarkably different from the value found using N-terphenylmaleimide as enophile (1.0 ± 0.2 kcal/mol). The two longer enophiles appear to be much better oriented than NPMI, as reflected by the greater degree of regiochemical control.

As mentioned in the results section, the transition temperatures for the reactant-doped cholesteric samples do not vary significantly with the structure of the enophile used. Transition temperature depression is generally used as a reflection of the degree of disruption that a solute imposes upon a liquid crystalline solvent.⁸ We had anticipated that the longer enophiles should be somewhat more disruptive to cholesteric order. The transition temperature data suggests that this is not the case. As well, the activation parameter results indicate that N-terphenylmaleimide is oriented very well within the liquid crystal and consequently should not be significantly disruptive to solvent order. A possible explanation for the small variation in transition temperature depression is that solvent disruption must be due predominantly to the maleimide portion of the enophiles while the aryl chain is acting primarily as an "anchor" that assists solute ordering. As a result, each enophile might impose about the

same degree of solvent disruption while the length of the aryl chain may influence how well the average orientation of the molecule is controlled in the mesogen.

One noteworthy feature not yet discussed is that the degree of regiochemical control in the two cholesteric phases differ. With the shortest enophile, the T5/T4a product ratio is about the same in both cholesteryl-4-chlorobenzoate and cholestanyl toluate. With the longer enophiles, there is a trend toward greater regiochemical control in C.C.B. than in C.T. This result is consistent with the differing order parameters for the two cholesteric solvents at 200°C.

It is known that the density, viscosity and order parameters for liquid crystalline solvents vary over the mesogenic temperature range.^{79,80} At lower temperatures, liquid crystalline phases are more rigidly ordered than they are at higher temperatures. At 200°C, C.C.B. and C.T. are in the lower and middle regions of their cholesteric temperature ranges respectively. Consequently, we expect that C.C.B. will be somewhat more rigid at this temperature than will be its counterpart. As we mentioned above, order parameters for cholesterics only vary by a small amount over the bulk of their liquid crystalline temperature range. The differences between the order parameters for these two mesogens at 200°C is going to be quite small. From the published data we estimate an order parameter for C.C.B. at 200°C of ca. 0.45-0.50 and for C.T. ca. 0.40-0.45.¹⁰⁷

The influence that this small order parameter difference has on reactivity depends on the enophile used. For NPMI, we have determined that the average orientation within the cholesteric solvents is rather poor. Consequently, the rather small differences in the order parameters for the cholesteric solvents have little effect on the reaction energetics. The longer enophiles however are much better oriented, within the cholesteric media. In these cases the order parameters of the solvents themselves now become more important in influencing how well the longer enophiles are oriented in

each solvent. The trend toward better regiochemical control in C.C.B. than in C.T. is consistent with the fact that the former should have a more rigid matrix at 200°C and should consequently result in a better average orientation of the reactants.

3.3.5. Reaction of 1 with N-Arylmaleimides in Smectic Liquid Crystalline Solvents

The results found for the smectic liquid crystalline solvent will now be discussed. Recent results have indicated that reactant solubilization in smectic phases is not always straightforward. There is growing evidence to suggest that even low concentrations of reactants in smectic mesogens may result in heterogeneous phase behaviour.^{8,60-62,81} Our results also suggest the possibility that the reactants may not be incorporated homogeneously within the smectic liquid crystal. Because of this complication, our results using the smectic liquid crystalline solvent S1544 will be presented now along with thermal microscopy results which suggest a heterogeneous reactant solubilization.

From Tables 3.3.-3.5. and from Figure 3.3., it is obvious that the largest influence of liquid crystalline order on the regiochemical control of this cycloaddition occurs when using the smectic B solvent, S1544. From Figure 3.3., the ratio of $\%(\text{5})/\%(4\text{a}+4\text{b}+3)$ is consistently larger for the smectic mesogen than for the other solvents.

This can be explained qualitatively in terms of the average orientation associated with the smectic mesophase. The order parameters for smectic mesogens are greater than those for cholesterics. Highly ordered smectic phases (such as smectic B) have order parameters typically around 0.9 while the less ordered phases (Smectic A or C) have order parameters of *ca.* 0.6-0.8.^{10,94,109,110} As a result, solute molecules

oriented homogeneously within a smectic matrix may be more highly ordered than they would be in cholesteric solvents. The energy of order would be higher and a greater influence on the activation parameters may be expected.

Quantitatively, our results in the smectic phase are more difficult to discuss. It is very difficult to speculate on how great an influence smectic phases may have on reaction energetics. From the thermodynamic studies of phase transitions and from order parameter data, we know that smectic phases are much more ordered than cholesteric or nematic phases. Consequently, it has been generally accepted that smectic phases should have the highest potential for orienting reactants and altering reactivity.

3.3.6. Relative Activation Parameters for the Reaction of **1** with N-Terphenylmaleimide in a Smectic Liquid Crystalline Solvent

In order to get a better idea of how smectic order influences reaction energetics, the differences in the free energies of activation for formation of **T5** and **T4a** in the smectic B phase and its model isotropic solvent were calculated (data in tables 3.3, 3.4 and 3.5) and are collected below.

TABLE 3.11. ($\Delta G^*_{4a} - \Delta G^*_5$ (kcal/mol)) for the reaction of **1** with each enophile in **S1544** (smectic B) and **S1409** (isotropic liquid)

	<u>S1544</u>	Solvent	<u>S1409</u>	Difference
N-phenylmaleimide	-0.10±0.03		-0.77±0.04	0.7±0.1
N-biphenylmaleimide	0.48±0.03		-0.57±0.04	1.1±0.1
N-terphenylmaleimide	1.22±0.05		-0.45±0.03	1.7±0.1

Comparing these results to those in the cholesteric mesogen (Table 3.10.), it is clear that the free energies of activation are influenced more dramatically in the smectic environment. The greater order of the smectic phase apparently results in larger differences in the free energies of activation.

The variable temperature study data for the reaction of 1 with N-terphenylmaleimide show some interesting results (Tables 3.8. and 3.9.). There is negligible influence of reaction temperature on the yield of adduct T5 in the model isotropic solvent, S1409. However, in the smectic solvent, S1544, the yield of adduct T5 increases with increasing reaction temperature. This suggests that with increasing temperature, the reactants are becoming better oriented and the regiochemical control of the reaction increases. This result is opposite to that observed in the cholesteric phases and indicates that there must be fundamental differences in the solubilization of the reactants in these two types of mesogens.

As well, the Eyring data indicates a fundamental difference in reactant solubilization within the smectic phase. Differences in the activation parameters for the formation of adducts T5 and T4a were calculated in smectic S1544 and isotropic S1409. In the isotropic solvent, S1409, the calculated values for $\Delta\Delta H^*$ and $\Delta\Delta S^*$ (figure 3.2) are very small and are identical (within experimental error) to those found for the model isotropic solvent C.B. .

However, for the reaction in S1544, the differences in the activation parameters ($\Delta\Delta H^* = 2 \pm 2$ kcal/mol and $\Delta\Delta S^* = -1 \pm 4$ e.u.) are *less* than those found in the cholesteric medium. This result is certainly unexpected on the basis of the results at 200°C alone.

We believe that the rather unexpected differences in the activation parameters may be due to heterogeneous solubilization of the reactants in the smectic phase. The differences in the activation parameters in S1544 may be a reflection of

changes in the composition of the mixture, as a function of temperature, superimposed on the thermodynamics of the reaction itself.

3.3.7. Heterogeneous Solubilization of Reactants in Smectic Liquid Crystalline Solvents

There is growing precedence for phase separation in solute-doped smectic liquid crystalline solvents.^{8,60-62,81} In Chapter 1, the work of Samori was described in which the bimolecular isomerization of two sulfonate esters was studied in a number of smectic mesogens. Using thermal microscopy and D.S.C., Samori concluded that the complicated kinetic behaviour of this system was the result of heterogeneous solubilization of the reactants in the smectic mesogen. We have observed very similar behaviour for the solubilization of a number of ketone solutes in the smectic phase of **CCH-4** (vide supra). These results will be briefly described here in order to compare it with the results for our cycloaddition reaction.

Using differential scanning calorimetry (D.S.C.), thermal microscopy (T.M.) and ²H N.M.R., it has been found that at concentrations greater than the solubility limit (typically ca. 1 mol%), the solute molecules exist not only in a smectic environment, but also in a ketone rich nematic phase. The proportions and concentrations of the solute in these two phases are temperature dependent.

For example, the phase diagram for binary mixtures of *p*-methoxy- β -phenylpropiophenone (**11**) (0-30 mol %) in **CCH-4** was constructed using D.S.C., thermal microscopy and ²H N.M.R and is shown below.

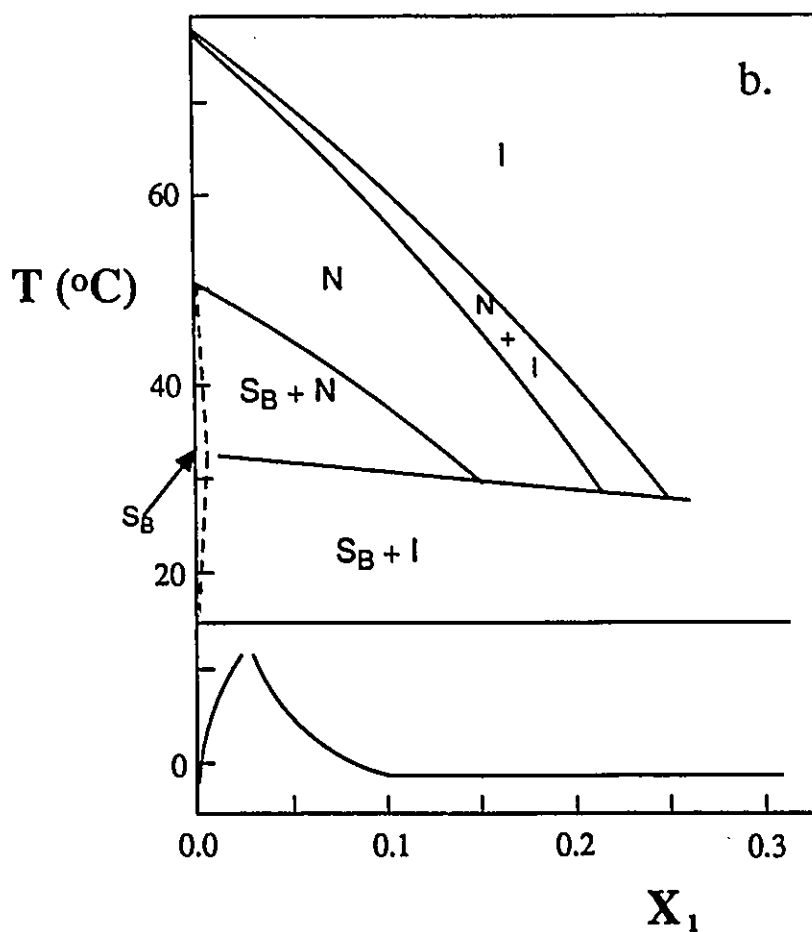


FIGURE 3.5.^a Phase diagram for p-methoxy- β -phenylpropiphenone in CCH-4 (0-30 mol%) from reference 39.

I, Isotropic; N, Nematic; S, Smectic;

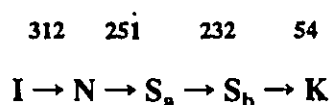
It can be seen from the phase diagram that even relatively small amounts of solute induce the formation of a heterogeneous mixture of two phases ($S_B + N$).

In the biphasic region of the phase diagram, the proportions and relative concentrations of the phases are temperature dependent. For example, a 2.5 mol% sample of the ketone in CCH-4 undergoes a nematic to ($S_B + N$) phase transition at ca. 46°C. On cooling through the biphasic region, the proportion of the smectic phase increases while that of the nematic phase decreases. As well, the concentrations of the ketone in each phase are continuously changing. On cooling, the nematic phase becomes progressively richer in ketone. Any order-induced alteration of reactivity for mixtures of composition in this region of the phase diagram is the combined result of ketone solubilization in two environments, where the reactant concentrations in each phase are temperature dependent.

3.3.8. Thermal Microscopy: 1 with TPMI in S1544

This type of heterogeneous solubilization may be responsible for the temperature-dependent behaviour we have seen for the cycloaddition reaction in S1544. We have tried, using thermal microscopy, to gain some information into the nature of the solubilization of the reactants within the smectic B phase of S1544. At the reactant concentrations used in our thermolyses (1.76wt% total) it is impossible to determine using thermal microscopy whether or not phase separation is occurring. We chose to increase the concentration of the reactants in the sample to 5wt% and compare the thermal microscopy of this sample to that of the neat mesogen. By comparing the behaviour of these samples using thermal microscopy, we hoped to establish whether or not phase separation is occurring in the 5wt% sample and perhaps speculate on the solvation of the reactants in our 1.7wt% thermolysis samples.

The pure smectic mesogen exhibits the following phase transitions;
(temperatures are °C)^{35,81}



For the neat liquid crystalline sample, the nematic phase is very fluid and, on tapping, the sample flows easily. The first transition at 251.0-251.5 °C results in a smectic A phase which is somewhat more ordered than the nematic phase but again it is quite fluid and is easily deformed by applying gentle pressure to the sample. The smectic B phase formed at 230.0-232.0 °C is distinctly less fluid than the previous two phases. On gentle tapping the smectic B phase is less mobile. Applying gentle pressure on the sample results in a plastic-like deformation of the texture. On cooling through the smectic B temperature range the sample requires greater amounts of force to cause a visible effect on the texture. The important point of this description of the neat mesogen is that in all cases the samples appear to be homogeneous and the entire sample responds uniformly to the applied stress.

For a sample of the reactants (5 wt%) in S1544, the behaviour is a little different. The transition from nematic to smectic A occurs over a lower and broader temperature range (247.0-245.0 °C) than for the neat mesogen. This phase does, however, appear to be homogeneous in nature. It has a texture that is very similar to the smectic A phase of the neat mesogen. Tapping on the sample results in uniform mobility of this phase. The transition to the smectic B phase was somewhat more difficult to detect (ca. 224-226 °C). Much of the sample is rather dark and the only visible change is the formation of some plain monodomains which are typical of the smectic B phase type. However, on tapping the slide, two phases of differing

mobilities can be seen. Some of the sample, including the smectic B-like monodomains, are less mobile than the bulk of the sample (ca. 80%) which is much more easily deformed. On cooling from 225 °C down to 180 °C, it looks as if the proportion of the sample that is more mobile becomes successively smaller and less mobile. It appears that phase separation is occurring and that the proportion of each phase changes with temperature.

These results indicate that at 5wt% reactants in S1544, phase separation is occurring. While it is difficult to tell using optical methods whether or not the 1.7wt% samples are behaving in the same manner, the results of our temperature studies are consistent with such behaviour.

Above *ca.* 225°C, thermal microscopy (of both the 5wt% and 1.76wt% reactant samples) indicates that the samples are homogeneous with a texture similar to that of the smectic A phase of the neat mesogen. Consequently, we believe that the reactants are homogeneously dissolved in a smectic A environment above *ca.* 225°C. The product yield data in table 3.9 are consistent with this. The control of reactivity is slightly greater at 230°C than at 240°C. This is consistent with the reactants being overall better oriented at the lower temperature.

Cooling the 5wt% sample below 228°C results in the formation of a biphasic environment in which one phase is more mobile than the other (possibly $S_B + S_A$). Because a smectic B phase is much more ordered than a smectic A phase, and on the basis of similar results found in the ketone/CCH-4 studies, it would be reasonable to suggest that the reactants may be concentrated in the S_A region. If this is also the case for the 1.76wt% sample, then reactivity may be dominated by that in the more mobile region.

The proportions of the two phases and the compositions of each will be temperature dependent. At higher temperatures, the S_A phase will comprise a higher

proportion of the sample and the effective concentration of the reactants in the S_A phase will be lower. On cooling, the proportion of S_A phase will decrease and the concentration of reactants in the S_A phase will increase and as a result, the solute induced disruption of the environment will also increase. The effect of this is that at lower temperatures the solutes will experience a less ordered environment and orientational control of the reaction should be reduced. This is exactly what we see from the product yields in Table 3.9.

This suggested explanation is consistent with the results from the variable temperature study. However, the results are far from conclusive. It is very difficult to tell using thermal microscopy at low reactant concentrations exactly what the phase behaviour is. It is clear from the 5wt% sample that phase separation does occur at these concentrations and that the mobilities and proportions of each phase change with temperature. More exhaustive studies will be required to determine exactly how the reactants are solubilized in the smectic B mesophase.

CHAPTER 4: SUMMARY AND CONCLUSIONS

4.1 Contributions of Our Study

There has been considerable interest in controlling chemical reactivity using liquid crystalline solvents as illustrated by the large number of papers recently published in this area. As our survey of the literature revealed, some of these studies have shown significant influences of orientational order on reactivity while a great many others have shown little or no effect. This indicates that while there is potential to develop this area of research, there is still much that is not yet understood. What is missing are more systematic studies where an established probe reaction has been utilized to investigate the factors which may influence the order-induced control of reactivity.

Our goal was to establish that liquid crystalline order could influence the reactivity of a thermal bimolecular reaction and then to investigate how solvent order and reactant structure may influence the observed effects. By investigating relative reactivity, the influence of diffusion and viscosity factors can be eliminated and any control of reactivity observed in liquid crystalline solvents can be directly attributed to orientational effects. We have in fact been able to alter thermal bimolecular reactivity and we have found some very interesting results concerning the influence of solvent type and enophile structure on the degree of regiochemical control.

A major contribution of our work has been to establish that even relatively weakly ordered liquid crystals such as cholesterics can have a significant influence on reaction energetics. This result, unlike many of the others obtained using cholesteric or

nematic phases, cannot be largely attributed to viscosity effects. This is strong evidence that cholesteric phases are indeed capable of altering reaction energetics to a significant extent. In fact, we have found not only that cholesteric order can influence reactivity, but also that by using longer, more rod-like enophiles, the effect on reaction energetics can be very large. Using the longest enophile investigated, N-terphenylmaleimide, we have shown that cholesteric order can have a very large influence on reactivity. This influence decreases with decreasing enophile length. This is a result of the fact that molecular shape is very important in determining the average orientation of the reactants. Because cholesteric phases are inherently very fluid like, it is reasonable that they may be more accommodating to solute molecules that are not structural mimics of the mesogen. From our results, it is certainly apparent that the rod-like shape of the solute is a critical factor in determining how well the average orientation is restricted.

Comparing the results in the smectic and cholesteric solvents, it can be seen that the former has a larger influence on the degree of regiochemical control. This is consistent with the generally held belief that more highly-ordered mesogens should have greater potential to orient solutes and alter reactivity. However, the degree of orientational order imposed on the reactants depends on how they are solvated within the smectic mesophase. Our work, in conjunction with other recently published results, has shown that the solubilization of reactants in smectic solvents may be fairly complicated. Techniques such as D.S.C., T.M. and ^2H N.M.R. are being used more frequently to help determine the nature of reactant solubilization within smectic liquid crystalline solvents. Smectic liquid crystals do appear to hold the greatest potential to control reaction energetics, however, the nature of reactant solubilization must be carefully considered. In general, the use of cholesteric phases may be simpler owing to the less complicated reactant solubilization behaviour.

4.2 Future Work

i, Cholesteric Solvents;

Our work using cholesteric solvents has shown that reactant shape has a dramatic influence on the degree of regiochemical control observed. Using rod-like solutes, we have found that the influence of cholesteric order on reaction energetics approaches the maximum that can be expected. For this reason, choosing an enophile that is a better structural match with the steroidal solvents will probably not result in much greater control of reactivity than has been demonstrated in this study. It appears that shape considerations may be very important in cholesteric solvents while structural factors may not be as critical. We have seen that maximum changes in reaction enthalpies of *ca.* 4-6 kcal/mol can be expected from cholesteric solvents. Consequently, we can expect to see an influence of cholesteric order when using fairly sensitive probe reactions which require large shape changes on reaction. It may be interesting to examine reactions of well oriented solutes which have more subtle orientational requirements for transition state formation. The purpose of this would be to help define how sensitive cholesteric solvents could be in distinguishing between reactive pathways for well oriented reactants. This would be very helpful in speculating how much cholesteric order may be expected to influence a given reaction.

ii, Smectic Solvents

It has been generally accepted that the rigid nature of smectic solvents should result in a greater potential to control reactivity. However, the possibility of

heterogeneous reactant solubilization adds an interesting new factor that contributes to the control of solute reactivity in smectic solvents.

In smectic solvents, structural similarity factors may be more important in determining how a solute is incorporated into the mesogen. Techniques such as ^2H N.M.R., differential scanning calorimetry and thermal microscopy are becoming indispensable in studying the complicated nature of reactant solubilization in liquid crystalline solvents. These techniques are required in conjunction with any studies of chemical reactivity in smectic solvents in order to discern how the reactants may be incorporated into the mesophase. While liquid crystalline solvents have not yet been widely utilized, investigations like ours may help to define the general utility of these interesting phases.

CHAPTER 5: EXPERIMENTAL SECTION

5.1. General

Melting points, transition temperatures and bulk phase behaviour were determined using a Mettler FP82 hot stage mounted on an Olympus BH-2 microscope (total magnification 100X). The hot stage was interfaced, through a Mettler FP80 central processor, with an I.B.M.-compatible 8086 computer and controlled via software written using the Asyst software package.

Analytical scale thermolyses and kinetic studies were performed with an insulated oil bath equipped with a Jumo-MS D.B.P. mercury thermoregulator, a Fisher Model 32 transistor relay and Dow Corning 710 silicon oil. Temperatures for the oil bath apparatus were monitored using a Cole-Parmer Model 8110-10 Type K thermocouple thermometer. Temperature flux was not greater than $\pm 1^\circ\text{C}$ during any experiment. Semi-preparative scale thermolyses were performed in a Parr Pressure Reaction Apparatus, model 4914 (2000 watts).

All ^1H NMR spectra were recorded with a Varian EM390 (90 MHz) or a Bruker AM500 (500.13 MHz) spectrometer using deuteriochloroform as solvent. All ^{13}C NMR spectra (except those of DMAD adducts X and II) were recorded with the Bruker AM500 spectrometer at 125.7 MHz. Spectra for adducts X and II were recorded with a Bruker WM250 spectrometer at 62.9 MHz. All chemical shifts are in parts per million downfield from TMS.

Mass spectra and exact masses were determined using a VG analytical ZAB-E mass spectrometer with a source temperature of 200°C and direct probe injection (E.I. 70eV).

Infrared spectra were recorded using a Perkin-Elmer model 283 infrared spectrometer calibrated with the 1601.8 cm^{-1} line of polystyrene using carbon tetrachloride as solvent.

Analytical high performance liquid chromatography was performed using a Gilson Isocratic H.P.L.C. system equipped with a model 302 pump, 5ml head, model 802B manometric module, Holochrome variable wavelength detector and a Rheodyne model 7125 injector. Normal phase analytical H.P.L.C. was performed using a Merck Hibar (4.6x220 mm) Si60 (10 μm) analytical column while reverse phase analytical separations were done using an Alltech (4.6x250mm) C18 (10 μm) column or a Brownlee (4.6x220mm) RP-18 Spheri-10 column. Data collection was performed using a Unitron microcomputer interfaced with the detector through an Adalab data acquisition/control card. The 0-10 mV signal was amplified to 0-1 V using an Adaamp analog amplifier (Interactive Microware, Inc.). Chromatogram acquisition and storage was performed using the Chromatohart (Interactive Microware, Inc.) software package. Peak areas were calculated by triangulation.

Semi-preparative H.P.L.C. separations were performed with the Gilson H.P.L.C. equipped with a 50 ml head. Normal phase separations were performed with an EM Reagents Lobar Si60 size B or Pharmacia column using the Holochrome variable wavelength detector or with an Isco 254 nm single wavelength detector. Semi-preparative reverse phase separations were performed using a Whatman Partisil M9 10/50 ODS-2 column.

5.2. Solvents

All solvents used for H.P.L.C. work were used as received; these included acetonitrile (Caledon HPLC), dichloromethane (Caledon HPLC), ethyl acetate (BDH

reagent) and hexane (Caledon HPLC). Other solvents used as received were methanol (Mallinckrodt anhydrous), acetic anhydride (BDH reagent) nitropropane (Eastman), chlorobenzene (Fischer Scientific), toluene (Caledon reagent) and carbon tetrachloride (Caledon reagent grade). Absolute ethanol was obtained by refluxing 95% ethanol over magnesium turnings and iodine for 24 hours followed by distillation. Pyridine (Caledon reagent) was dried by refluxing over sodium hydroxide and distilling under nitrogen. Dry ethyl acetate was obtained by refluxing for several hours with acetic anhydride and distilling. Benzene- d_6 and deuteriochloroform were used as received from Merck Sharpe and Dohme. Spectroscopic grade carbon tetrachloride was purchased from Fischer Scientific and stored over molecular sieves.

5.3. Preparation and Purification of Compounds

5.3.1. Preparation and Purification of Liquid Crystalline and Model Isotropic Liquid Compounds

The smectic solvent, 4-(trans-pentylcyclohexyl)-4'-(propylcyclohexyl) biphenyl (**1544**) and the model isotropic solvent, 4-(trans-pentylcyclohexyl)-4-(ethyl) biphenyl (**1409**) were both used as received from E. Merck Co..

The cholesteric liquid crystals were prepared by heating mixtures of the steroidal alcohol (cholesterol or 3β -cholestanol) with the appropriate acid chloride, as outlined below.

Preparation of Acid Chlorides

The acid chlorides, 4-chlorobenzoyl chloride, 4-toluoyl chloride and benzoyl chloride were prepared by refluxing the corresponding carboxylic acid with a 50% excess of freshly distilled thionyl chloride under nitrogen for approximately 10 hours.

Excess thionyl chloride was removed by distillation. 4-Chlorobenzoyl chloride was further purified by vacuum distillation (*ca.* 2mm Hg, b.p.=75 °C) giving a 90% yield. The other acid chlorides were used without further purification. Propionyl chloride was used as received from BDH.

Preparation of Cholesteryl-4-chlorobenzoate (C.C.B.), Cholesteryl Benzoate (C.B.), Cholestanyl-4-toluate (C.T.) and Cholestanyl Propionate (C.P.)

The cholesteric liquid crystals were prepared by mixing equimolar mixtures of the steroidal alcohol (cholesterol or 3 β -cholestanol) with the appropriate acid chloride (*ca.* 9.8 x 10⁻² mol of each) in dry pyridine (*ca.* 40ml) and heating at 50-60 °C overnight. Reaction mixtures were quenched with water and the products extracted with dichloromethane. The organic layer was washed successively with 5% aq. HCl (3 x 50 ml), 5% aq. sodium bicarbonate (3 x 50 ml) and water, (2 x 50 ml), dried over sodium sulphate, filtered, and the solvent was evaporated.

For C.C.B., C.B. and C.P. the product was purified by column chromatography (silica gel) using hexanes as eluant to give a white solid in 60-80 % yield.

C.C.B. was recrystallized twice from 95% ethanol/ methylene chloride, giving a 67% yield.

K – Ch 170-174 °C (lit. 165 °C)

Ch – I 240-245 °C (lit. 240 °C).

C.B. and C.P. were each recrystallized from 95% ethanol.

C.B. K–Ch 137.0-139.0 °C (lit. 136.5-137.0 °C)

Ch–I 155.0-157.0 °C (lit. 155.0 °C)

C.P. K–I 126.0-128.0 °C (lit. 124-125 °C)

To prepare cholestanyl-4-toluate, ethanol was added to quench the reaction. The product was purified by chromatography using alumina as the stationary phase and 60% hexane/methylene chloride as the elutant. The product was recrystallized twice from chloroform/ethanol giving a yield of 37%.

K – Ch 173-175 °C (lit. 172 °C)

Ch – I 227-230 °C (lit. 225 °C)

5.3.2. Preparation and Purification of Reactants

N-Phenylmaleimide (NPMI):

N-phenylmaleimide (Sigma Chemical Company) was recrystallized twice from acetone and dried in a dessicator over phosphorous pentoxide.

M.P. = 89.5-90 °C (lit. 90-91 °C).

Preparation of N-Biphenylmaleimide (BPMI):

N-Biphenylmaleimide was prepared from 4-aminobiphenyl and maleic anhydride using the method of Crivello.¹¹¹ Maleic anhydride (1.0 g, 1.0×10^{-2} mol) was dissolved in *ca.* 20 mL of acetone. Addition of 4-aminobiphenyl (0.9 g, 5.0×10^{-3} mol) gave an immediate yellow precipitate of the corresponding amic acid. The mixture was stirred for 60 minutes under gentle reflux. Triethyl amine (0.25 mL) and sodium acetate (0.02 mg) were then added directly to the refluxing mixture. Acetic anhydride was added slowly over 3 hours with gentle warming, during which time the amic acid gradually dissolved. On cooling, a bright yellow solid precipitated. The mixture was filtered and the solid was purified by silica column chromatography with 2% acetonitrile/methylene chloride as eluant followed by two recrystallizations from

acetone, yielding bright yellow needles (1.5 g, 6.0×10^{-3} mol, 40%).

M.P. = 190.0-190.5 °C (lit. 189-190 °C)

I.R. cm^{-1} (KBr) 3100(w), 1705(s,br), 1509 (m), 1490(m), 1398(s), 1160(m), 1148(m), 1007(w), 948(w), 840(m), 831(m), 766(m), 757(m), 729(m), 721(m), 717(m), 683(s)

$^1\text{H N.M.R.}$ (ppm); $\delta=6.6$ (s,2H), 7.0-7.5 (m,9H)

Preparation of N-(p-Terphenyl)maleimide (TPMI):

(i) Preparation of 4-Nitro-p-terphenyl;

p-Terphenyl, obtained from Aldrich, was used as received. Anhydrous nitric acid (sp. gr. > 1.53) was prepared by twice distilling nitric acid from an equal volume of sulphuric acid in a nitrogen atmosphere and collecting a volume of the first distillate equal to approximately half the volume of nitric acid used.

4-Nitro-p-terphenyl was prepared by the method of Splies.¹¹² To a suspension of p-terphenyl (6.0 g, 2.6×10^{-2} mol) in 30 ml glacial acetic acid (100°C), a solution of 1.3 ml anhydrous nitric acid in 2.5 ml of glacial acetic acid was added dropwise over 3 hours. The reaction vessel was cooled on an ice bath and the product was collected by vacuum filtration. The crude 4-nitro-p-terphenyl was purified on a silica gravity column (40% methylene chloride/hexane), recrystallized twice from 2-nitropropane, and washed with ethanol. (4.6 g, 1.7×10^{-2} mol, 64%)

M.P. = 212-216 °C (lit. 209-213 °C)

(ii) Reduction of 4-Nitro-p-terphenyl to 4-Amino-p-terphenyl;

Reduction of 4-nitro-p-terphenyl was performed using the method of Bellamy.¹¹³ 4-Nitro-p-terphenyl (1 g, 3.6×10^{-3} mol) and excess $\text{SnCl}_2 \cdot 2\text{H}_2\text{O}$ (3.8 g, 1.8×10^{-2} mol) were dissolved in ca. 20ml of ethyl acetate and heated to 80 °C

overnight. The solid product obtained on cooling was recrystallized once from 95% ethanol. (0.6 g, 2.6×10^{-3} mol, 80%).

M.P. = 185-188 °C (lit. 186-193 °C).

(iii) Preparation of TPMI from 4-Amino-p-terphenyl;

The method used is similar to that of Crivello.¹¹¹ Maleic anhydride (300 mg, 3.1×10^{-3} mol) was dissolved in 4 ml of acetone. Addition of 4-amino-p-terphenyl (500 mg, 2.04×10^{-3} mol) resulted in the immediate formation of a precipitate, presumed to be the amic acid, which was collected and dried over P_2O_5 . The solid was dissolved in a solution of ca. 5 ml of acetic anhydride and 100 mg of flame-dried sodium acetate. After heating for 3-4 hours at 90°C a precipitate was formed. The reaction mixture was cooled and the resultant solid was collected and washed with acetone/water and recrystallized twice from acetone to yield a pale yellow solid. (550 mg, 1.7×10^{-3} mol, 83%)

M.P. = 293-303 °C (decomp.)

I.R. cm^{-1} (KBr); 3095(w), 1705(s), 1503(w), 1481(m), 1394(m), 1153(w), 1139(w), 1009(w) 939(w), 822(m), 812(m), 757(w), 751(w), 718(w), 676(m)

1H N.M.R. (ppm); ($CDCl_3$) δ =6.8 (s, 2H), 7.1-7.7 (m, 13H)

exact mass; calculated 325.1103

 found 325.1105

Preparation of Cholesta-5,7-dienyl-3 β -yl acetate (1**);**

7-Dehydrocholesterol (2.5 g, 6.5×10^{-3} mol) in acetic anhydride (12 mL, 1.2×10^{-1} mol) was refluxed under nitrogen for 2 hours. The reaction mixture was cooled and the product was recrystallized thrice from acetone and washed with cold methanol affording a white solid. (2.1 g, 5.0×10^{-3} mol, 75%)

M.P. = 125-127 °C (lit. 129-130 °C)

5.4. Thermolysis of N-Arylmaleimides with (1)

5.4.1. General Sample Preparation

All thermolyses were carried out in sealed Pyrex tubes which had been treated with 10% aqueous sodium hydroxide for *ca.* eight hours and then rinsed with water before use.

Analytical samples were prepared using 7mm Pyrex tubing. To 100 mg samples of each solvent were added 1mg (2.3×10^{-6} mol) of the diene and an equimolar amount of the appropriate enophile. Samples were dissolved in *ca.* 2mL of methylene chloride which was evaporated off and the sample then placed under vacuum for several hours. Aliquots of the reactant-doped mesogen (*ca.* 20-30 mg each) were placed into the Pyrex tubes which were vacuum sealed after three freeze, pump and thaw cycles. Thermolyses were performed in the oil bath apparatus for either two or four hours (6 or 12 hrs for TPMI+1 in S1544 samples) after which time the samples were opened, dissolved in methylene chloride, and the crude mixtures analyzed by H.P.L.C.

Semi-preparative scale samples using NPMI or BPMI as enophile were prepared by adding *ca.* 300mg (7.0×10^{-4} mol) of 1 to an equimolar amount of the enophile and dissolving in *ca.* 34ml of dry benzene. The reaction mixture was then divided among three base-washed 5/8 in. O.D. Pyrex tubes. The tubes were degassed using three freeze, pump and thaw cycles, vacuum sealed and placed in the high pressure reaction vessel at 200 °C for *ca.* 4 hours. The tubes were then opened and the crude reaction products analyzed by analytical H.P.L.C.. Products were isolated by semi-preparative cyclic chromatography. (*vide infra*)

The semi-preparative scale reaction of 1 with TPMI was performed in a cholesteric liquid crystalline solvent in order to increase the yield of T5. 150 mg (3.5×10^{-4} mol) of 1, an equimolar amount of TPMI and 15g of C.C.B. were dissolved in *ca.* 10ml of methylene chloride. The methylene chloride was removed by evaporation and the resulting mixture was placed in a Pyrex tube, vacuum sealed, and heated at 200 °C for 4 hours. The liquid crystal was removed by flash chromatography using a silica column and hexanes as the eluant. The product mixture was then separated by semi-preparative liquid chromatography. (*vide infra*)

5.4.2. Reaction of N-Arylmaleimides with 1

Reaction conditions were determined by monitoring the course of the reaction of equimolar amounts of 1 and NPMI (1.4×10^{-5} mol of each) in benzene- d_6 (6 ml; 1.5 wt% total reactants) by ^1H N.M.R. and H.P.L.C.. The reaction appears to proceed to *ca.* 70% completion in 4 hours at 200 °C.

Product isolation from the semi-preparative scale reaction mixtures were virtually identical in each case. Cyclic chromatography was used starting with 100% methylene chloride as the eluant. The sample was cycled twice in order to separate it into two fractions; (5+4a) and (4b+3). The first fraction was then recycled twice and the products were isolated. For the reaction with NPMI, products N4b and N3 were separable by normal phase L.C. with one cycle using 2% $\text{CH}_3\text{CN}/\text{CH}_2\text{Cl}_2$ as the eluant. For the other enophiles, reverse phase chromatography using 95% $\text{CH}_3\text{CN}/\text{H}_2\text{O}$ as the eluant was required. No cycling was required to isolate the products using reverse phase L.C.. Flow rates used for all normal phase semi-preparative work were *ca.* 8-10 ml min^{-1} while for the reverse phase semi-preparative work (Whatman ODS Column) a flow rate of 7 ml min^{-1} was used. The isolated adducts were recrystallized several times from methanol or methanol/chloroform.

Analytical H.P.L.C. Analysis; NPMI/1 ADDUCTS

Column; Merck Hibar (4.6x220mm) Si60 (10 μ m)

Solvent; 2% CH₃CN/CH₂Cl₂

Flow Rate; 1 mL min⁻¹

Analytical Wavelength; 235 nm

Retention times; 1; 4 min, NPMI; 6 min, N4a 13 min, N5; 14 min, N4b; 19 min, N3; 23.5 min

N.B. The ¹H and ¹³C N.M.R. data for all adducts are collected in Chapter 2 and in Appendices 1-3.

ADDUCT N5;

M.P.= 170.0-172.5 °C

I.R. cm⁻¹ (KBr); 2957(s,br.), 2876(m), 1714(s,br.) 1499(m),

1467(w), 1455(w), 1395(s), 1378(m), 1359(m), 1234(s,br.), 1209(w), 1180(s,br.),

1158(w), 1034(s) 958 (w), 939(w), 793(w), 776(w), 748(w), 691(m).

mass spec.; m/z (I) 524(5), 424(2), 365(100), 349(5), 195(6), 157(33), 119(11), 95(10)

exact mass; calculated 599.3975

 found 599.3967

ADDUCT N4a;

M.P.= 124.0-126.0 °C

I.R. cm⁻¹ (KBr); 2959(s,br.), 2879(m), 1715(s,br.), 1500(m), 1467(m), 1459(m),

1385(s), 1376(s), 1244(s,br.), 1215(w) 1179(s,br.), 1034 (s), 949(w), 931(w), 799(w),

755(w), 742(w), 693(w).

mass spec.; m/z (I) 524(1), 424(3), 364(100), 349(15), 251(30), 197(18), 157(16)

exact mass; calculated 599.3975

 found 599.3961

ADDUCT N4b;

M.P.= 78.5-81.0 °C

I.R. cm^{-1} (KBr); 2960(s,br.), 2878(m), 1719(s,br.), 1501(m), 1468(w), 1458(w),

1378(s), 1369(s), 1260(s), 1248(s.br.), 1174(s,br.), 1028(s,br.), 952(w), 938(w), 799(m),

756(w), 738(w), 694(m).

mass spec.; m/z (I) 524(2), 424(2), 365(100), 349(7), 251(10), 197(8), 157(7), 119(7).

exact mass; calculated 599.3975

 found 599.397

ADDUCT N3;

M.P.= 96.5-98.0 °C

I.R. cm^{-1} (KBr); 2962(s,br.), 2879(m), 1718(s,br.), 1500(m), 1468(w), 1458(w),

1380(s,br.), 1368(s), 1246(s,br.), 1186(m), 1029(m), 919(w), 897(w), 760(w), 730(w),

688(w).

mass spec.; m/z (I) 599(1), 539(100), 524(20), 365(5), 351(4), 237(8), 174(50), 129(20)

exact mass; calculated 599.3975

 found 599.3976

Analytical H.P.L.C. Analysis; BPMI/1 ADDUCTS

Column; Merck Hibar (4.6x220mm) Si60 (10 μ m)

Solvent; 2% CH₃CN/CH₂Cl₂

Flow Rate; 1 mL min⁻¹

Analytical Wavelength; 280 nm

Retention times; 1; 4 min, BPMI; 5.5 min,

B5; 7.5 min, B4a; 8 min, B4b; 11 min, B3; 11 min

ADDUCT B5

M.P.= 183.5-185.0 °C

I.R. cm⁻¹ (KBr); 2957(s,br.), 2877(m), 1716(s,br), 1522(m), 1486(m), 1466(w),
1451(w), 1376(s,br.), 1245(s,br.), 1172(m,br.), 1026(m), 836(w). 758(m), 692(m),
660(w).

mass spec.; m/z (I) 616(1), 615(3), 600(4), 365(100), 366(35), 364(32), 251(22),
249(24), 195(15).

exact mass; calculated 675.4287
 found 675.4314

anal.; calc.; C 79.96 H 8.50
 found; C 79.96 H 8.56

Adduct B4a

M.P.= 100.5-101.5 °C

I.R. cm⁻¹ (KBr); 2956(s,br.), 2876(m), 1714(s,br.), 1522(m), 1485(m), 1466(w),
1434(w), 1376(s,br.), 1241(s,br.), 1172(m,br.), 1027(m, br.), 833(m), 757(m), 692(m),
662(w)

mass spec.; m/z (I) 615(2), 366(34), 365(100), 364(47), 251(25), 249(50), 237(17),
219(13), 195(32).

exact mass; calc. 675.4287
 found 675.4281

anal.; calc. C 79.96 H 8.50
 found C 79.44 H 8.52

Adduct B4b

M.P.= 221.0-223.0 °C

I.R. cm⁻¹ (KBr); 2959(s,br.), 2875(m), 1716(s,br.), 1505(w), 1486(m), 1464(w),
1444(w), 1376(s,br.), 1243(s,br.), 1173(m,br.), 1025(m), 817(w), 759(m), 690(m),
664(w).

mass spec.; m/z (I) 675(2), 616(14), 366(37), 365(100), 364(42), 251(22), 249(15),
237(4), 219(9), 195(19).

exact mass; calc. 675.4287
 found 675.4284

anal.; calc. C 79.96 H 8.50
 found C 79.57 H 8.40

Adduct B3

M.P.= 120.0-122.0 °C

I.R. cm⁻¹(KBr); 2956(s,br.), 2875(m), 1715(s,br.), 1520(m), 1486(m), 1465(w),
1445(w), 1377(s,br.), 1244(s,br.), 1180(m), 1027(m), 832(m), 760(m), 739(m), 694(m),
665(w).

mass spec.; m/z (I) 675.3(48.2), 367(30), 366(100), 365(26), 364(15), 351(14),
253(18),250(19), 251(11), 249(89), 195(16)

exact mass; calc. 675.4287
 found 675.4289

Analytical H.P.L.C. Analysis; TPMI/1 ADDUCTS

Column; Merck Hibar (4.6x220mm) Si60 (10 μ m)

Solvent; 2% CH₃CN/CH₂Cl₂

Flow Rate; 1 mL min⁻¹

Analytical Wavelength; 280 nm

Retention times; 1; 4 min, TPMI; 5 min, T5; 6 min, T4a; 7 min, T4b; 10 min, T3; 10 min

Adduct T5

M.P.= 162.0-166.0 °C

I.R. cm⁻¹ (KBr); 2937(s,br.), 2860(m), 1715(s,br.), 1510(m), 1485(w), 1466(m), 1384(s), 1240(s,br.), 1166(m,br.), 1032(m), 824(m), 760(m), 730(w), 692(w).

mass spec.; m/z (I) 751(0.5), 424(2), 367(7), 366(33), 365(100), 364(38), 325(21), 271(12), 213(17) 157(31).

exact mass; calc. 751.4601
 found 751.4579

Adduct T4a

M.P.= 147.5-149.5 °C

I.R. cm⁻¹ (KBr); 2939(s,br.), 2861(s), 1713(s,br), 1508(w), 1487(m), 1465(m), 1380(s,br.), 1240(s,br), 1169(m,br.), 1029(w), 820(w), 760(m), 730(w), 691(w).

mass spec.; m/z (I) 751(0.6), 424(2), 367(6), 366(32), 365(100), 364(47), 325(21),

271(14), 157(10).

exact mass; calc. 751.4601
 found 751.4579

Adduct T4b

M.P.= 182.0-185.0 °C

**I.R. cm^{-1} (CCl_4); 2942(s,br.), 2862(m), 1715(s,br.), 1478(m), 1459(w), 1370(s,br.),
1230(m,br.), 1167(m,br.), 1020(m, br.), 683(w).**

**mass spec.; m/z (I) 751(1), 424(2), 367(8), 366(38), 365(100), 364(52), 325(34),
271(18).**

exact mass; calc. 751.4601
 found 751.4579

Adduct T3

M.P.= 119.5-123.0 °C

**I.R. cm^{-1} (KBr); 2959(s,br.), 2878(s), 1715(s,br.), 1508(w), 1485(m), 1467(m,br.),
1379(s,br.), 1244(s,br.), 1179(m,br.), 1028(w), 820(m), 762(m), 745(w), 732(w),
691(m).**

mass spec.; m/z (I) 751(77), 366(100), 325(82), 271(20), 195(12),

exact mass; calc. 751.4601
 found 751.4606

APPENDIX 1

¹H and ¹³C CHEMICAL SHIFTS (ppm); ADDUCTS OF N-BIPHENYLMALEIMIDE WITH CHOLESTA-5,7-DIEN-3 β -YL ACETATE (I)

Solvent; CDCl ₃										
ADDUCT	(B3)		(B4a)		(B4b)		(B5)		(I) ⁸⁸	
NUMBER	¹ H	¹³ C	¹ H	¹³ C	¹ H	¹³ C	¹ H	¹³ C	¹ H	¹³ C
1 α	1.58	31.95	1.23	36.60	1.24	36.60	1.32	37.12	1.30	37.89
1 β	1.78	-----	1.82	-----	1.78	-----	1.98	-----	1.79	-----
2 α	2.06	27.27	1.99	28.24	1.87	28.32	1.93	28.34	1.89	27.95
2 β	1.65	-----	1.61	-----	1.55	-----	1.67	-----	1.53	-----
3 α	5.33	70.07	4.66	73.72	4.61	73.75	4.55	74.67	4.62	72.80
4 α	2.85	35.07	2.44	38.21	2.45	38.38	2.36	38.89	2.43	37.03
4 β	2.06	-----	2.30	-----	2.34	-----	2.34	-----	2.28	-----
5	-----	46.41	-----	125.86	-----	125.89	-----	126.86	-----	138.44
6	6.24	136.27	5.05	119.86	5.51	121.96	5.17	118.11	5.48	120.19
7	5.83	131.06	3.64	37.97	3.16	40.47	3.53	39.62	5.31	116.25
8	-----	45.50	-----	147.18	-----	148.23	-----	143.79	-----	141.49
9	1.71	55.40	1.95	45.66	2.25	44.51	-----	137.14	1.93	46.02
10	-----	44.21	-----	39.05	-----	39.26	-----	38.99	-----	37.03
11 α	2.57	23.71	1.63	19.73	1.64	19.69	2.20	23.27	1.60	22.50
11 β	1.43	-----	1.54	-----	1.54	-----	2.10	-----	1.49	-----

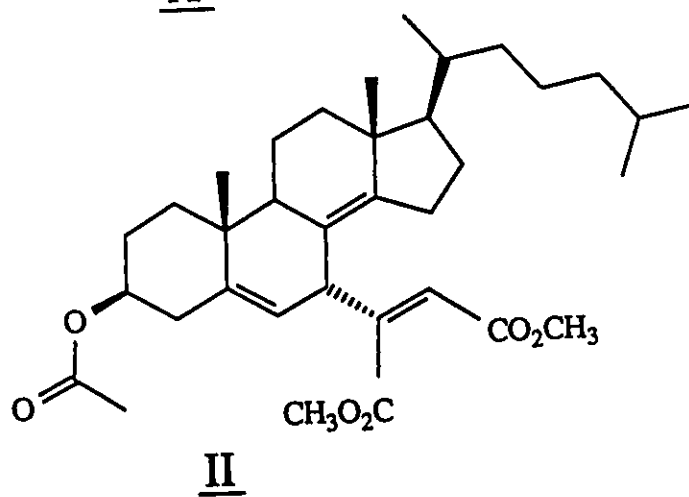
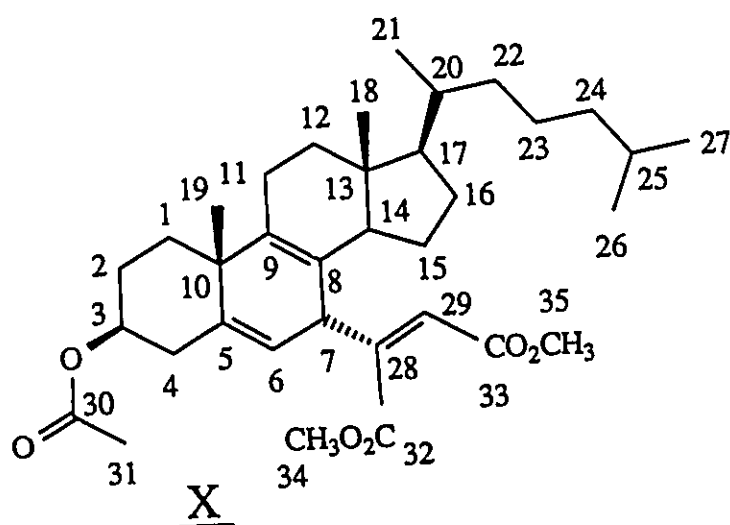
APPENDIX 1 (CONTINUED)

ADDUCT (B3)	(B4a)		(B4b)		(B5)		(1) ⁸⁸			
	¹ H	¹³ C	¹ H	¹³ C	¹ H	¹³ C	¹ H	¹³ C		
12 α	1.11	39.49	1.10	37.84	1.16	37.67	1.30	36.71	1.13	39.11
12 β	2.03	-----	1.97	-----	2.01	-----	1.98	-----	2.00	-----
13	----	41.36	----	43.82	----	44.11	----	42.91	----	42.85
14	1.12	55.69	----	146.55	----	144.02	1.85	50.65	1.83	54.42
15 α	1.39	23.45	2.38	25.79	2.27	26.70	1.81	24.01	1.63	22.98
15 β	1.39	-----	2.35	-----	2.17	-----	1.37	-----	1.33	-----
16 α	1.31	28.27	1.43	27.39	1.42	27.31	1.35	29.31	1.29	22.98
16 β	1.90	-----	1.88	-----	1.84	-----	1.89	-----	1.91	-----
17	1.07	54.03	1.11	57.97	1.15	58.28	1.10	54.80	1.09	55.87
18	0.96	19.22	0.90	18.36	0.90	18.16	0.65	12.20	0.54	11.76
19	0.74	13.04	0.91	19.66	0.89	19.81	1.20	24.23	0.86	16.10
20	1.39	35.95	1.49	35.05	1.45	35.21	1.33	36.72	1.31	36.09
21	0.92	19.66	0.93	19.81	0.93	19.95	0.89	19.36	0.87	18.81
22	1.03	36.58	1.08	36.52	1.03	36.53	0.95	36.80	0.95	36.60
	1.36	-----	1.49	-----	1.26	-----	1.33	-----	1.04	-----
23	1.34	24.43	1.36	24.38	1.36	24.60	1.29	24.46	1.28	23.84
	1.15	-----	1.10	-----	1.12	-----	1.15	-----	1.03	-----
24	1.11	40.09	1.12	40.10	1.10	40.10	1.08	40.10	1.00	39.46
	1.11	-----	1.12	-----	1.10	-----	1.08	-----	1.00	-----
25	1.51	28.61	1.50	28.61	1.51	28.59	1.46	28.63	1.45	27.95

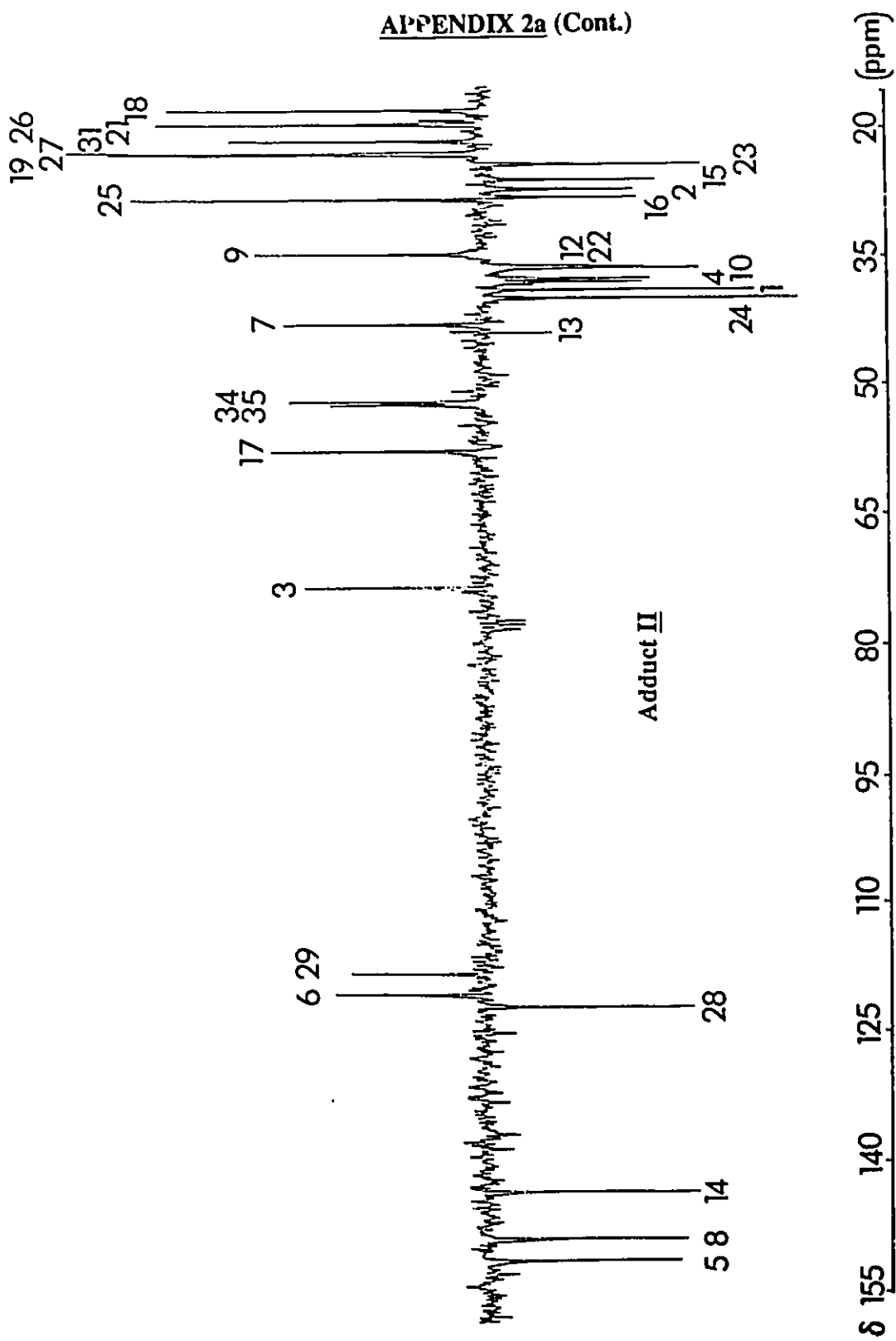
APPENDIX I (CONTINUED)

ADDUCT	(B3)		(B4a)		(B4b)		(B5)		(1) ⁸⁸	
Carbon										
Number	¹ H	¹³ C	¹ H	¹³ C	¹ H	¹³ C	¹ H	¹³ C	¹ H	¹³ C
26	0.86	23.14	0.86	23.40	0.84	23.41	0.82	23.40	0.79	22.98
27	0.85	23.39	0.85	23.14	0.85	23.14	0.80	23.15	0.80	22.76
28	3.40	42.95	3.17	45.02	3.09	46.17	3.27	43.53	----	----
29	2.77	57.21	2.93	32.17	2.93	34.40	2.55	30.81	----	----
	----	----	2.75	----	2.70	----	2.52	----	----	----
30	----	170.87	----	171.00	----	170.94	----	170.63	----	170.50
31	2.02	21.91	2.02	21.93	1.98	21.96	1.96	21.90	1.96	21.33
32	----	176.71	----	176.29	----	176.22	----	176.40	----	----
33	----	176.90	----	178.39	----	178.90	----	178.75	----	----
AROMATIC RESONANCES ^a										
Bp1	----	131.76	----	131.66	----	131.67	----	131.63		
Bp4	----	140.98	----	142.07	----	142.25	----	142.14		
Bp5	----	142.04	----	141.00	----	140.96	----	140.86		
Bp8	----	128.16	----	128.20	----	128.20	----	128.16		
Bp2/12	----	129.39	----	129.40	----	129.40	----	129.40		
Bp3/11	----	128.32	----	128.44	----	128.65	----	128.59		
Bp6/10	----	127.81	----	127.83	----	127.89	----	127.89		
Bp7/9	----	127.36	----	127.18	----	127.38	----	127.43		

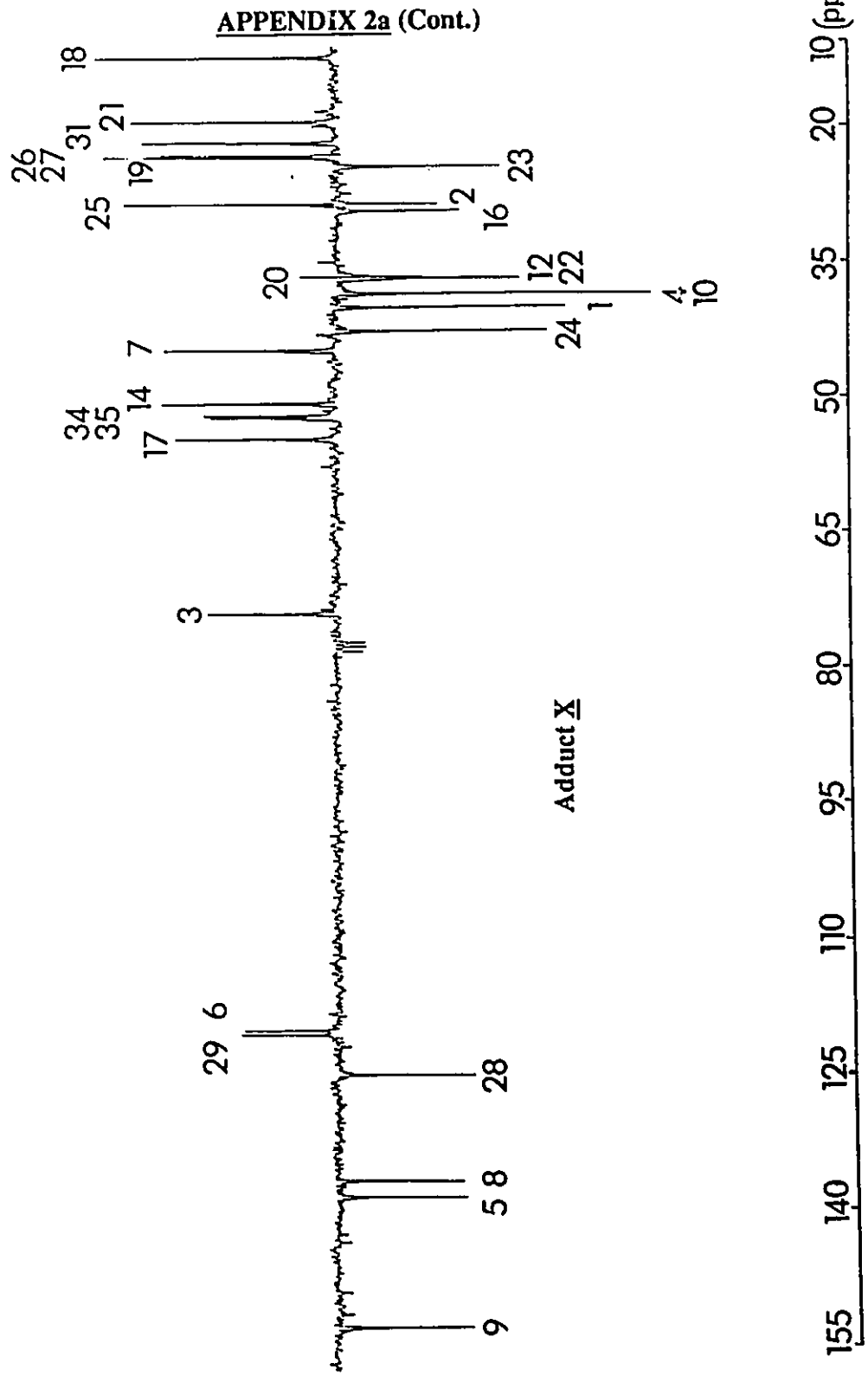
^a All adducts of biphenyl maleimide give aromatic proton resonances at $\delta = 7.2-7.9$ (m, 9H).

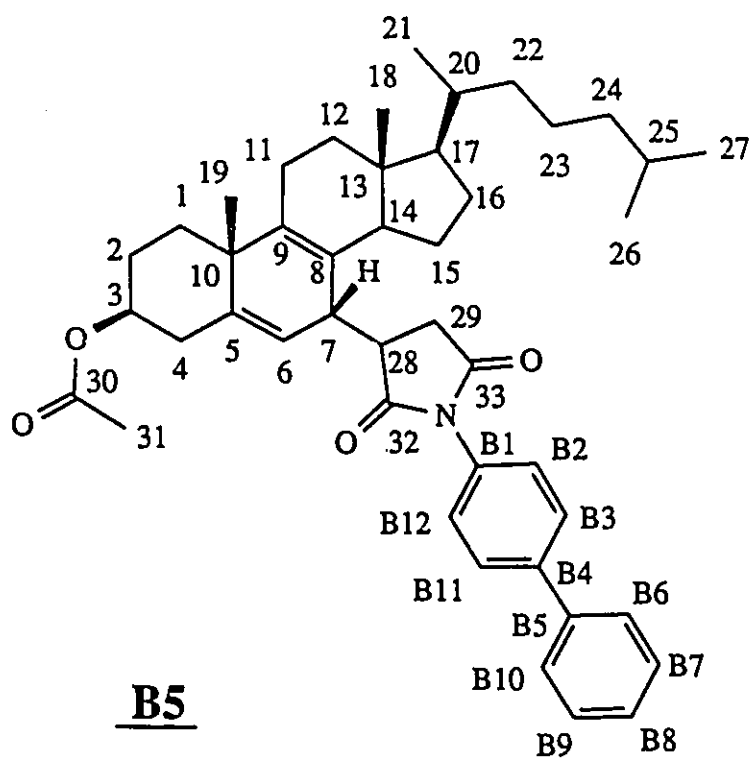
APPENDIX 2a¹³C SPECTRA OF ADDUCTS X AND II (2 PAGES)

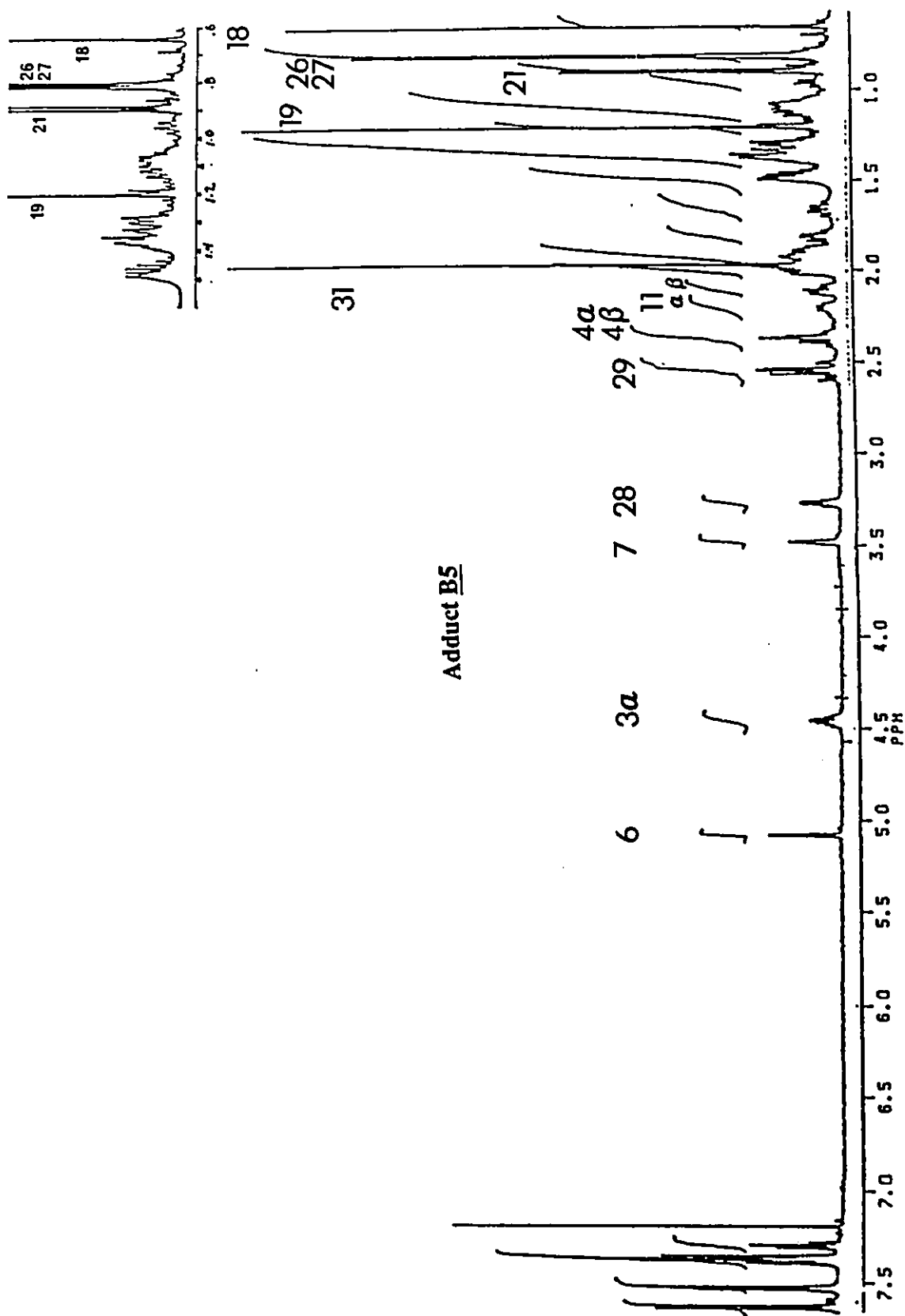
APPENDIX 2a (Cont.)



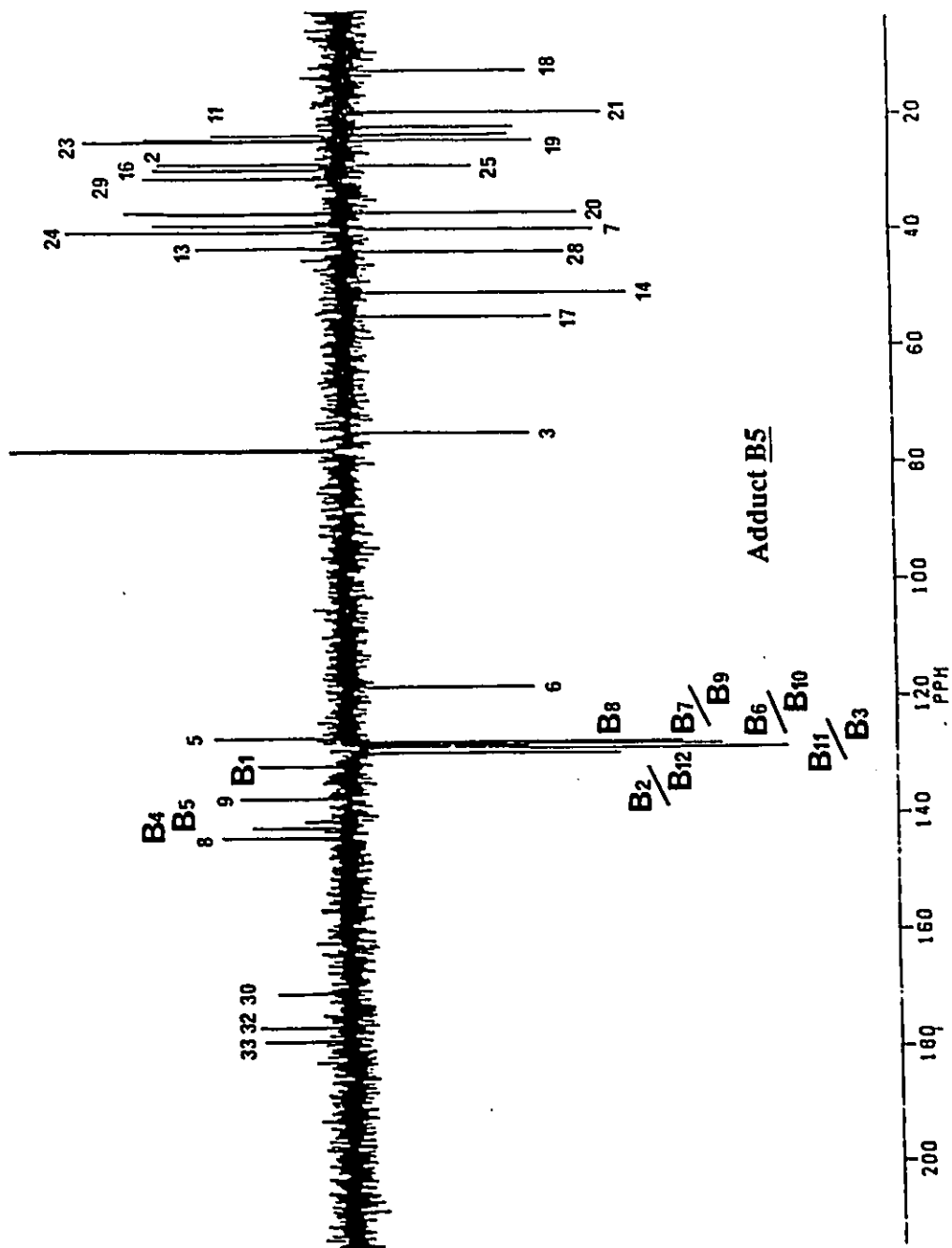
Adduct II



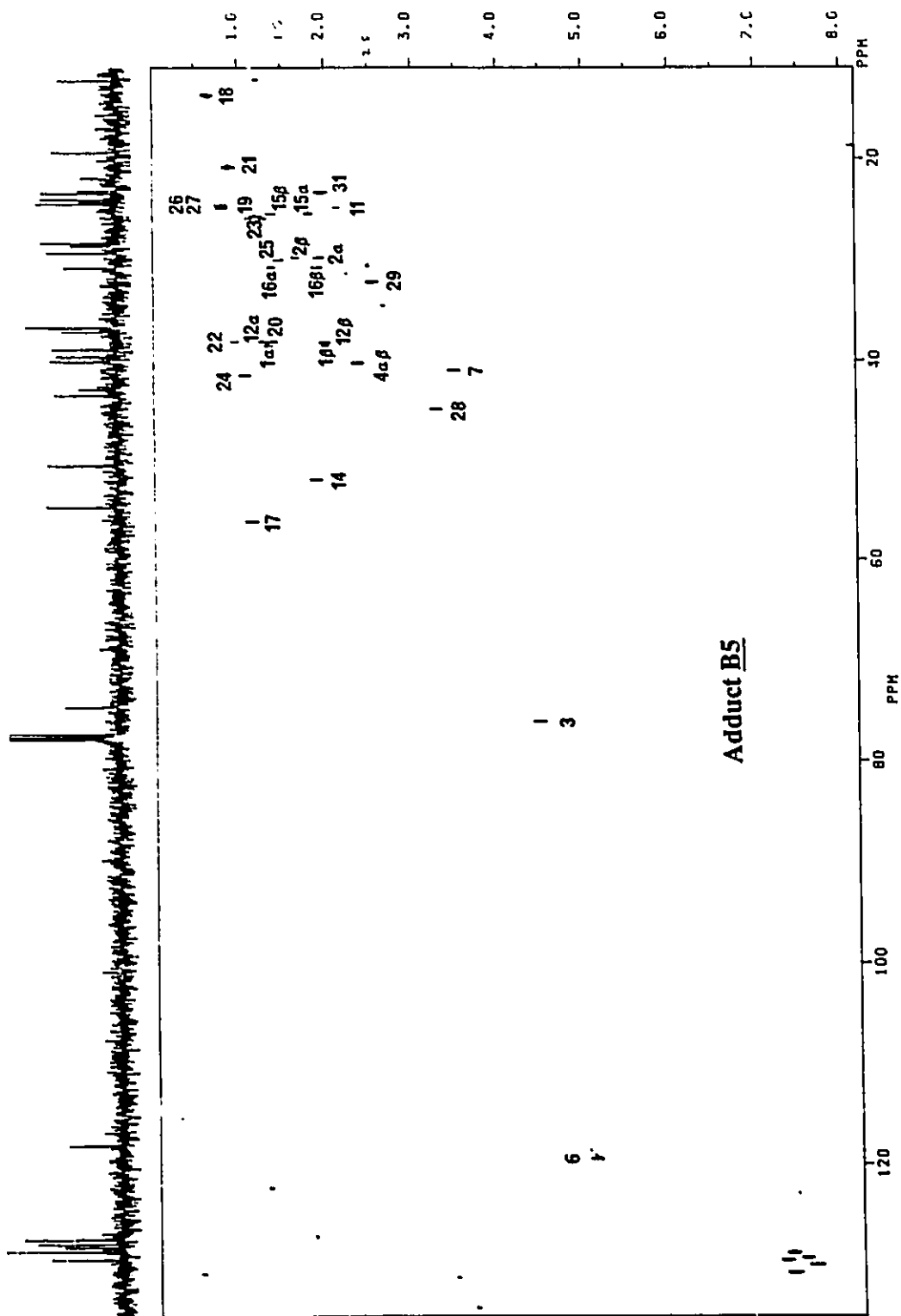
APPENDIX 2b ^1H and ^{13}C SPECTRA ADDUCT B5 (6 PAGES)

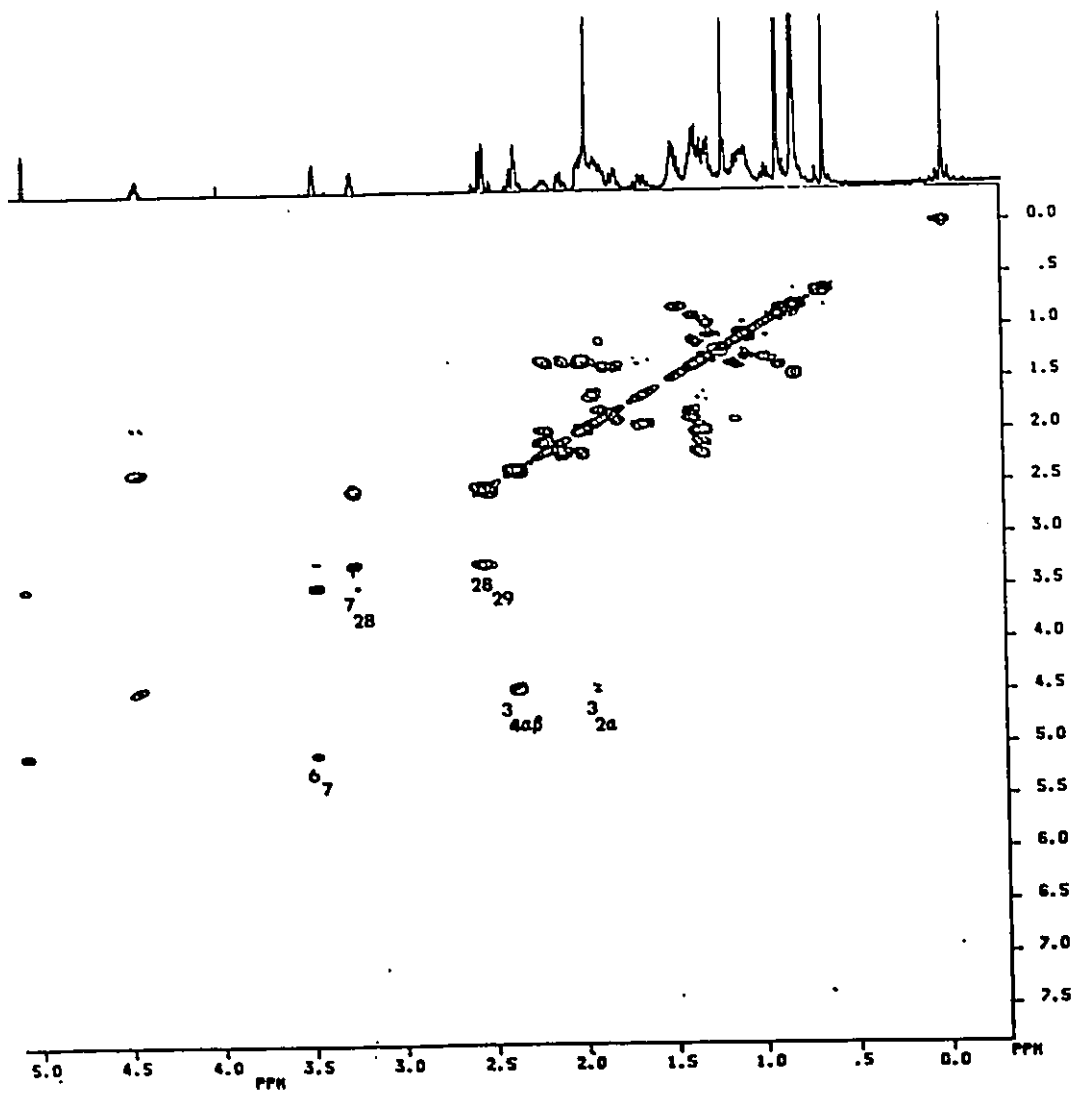


APPENDIX 2b (Cont.)

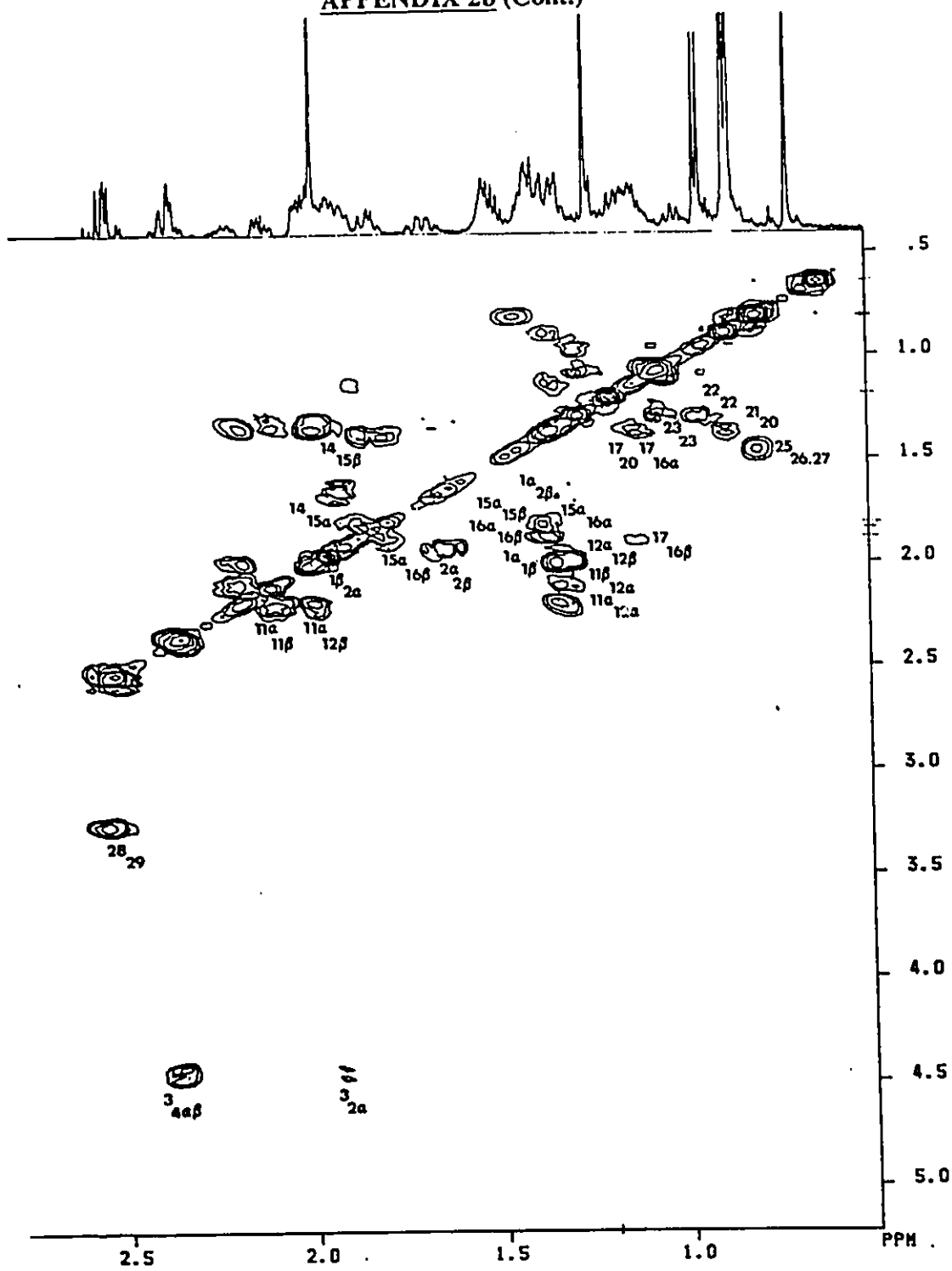


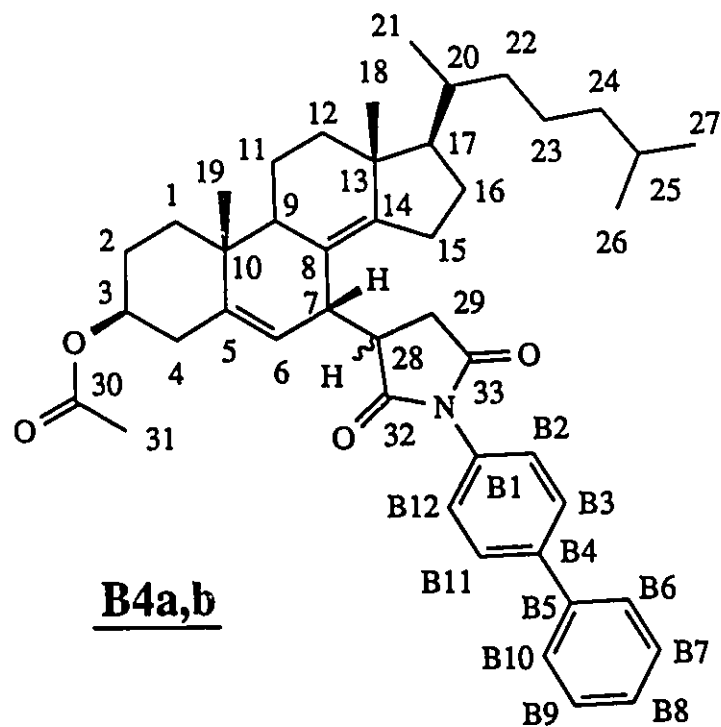
APPENDIX 2b (Cont.)



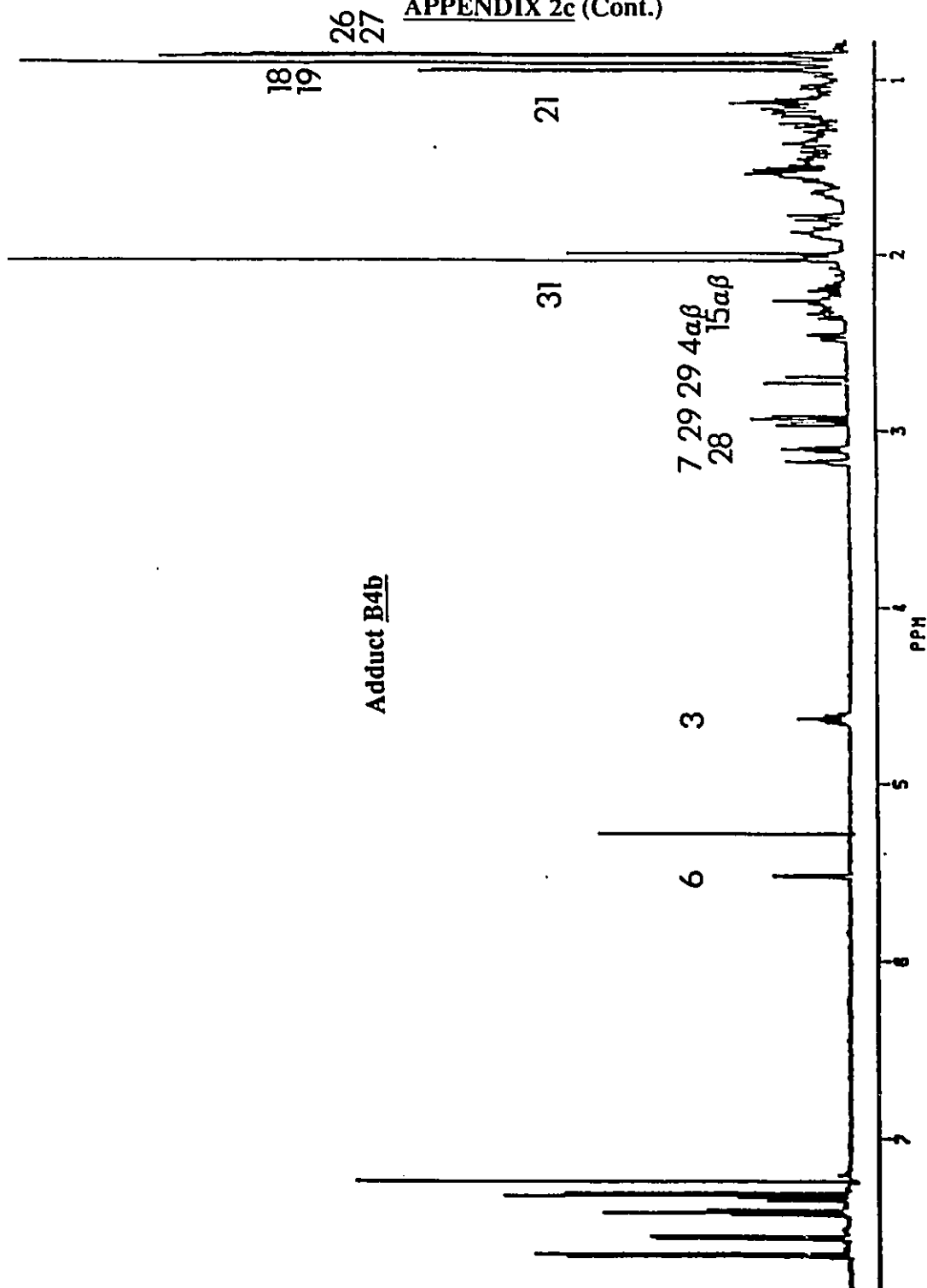
APPENDIX 2b (Cont.)**Adduct B5**

APPENDIX 2b (Cont.)

Adduct B5

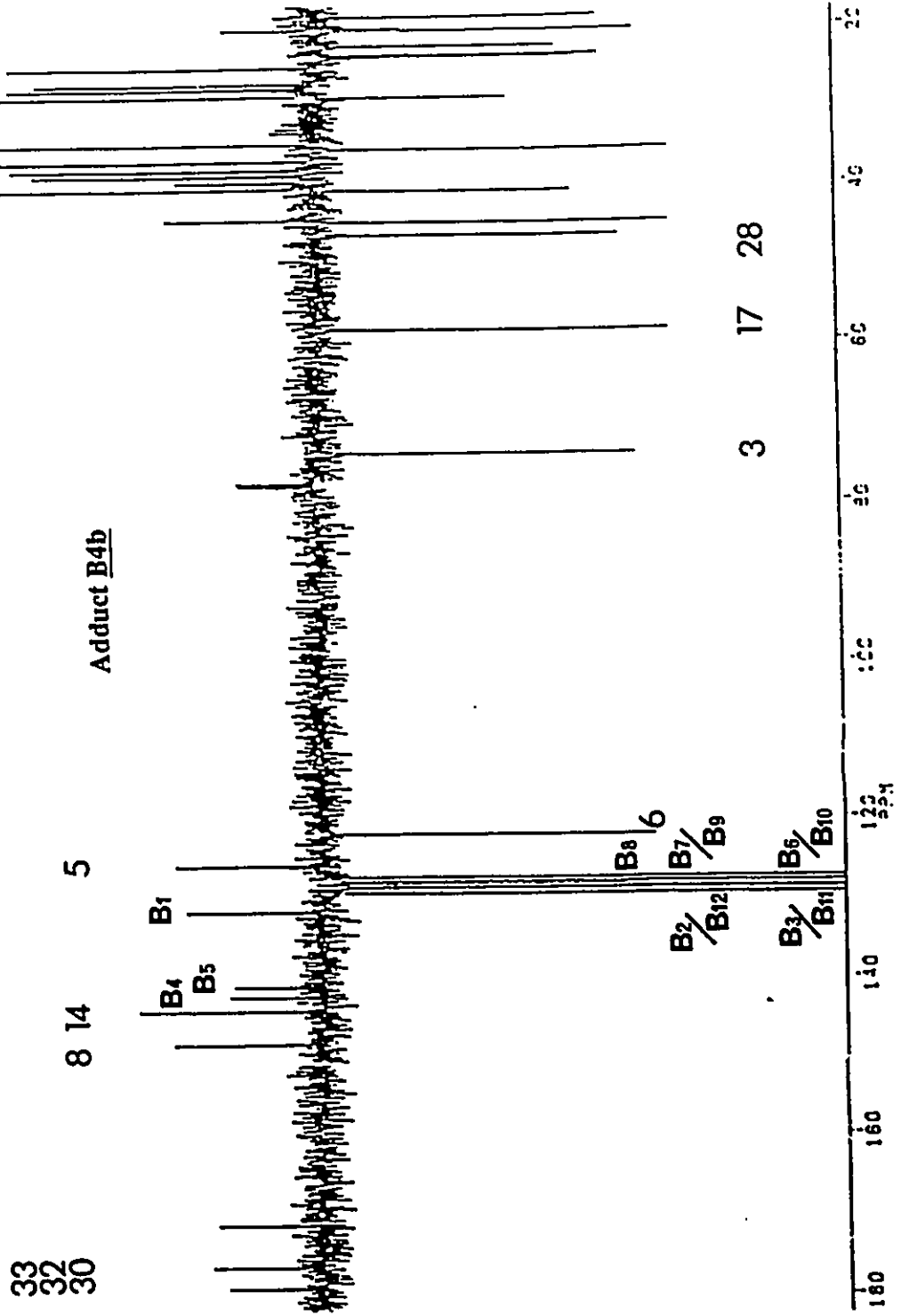
APPENDIX 2c ^1H and ^{13}C SPECTRA ADDUCTS B4a,b (11 PAGES)

APPENDIX 2c (Cont.)

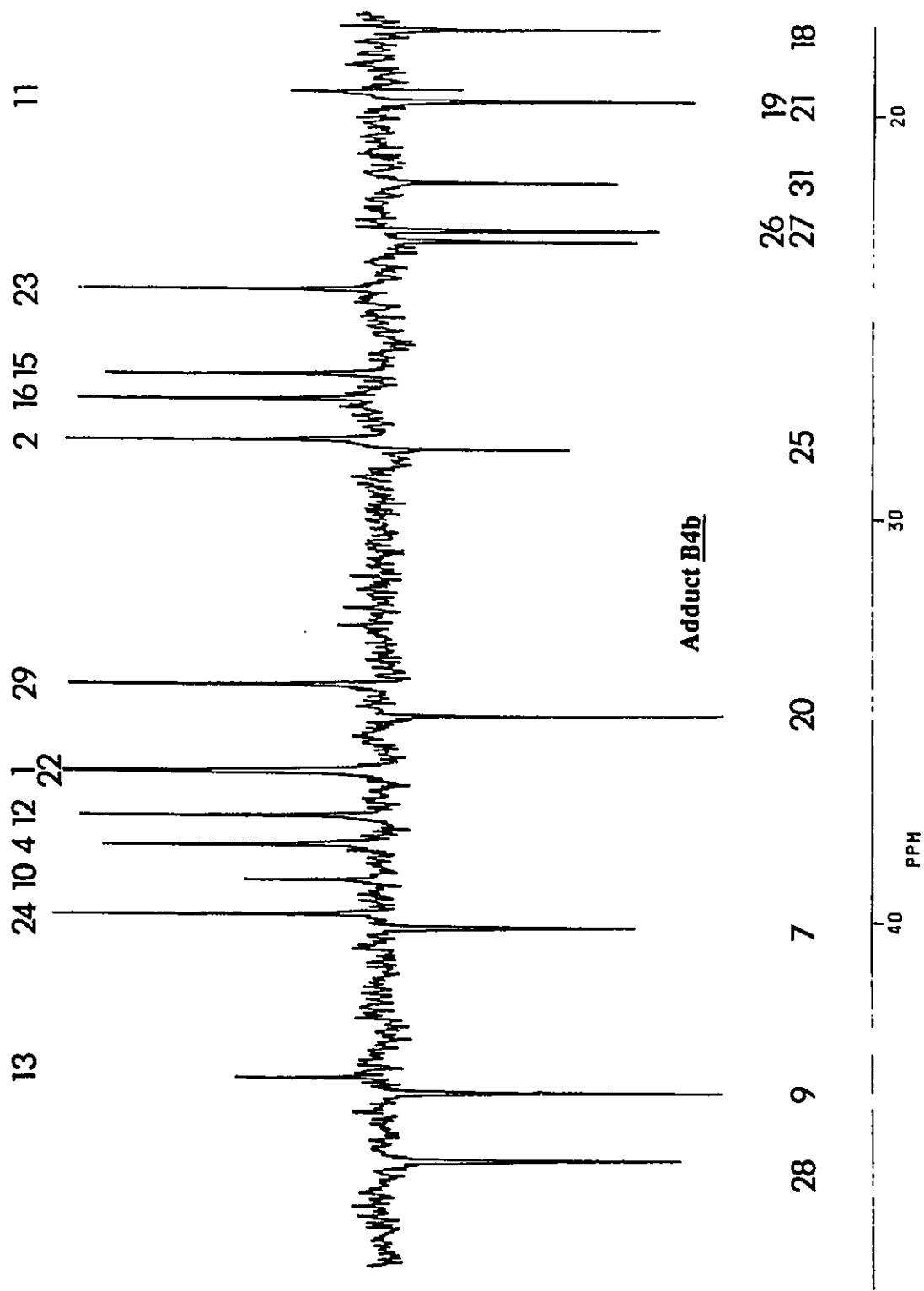


Adduct B4b

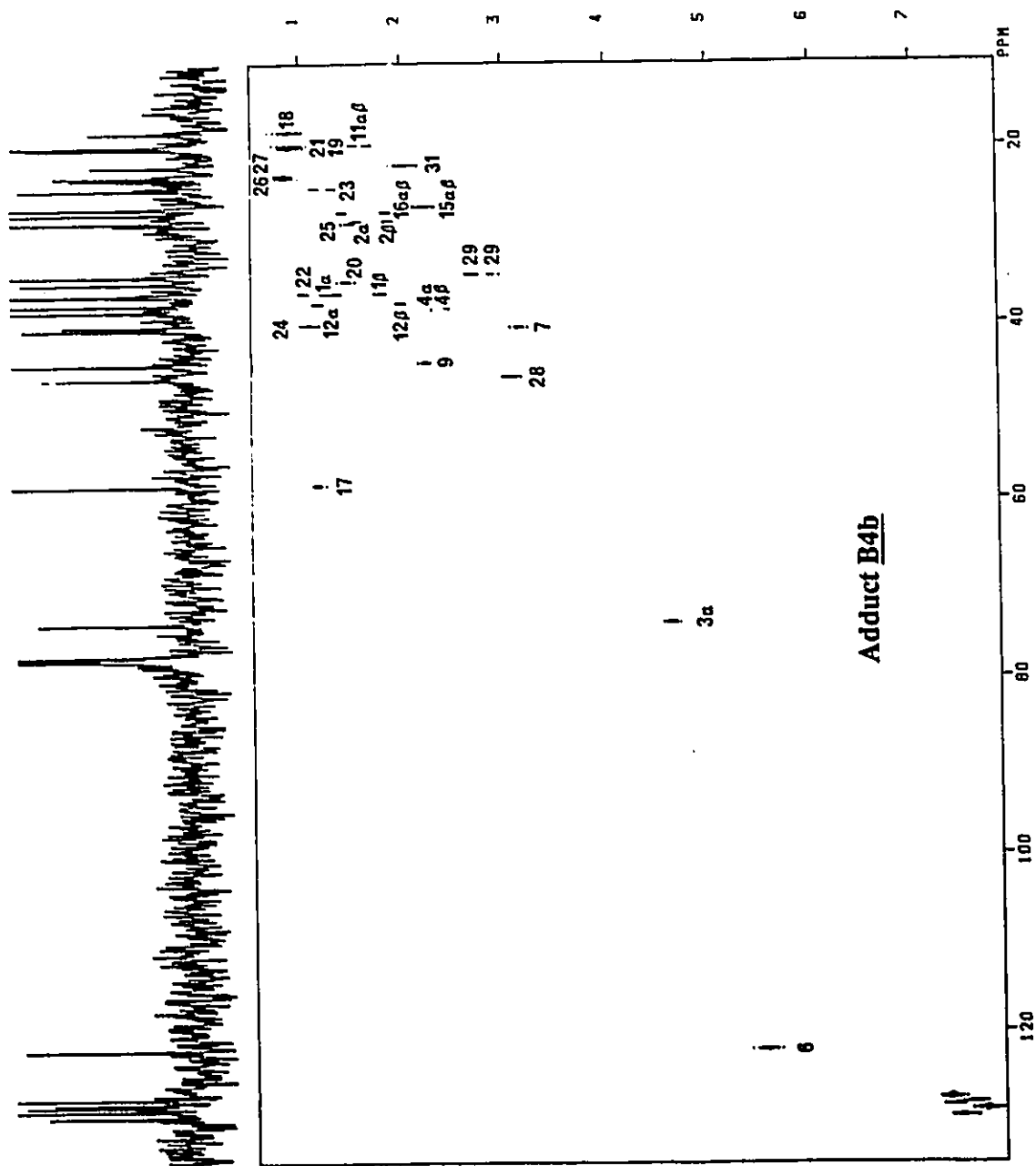
APPENDIX 2c (Cont.)



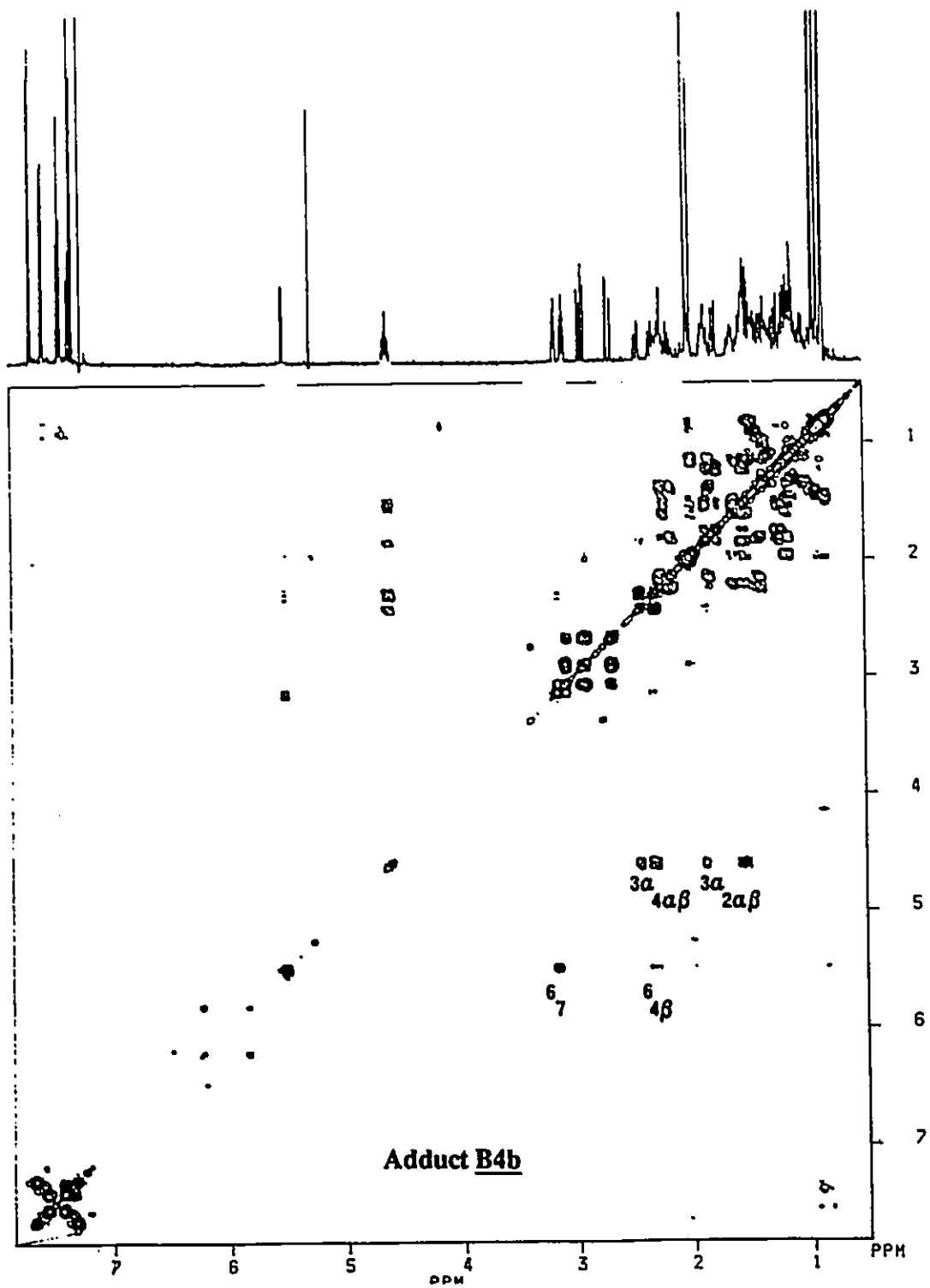
APPENDIX 2c (Cont.)



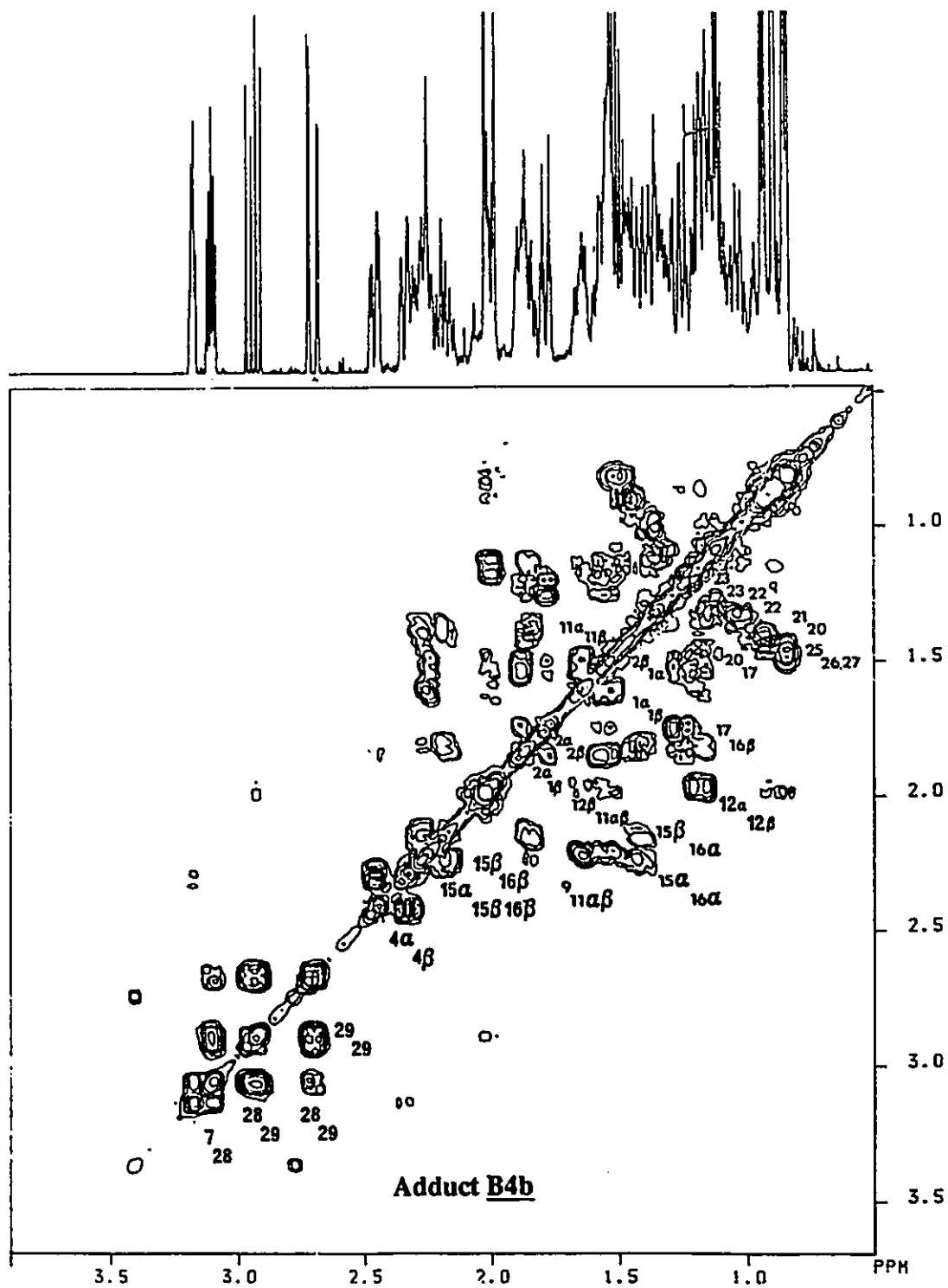
APPENDIX 2c (Cont.)



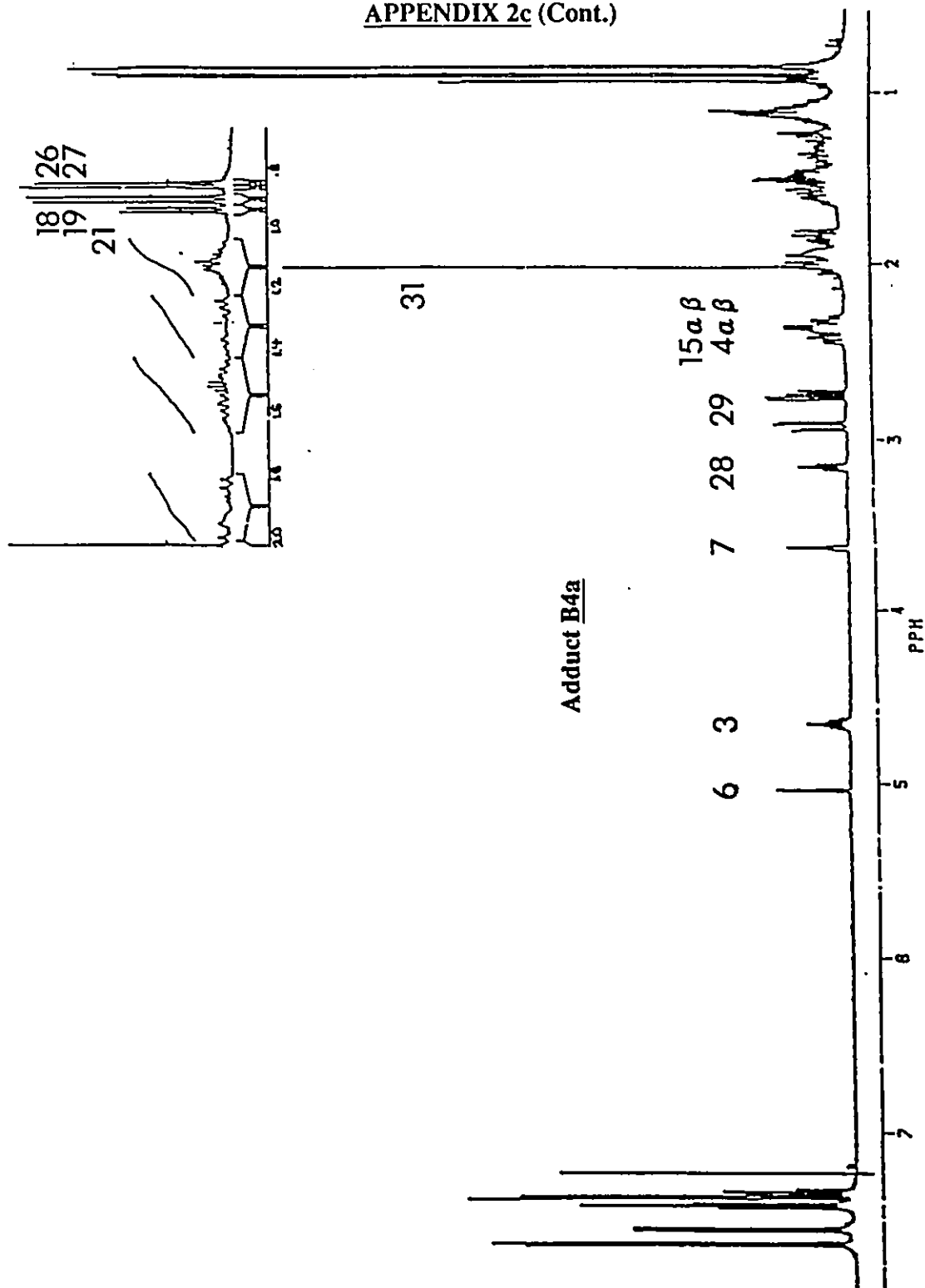
APPENDIX 2c (Cont.)



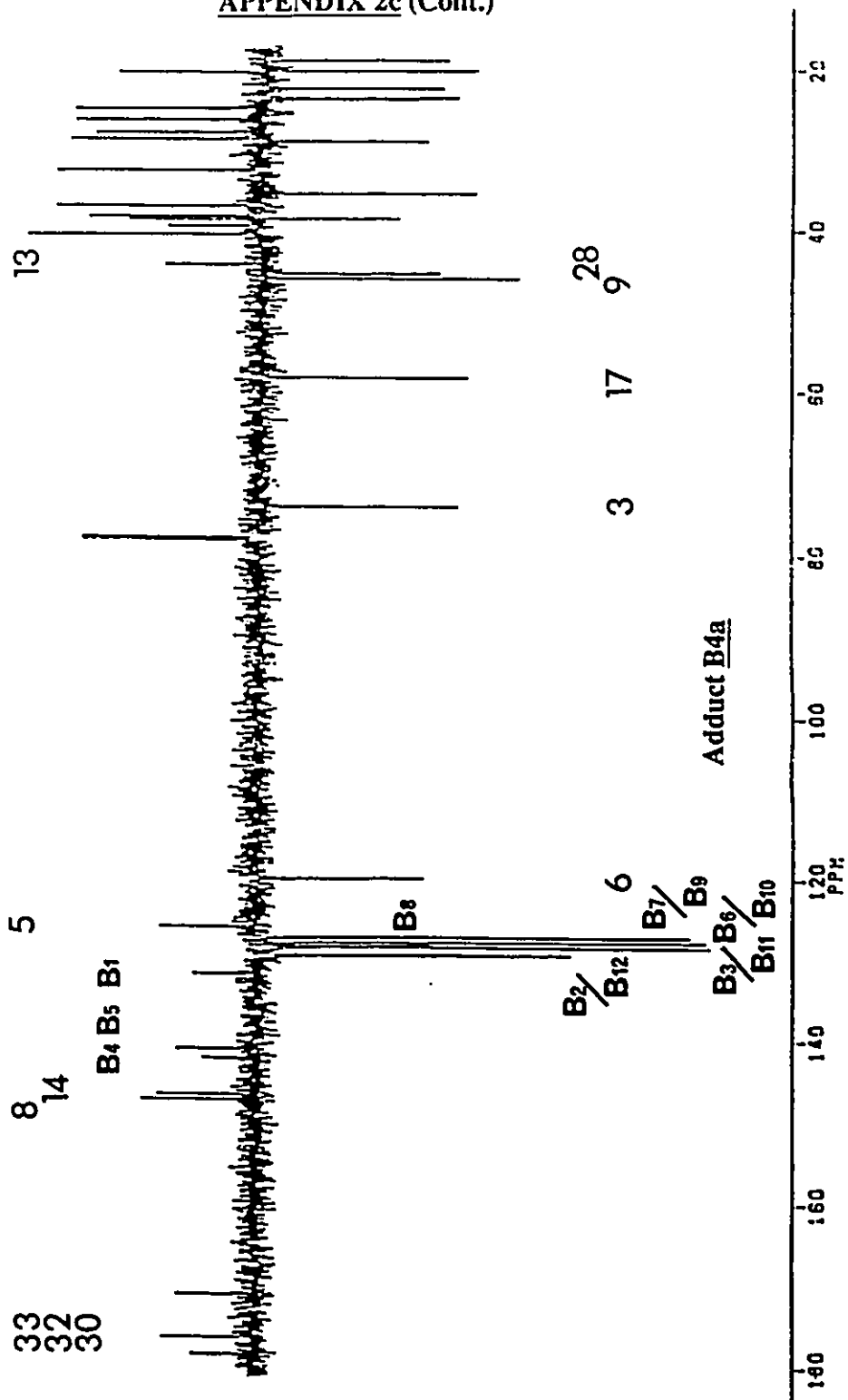
APPENDIX 2c (Cont.)

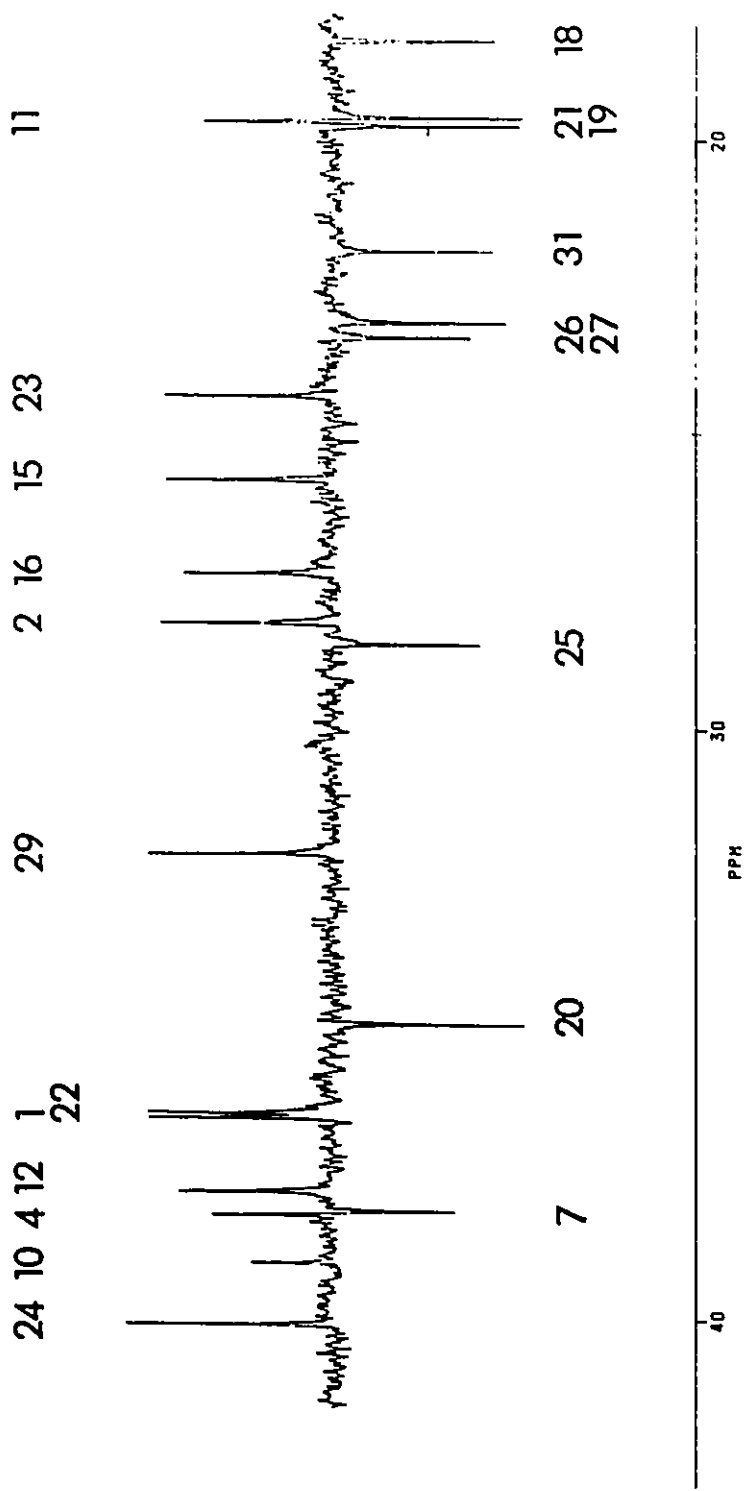


APPENDIX 2c (Cont.)

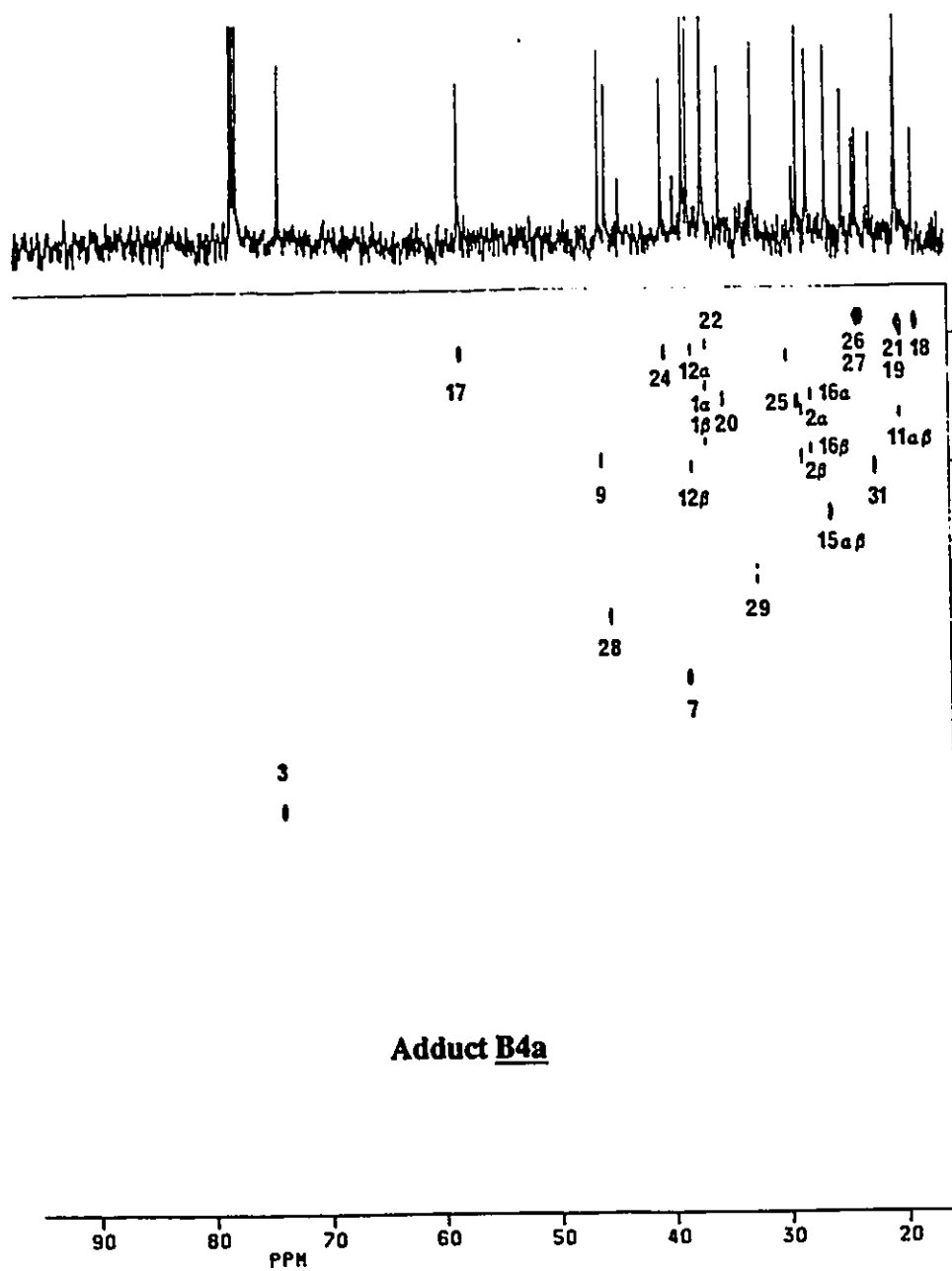


APPENDIX 2c (Cont.)

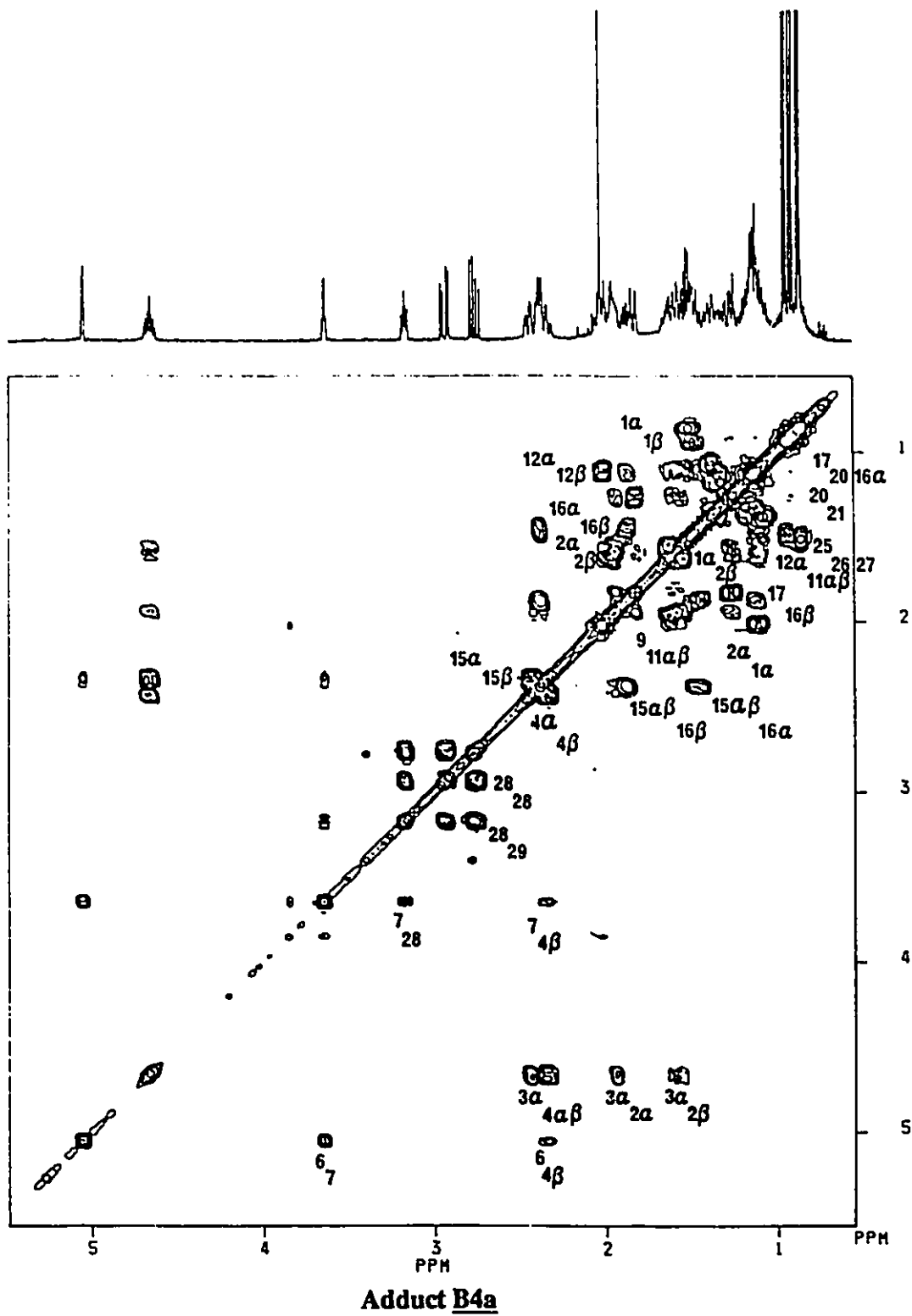


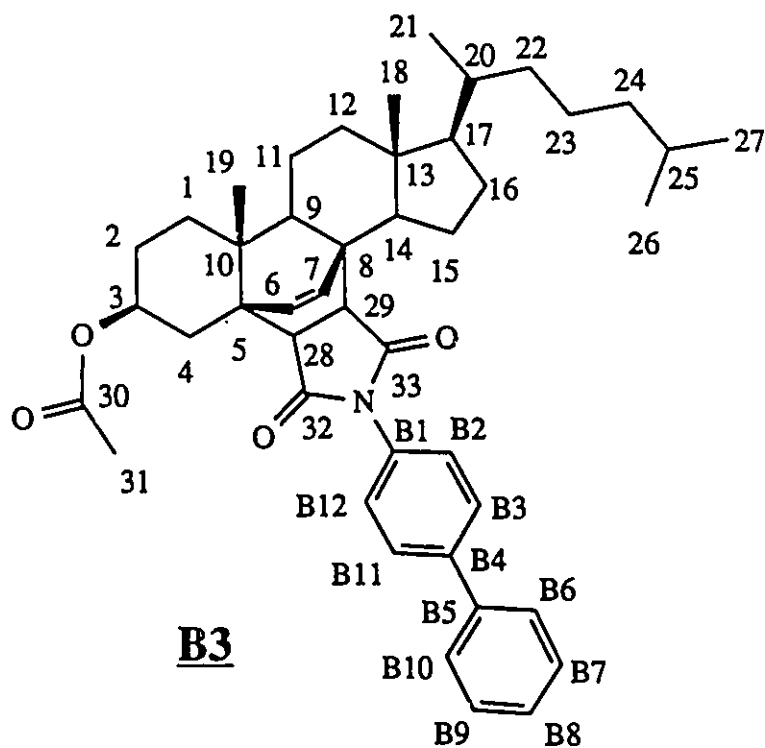


Adduct B4a

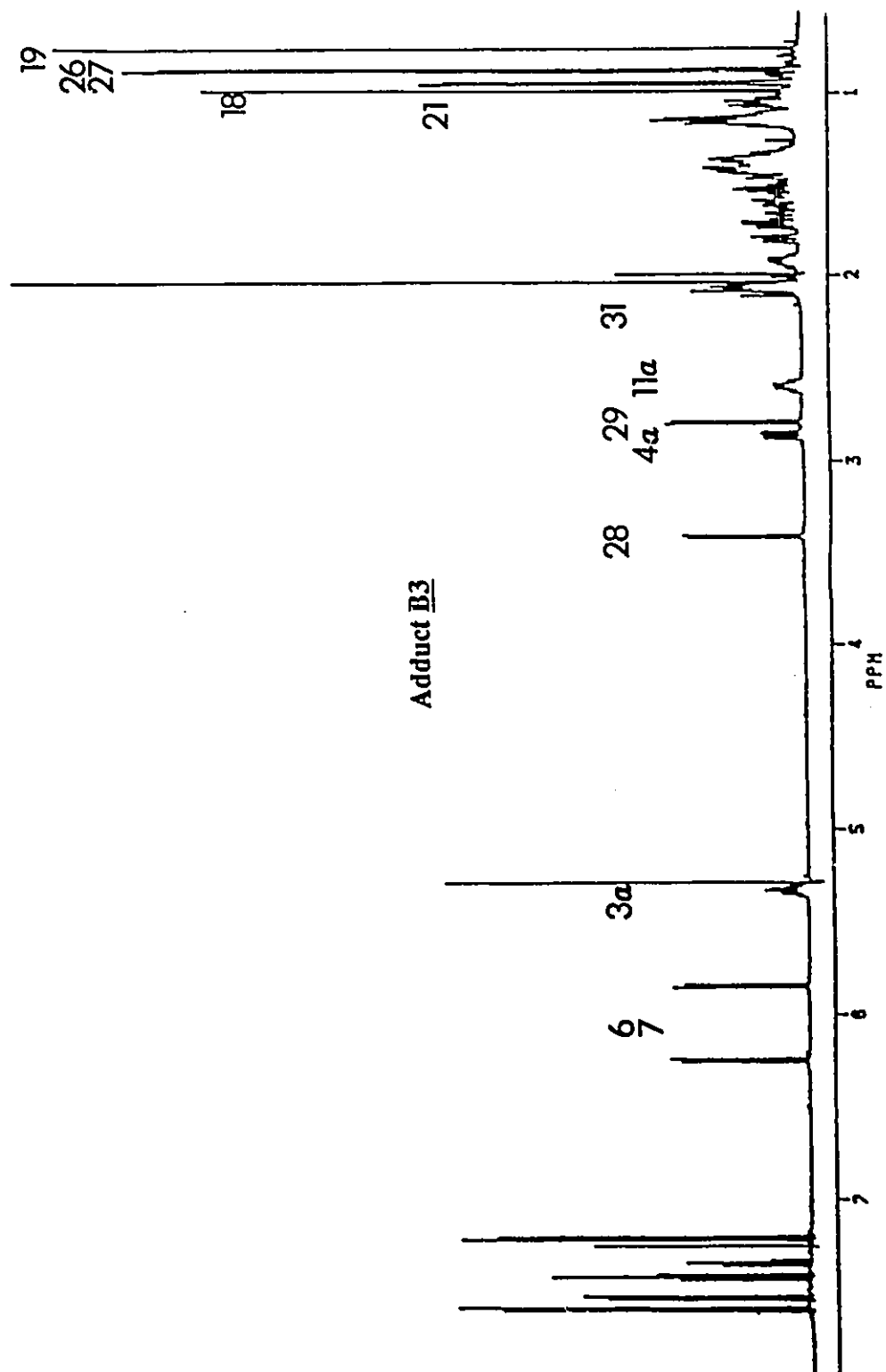
APPENDIX 2c (Cont.)

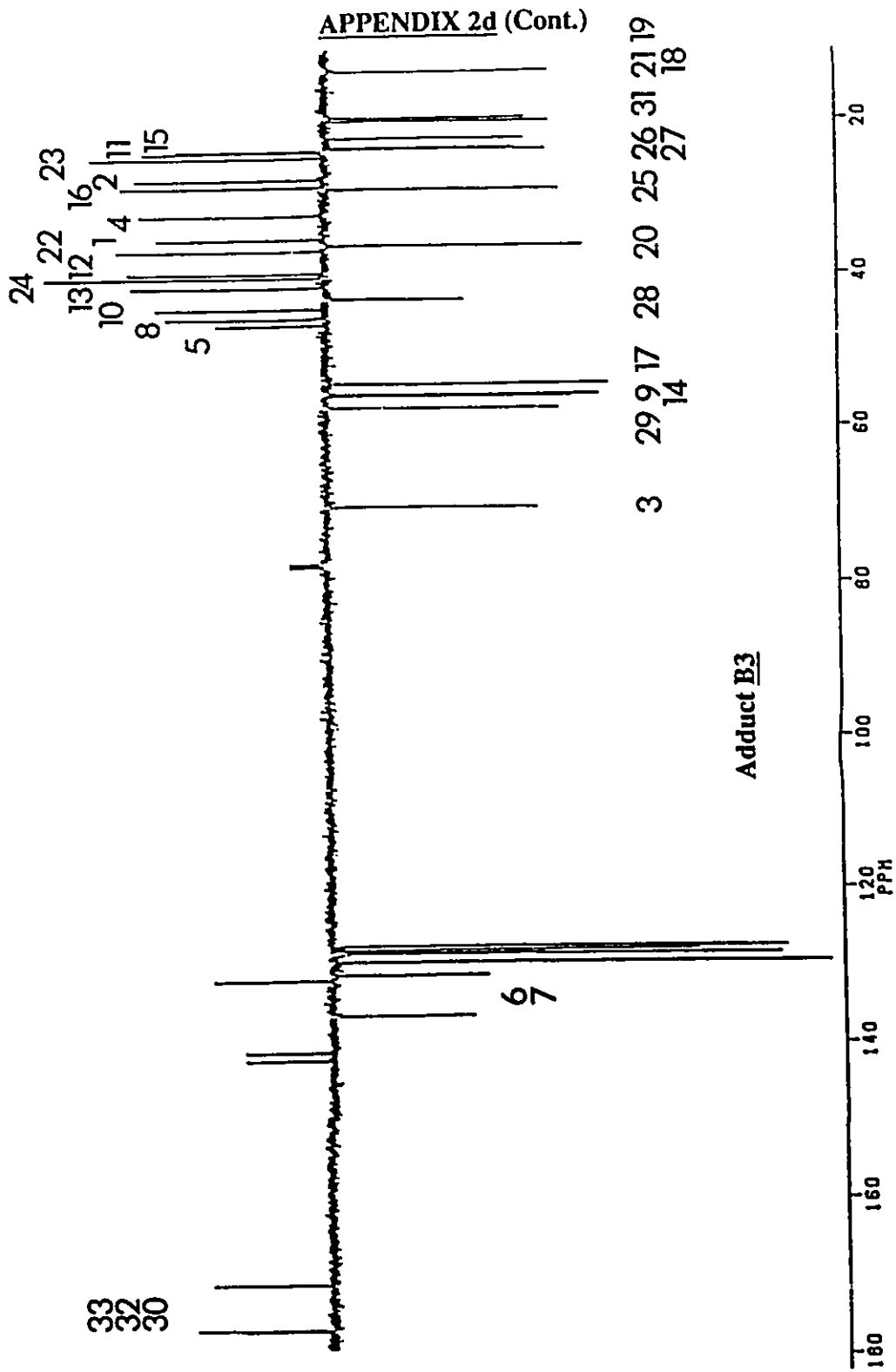
APPENDIX 2c (Cont.)



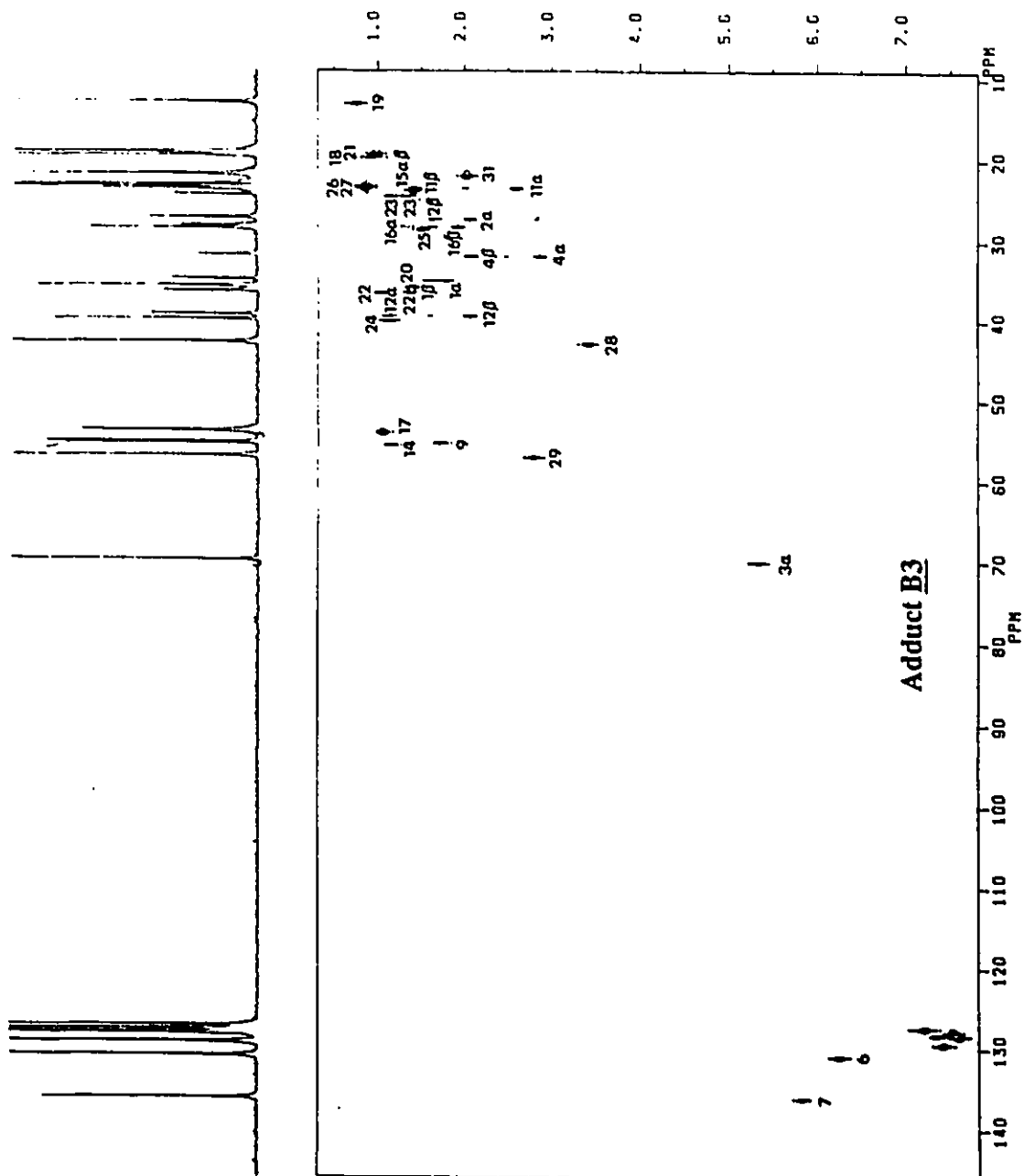
APPENDIX 2d ^1H and ^{13}C SPECTRA ADDUCT B3 (5 PAGES)

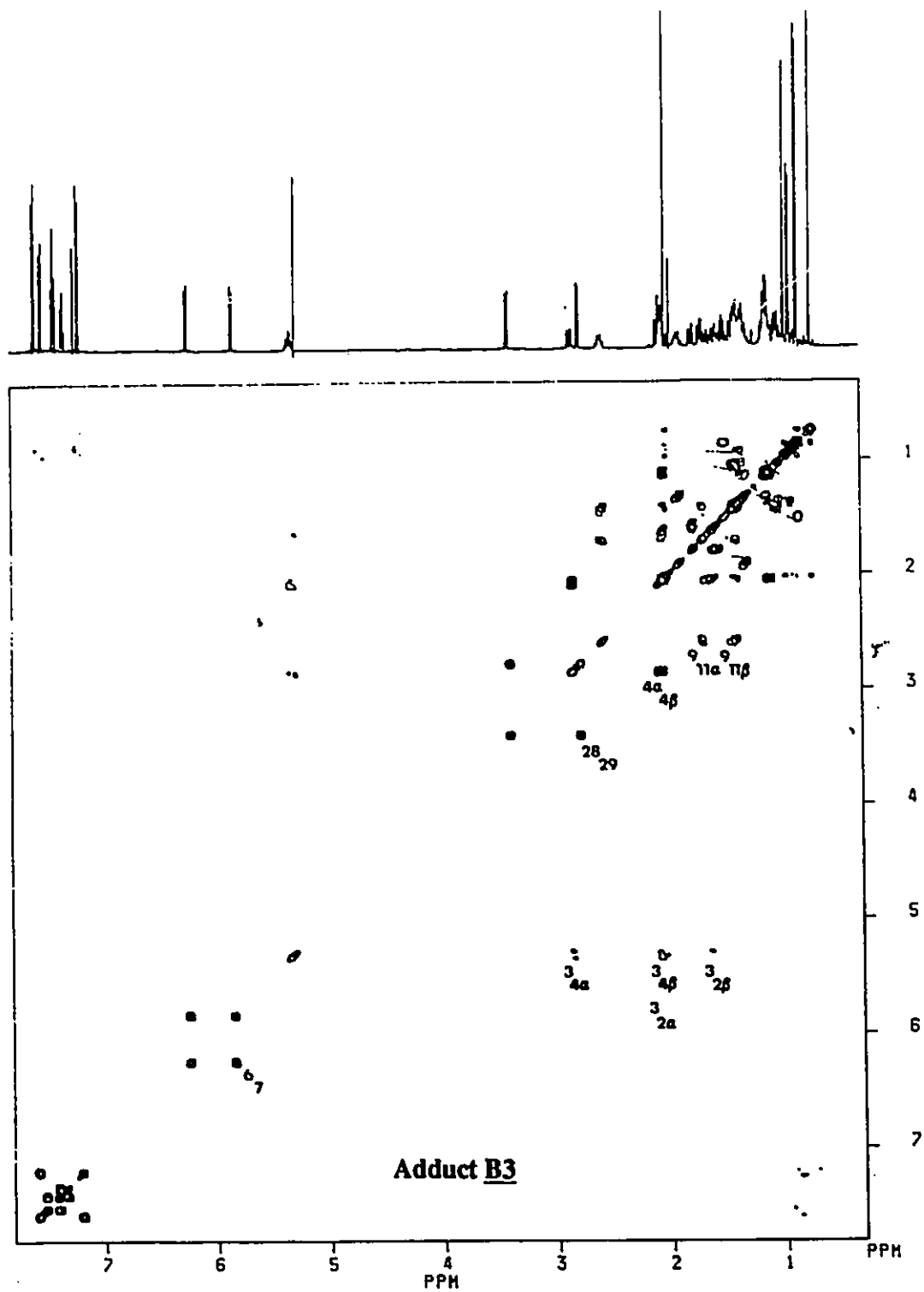
APPENDIX 2d (Cont.)



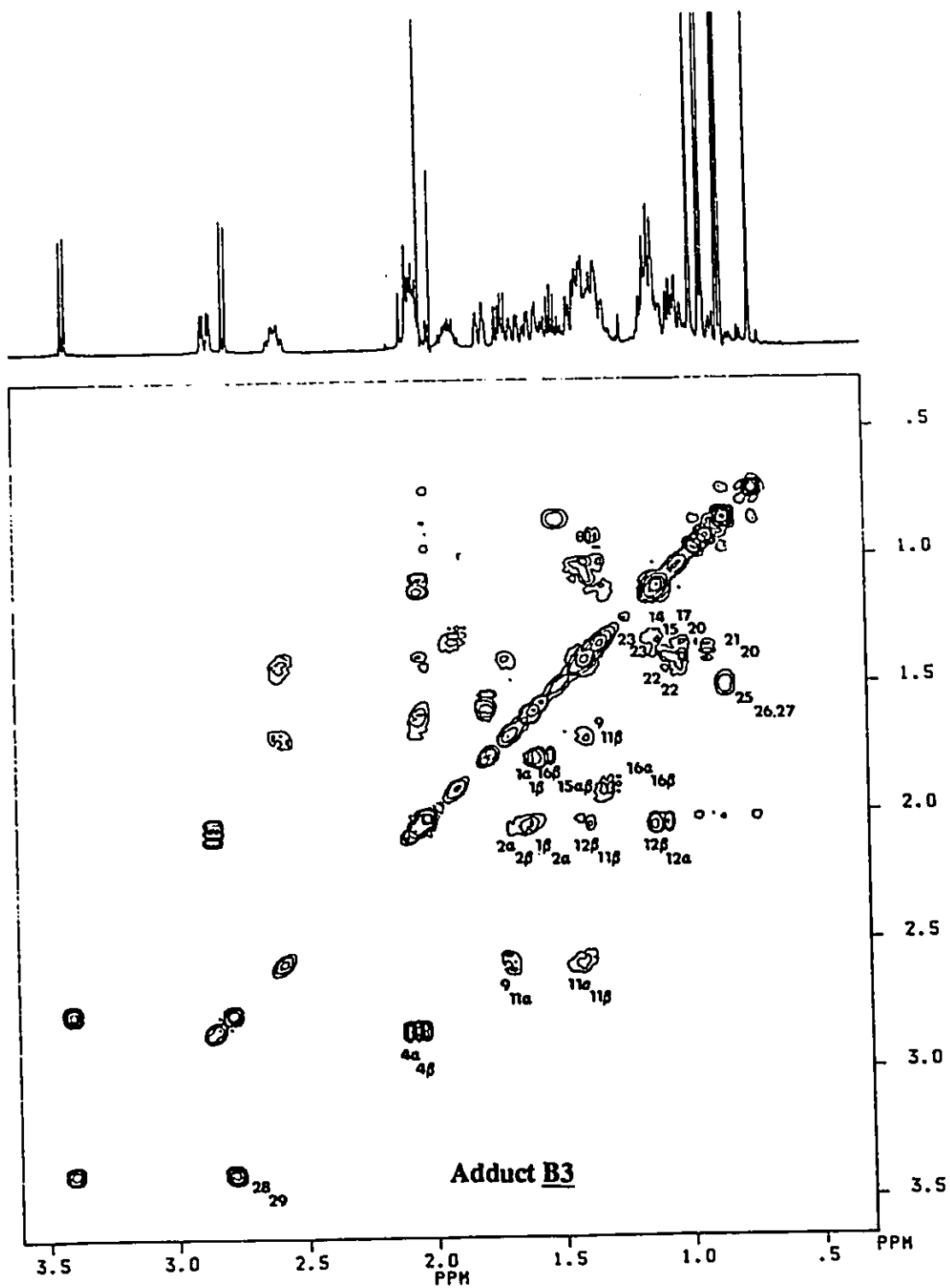


APPENDIX 2d (Cont.)



APPENDIX 2d (Cont.)

APPENDIX 2d (Cont.)



APPENDIX 3a**COMPARISON OF ¹H NMR SPECTRA: ENE ADDUCTS N5 and T5****Solvent; CDCl₃**

<u>N5</u>			<u>T5</u>		
δ (ppm)	proton(s)		δ (ppm)	proton(s)	
7.30-7.50	(m, 5H)	arom. ring	7.20-7.90	(m, 13H)	arom. ring
5.10	(d, 1H)	6	5.08	(d, 1H)	6
4.49	(m, 1H)	3 α	4.48	(m, 1H)	3 α
3.50	(m, 1H)	7	3.50	(m, 1H)	7
3.29	(q, 1H)	28	3.30	(q, 1H)	28
2.57	(dd, 1H)	29 α	2.60	(dd, 1H)	29 α
2.54	(dd, 1H)	29 β	2.56	(dd, 1H)	29 β
2.37-2.42	(m, 2H)	4 α ,4 β	2.32-2.40	(m, 2H)	4 α ,4 β
2.20	(m, 1H)	11 α	2.15-2.30	(m, 1H)	11 α
2.15	(m, 1H)	11 β	2.05-2.15	(m, 1H)	11 β
2.01	(s, 3H)	31	1.96	(s, 3H)	31
1.90-2.05	(m, 5H)	12 β ,1 β ,16 β 14,2 α	1.88-2.05	(m,5H)	12 β ,1 β ,16 β 14,2 α
1.80-1.85	(m, 1H)	15 α	1.74-1.86	(m, 1H)	15 α
1.69-1.72	(m, 1H)	2 β	1.65-1.75	(m, 1H)	2 β
1.48-1.52	(m, 1H)	25	1.45-1.55	(m, 1H)	25
1.30-1.45	(m, 7H)	1 α ,12 α ,15 β 16 α ,20, 22(1),23(1)	1.30-1.45	(m, 7H)	1 α ,12 α ,15 β 16 α ,20 22(1),23(1)

APPENDIX 3a(cont.)

<u>N5</u>			<u>T5</u>		
δ (ppm)	proton(s)		δ (ppm)	proton(s)	
1.24	(s, 3H)	19	1.22	(s, 3H)	19
1.08-1.20	(m, 4H)	17,23(1) 24(2)	1.05-1.18	(m, 4H)	17,23(1) 24(2)
0.85-1.00	(m, 1H)	22(1)	0.90-1.02	(m, 1H)	22(1)
0.93	(d, 3H)	21	0.89	(d, 3H)	21
0.86	(d, 3H)	26	0.80-0.81	(d, 3H)	26
0.85	(d, 3H)	27		(d, 3H)	27
0.65	(s, 3H)	18	0.60	(s, 3H)	18
TOTAL 53 PROTONS			TOTAL 61 PROTONS		

APPENDIX 3bCOMPARISON OF ¹H NMR SPECTRA: ENE ADDUCTS N4a and T4aSolvent; CDCl₃

<u>N4a</u>			<u>T4a</u>		
δ(ppm)	proton(s)		δ(ppm)	proton(s)	
7.20-7.45	(m, 5H)	arom. ring	7.20-7.70	(m, 5H)	arom. ring
5.02	(dd, 1H)	6	5.01	(d, 1H)	6
4.60-4.67	(m, 1H)	3α	4.55-4.65	(m, 1H)	3α
3.61	(dd, 1H)	7	3.61	(dd, 1H)	7
3.10-3.15	(m, 1H)	28	3.11-3.16	(m, 1H)	28
2.87-2.92	(dd, 1H)	29α	2.85-2.95	(dd, 1H)	29α
2.69-2.75	(dd, 1H)	29β	2.73-2.82	(dd, 1H)	29β
2.28-2.45	(m, 4H)	4α, 4β, 15α, 15β	2.25-2.45	(m, 4H)	4α, 4β, 15α, 15β
2.00	(s, 3H)	31	1.98	(s, 3H)	31
1.78-2.04	(m, 5H)	2α, 9, 16α, 1β, 12β	1.73-2.02	(m, 5H)	2β, 9, 16α, 1β, 12β
1.44-1.65	(m, 5H)	11α, 2α, 11β, 25, 20	1.45-1.63	(m, 5H)	11α, 2α, 11β, 25, 20
1.21-1.44	(m, 4H)	16β, 23(1), 1α, 22(1)	1.22-1.45	(m, 4H)	16β, 23(1), 1α, 22(1)
1.02-1.18	(m, 6H)	24(2), 12α, 22(1), 23(1), 17	1.00-1.18	(m, 6H)	24(2), 12α, 17, 22(1), 23(1), 17

APPENDIX 3b (cont)

<u>N4a</u>			<u>T4a</u>		
δ (ppm)	proton(s)		δ (ppm)	proton(s)	
0.92	(d, 3H)	21	0.90	(d, 3H)	21
0.89	(s, 3H)	18	0.88	(s, 3H)	18
0.88	(s, 3H)	19	0.85	(s, 3H)	19
0.85-0.86 (2 singlets, 6H)			0.79-0.80 (2 singlets, 6H)		
		26,27			26,27

TOTAL 53 PROTONS**TOTAL 61 PROTONS**

APPENDIX 3c**COMPARISON OF ¹H NMR SPECTRA: ENE ADDUCTS N4b and T4b**Solvent; CDCl₃

<u>N4b</u>			<u>T4b</u>		
δ(ppm)	proton(s)		δ(ppm)	proton(s)	
7.20-7.50	(m, 5H)	arom. ring	7.25-7.75	(m, 13H)	arom. ring
5.49	(dd, 1H)	6	5.51	(d, 1H)	6
4.60-4.67	(m, 1H)	3α	4.60-4.70	(m, 1H)	3α
3.12-3.15	(m, 1H)	7	3.15-3.19	(m, 1H)	7
3.04-3.09	(q, 1H)	28	3.08-3.15	(m, 1H)	28
2.88-2.94	(dd, 1H)	29α	2.90-2.98	(dd, 1H)	29α
2.64-2.69	(dd, 1H)	29β	2.67-2.75	(dd, 1H)	29β
2.40-2.45	(m, 1H)	4α	2.41-2.49	(m, 1H)	4α
2.28-2.34	(m, 1H)	4β	2.30-2.37	(m, 1H)	4β
2.20-2.25	(m, 2H)	15α,9	2.22-2.28	(m, 2H)	15α,9
2.13-2.18	(m, 1H)	15β	2.15-2.22	(m, 1H)	15β
2.01	(s, 3H)	31	2.03	(s, 3H)	31
1.97-2.00	(m, 1H)	12β	1.96-2.01	(m, 1H)	12β
1.80-1.90	(m, 2H)	2β,16α	1.82-1.91	(m, 2H)	2β,16α
1.75-1.80	(m, 1H)	1β	1.76-1.81	(m, 1H)	1β
1.58-1.66	(m, 2H)	11α,2α	1.57-1.67	(m, 2H)	11α,2α
1.30-1.58	(m, 5H)	23,16β,20, 25,11β	1.32-1.57	(m, 5H)	23,16β,20 25,11β
1.20-1.28	(m, 2H)	1α,22	1.20-1.27	(m, 2H)	1α,22

APPENDIX 3c(cont.)

<u>N4b</u>			<u>T4b</u>		
δ (ppm)	proton(s)		δ (ppm)	proton(s)	
1.00-1.20	(m, 6H)	22,24 23,17,12 α	1.00-1.18	(m, 6H)	22,24 23,17,12 α
0.92	(d, 3H)	21	0.95	(d, 3H)	21
0.89	(s, 3H)	18	0.90	(s, 3H)	18
0.87	(s, 3H)	19	0.89	(s, 3H)	19
0.86	(d, 3H)	26	0.85	(d, 3H)	26
0.85	(d, 3H)	27	0.84	(d, 3H)	27
TOTAL 53 PROTONS			TOTAL 61 PROTONS		

APPENDIX 3dCOMPARISON OF ¹H NMR SPECTRA: ENE ADDUCTS N3 and T3Solvent; CDCl₃

<u>N3</u>			<u>T3</u>		
δ(ppm)	proton(s)		δ(ppm)	proton(s)	
7.08-7.45	(m, 5H)	arom. ring	7.20-7.70	(m, 13H)	arom. ring
6.20	(d, 1H)	6	6.24	(d, 1H)	6
5.80	(d, 1H)	7	5.84	(d, 1H)	7
5.25-5.31	(m, 1H)	3α	5.29-5.35	(m, 1H)	3α
3.34-3.36	(d, 1H)	28	3.40-3.42	(d, 1H)	28
2.80-2.84	(dd, 1H)	4α	2.83-2.87	(dd, 1H)	4α
2.72-2.74	(dd, 1H)	29	2.77-2.79	(dd, 1H)	29
2.53-2.56	(m, 1H)	11α	2.57-2.61	(m, 1H)	11α
2.00-2.04	(m, 3H)	4β, 2α, 12β	2.02-2.06	(m, 3H)	4β, 2α, 12β
1.99	(s, 3H)	31	2.02	(s, 3H)	31
1.85-1.90	(m, 1H)	16β	1.88-1.92	(m, 1H)	16β
1.74-1.76	(m, 1H)	1β	1.78-1.80	(m, 1H)	1β
1.64-1.69	(m, 1H)	9	1.69-1.73	(m, 1H)	9
1.53-1.62	(m, 2H)	2β, 1α	1.56-1.66	(m, 2H)	2β, 1α
1.48-1.52	(m, 1H)	25	1.49-1.53	(m, 1H)	25
1.26-1.41	(m, 7H)	11β, 15α, 22, 23α, 15β 16α, 20	1.30-1.45	(m, 7H)	11β, 15α, 15β 22, 23α 16α, 20

APPENDIX 3d(cont.)

<u>N3</u>			<u>T3</u>		
δ (ppm)	proton(s)		δ (ppm)	proton(s)	
1.06-1.15 (m, 5H)		23,14,12 α 24 α ,24 β	1.08-1.17	(m, 5H)	23,14,12 α 24 α ,24 β
0.97-1.03	(m, 2H)	17,22	1.00-1.07	(m, 2H)	17,22
0.94	(s, 3H)	18	0.98	(s, 3H)	18
0.90	(d, 3H)	21	0.93	(d, 3H)	21
0.84	(d, 3H)	26	0.87	(d, 3H)	26
0.83	(d, 3H)	27	0.85	(d, 3H)	27
0.71	(s, 3H)	19	0.74	(m, 3H)	19

TOTAL 53 PROTONS

TOTAL 61 PROTONS

APPENDIX 4

ERROR ANALYSES

N.B. All error analyses were calculated according to published procedures, see for example D.A. Skoog and D.M. West, "Fundamentals of Analytical Chemistry", CBS College Publishing, Philadelphia, PA. (1982)

1, Errors in Product Yields (Tables 3.3-3.9).

Errors in all product yields are reported as $\pm 0.6\%$ (abs. error, 95% con. lim.).

To obtain this value, the % yield of adduct T5 was determined for 7 independent and identical samples and the standard deviation calculated from the equation;

$$S = \frac{\sum(x_i - \bar{x})^2}{N-1}^{1/2}$$

The 95% con. lim. was then calculated using the equation

$$\mu = \bar{x} \pm \frac{tS}{N^{1/2}} \quad \text{Where } t=2.45$$

This procedure was repeated for 8 trials of the same sample. In both cases, the 95% confidence limits were identical. ($\pm 0.6\%$ abs.).

2, Errors in Slopes and Intercepts of Eyring Plots

Errors in the Eyring plots were reported as ± 2 standard deviations of the slope. Errors in the intercepts were calculated from the worst slopes using the equation $a = y - bx$.

3, Propagation of Errors

The propagation of errors was performed according to published procedures; See reference above. All uncertainties are reported as absolute errors.

CHAPTER 6: REFERENCES

1. (a) Y. Murakami, *Top. Curr. Chem.*, **115**, 107, (1983). (b) D.J. Cram and K.N. Trueblood, *Top. Curr. Chem.*, **98**, 43, (1982)
2. V. Ramamurthy, *Tetrahedron*, **42**, 5753, (1986) and references cited therein.
3. J.L. Atwood, J.E.D. Davies, D.D. MacNichol, Eds.; **"Inclusion Compounds"**, Academic Press: London, (1984) Vol. 2 and 3
4. M.L. Bender, M. Komiyama, **"Cyclodextrin Chemistry"**, Springer, Berlin (1978)
5. W. Saenger, *Angew. Chem., Int. Ed. Engl.*, **19**, 344, (1980)
6. Y. Kotake and E.G. Janzen, *J. Am. Chem. Soc.*, **111** 5138, (1989) and references cited therein
7. K.K. Unger, **"Porous Silica"**, Elsevier Scientific, Amsterdam (1979).
8. R.G. Weiss, *Tetrahedron*, **44**, 3413, (1988)
For a Comprehensive review of the structure and properties of liquid crystals and leading references see;
9. (a) S. Chandrasekhar, **"Liquid Crystals"**, Cambridge University Press, London (1977) (b) H. Kelker and R. Hatz, **"Handbook of Liquid Crystals"**, Verlag Chemie, Weinheim. 1980. (c) F.D. Saeva (ed.), **"Liquid Crystals. The Fourth State of Matter"**, Marcel Dekker, Inc., New York. 1979. (d) G. Vertogen and W.H. de Jeu, **"Thermotropic Liquid Crystals, Fundamentals"**, Springer-Verlag, Berlin. 1987. (e) D. Demus and L. Richter, **"Textures of Liquid Crystals"**, Verlag Chemie, Weinheim. 1978. (f) G.H. Brown, (ed.), **"Advances in Liquid Crystals"**, Academic Press, New York.

1982. Volumes 1,2,3,4,5. (g) G.H. Brown and P.P. Crooker, **Chemical and Engineering News**, Special Report, Jan. 31, 1983. P. 24.
10. G.W. Gray and J.W. Goodby, "Smectic Liquid Crystals Textures and Structures", Leonard Hill, London. 1984. and references cited therein.
 11. (a) M. Miesowicz, *Nature*, 17, 261, (1935)
(b) M. Miesowicz, *Nature*, 158, 27, (1946)
 12. A.E. White, P.E. Cladis and S. Torza, *Mol. Cryst. Liq. Cryst.*, 43, 13, (1977)
 13. (a) Ch. Gahwiller, *Phys. Rev. Lett.*, 28, 1554, (1972). (b) Ch. Gahwiller, *Mol. Cryst. Liq. Cryst.*, 20, 301, (1973). (c) J.W. Summerford, J.R. Boyd and B.A. Lowry, *J. Appl. Phys.*, 46, 970, (1975).
(d) P. Martinoty and S. Candau, *Mol. Cryst. Liq. Cryst.*, 14, 243, (1971). (e) S. Meiboom and R.C. Hewitt, *Phys. Rev. Lett.*, 30, 261, (1973)
 14. "Chemical Rubber Co. Handbook of Chemistry and Physics", 63rd edition, CRC Press Inc. Boca Raton, Florida (1982)
 15. K. Sakamoto, R.S. Porter and J.F. Johnson, *Mol. Cryst. Liq. Cryst.*, 8, 443, (1969)
 16. R.S. Porter, C. Griffen and J.F. Johnson, *Mol. Cryst. Liq. Cryst.*, 25, 131, (1974)
 17. E.M. Friedman and R.S. Porter, *Mol. Cryst. Liq. Cryst.*, 31, 47, (1975)
 18. H. Knepe, F. Schneider and N.K. Sharma, *J. Chem. Phys.*, 77(6), 3203, (1982)
 19. H. Knepe and F. Schneider, *Mol. Cryst. Liq. Cryst.* 65, 23, (1981)
 20. H. Hakemi and M.M. Labes, *J. Chem. Phys.*, 61(10), 4020, (1974)
 21. H. Hervet, W. Urbach and F. Rondelez, *J. Chem. Phys.*, 68(6), 2725, (1978)
 22. M.E. Moseley and A. Loewenstein, *Mol. Cryst. Liq. Cryst.*, 90, 117, (1982)

23. C.K. Yun and A.G. Fredrickson, *Mol. Cryst. Liq. Cryst.*, **12**, 73, (1970)
24. K. Chu, N.K. Ailawadi and D.S. Moroi, *Mol. Cryst. Liq. Cryst.*, **38**, 45, (1977)
25. J.A. Murphy, J.W. Doane, Y.Y. Hsu and D.L. Fishel, *Mol. Cryst. Liq. Cryst.*, **22**, 133, (1973)
26. E. Meirovitch and J. H. Freed, *J. Phys. Chem.*, **88**, 4995 (1984) and references cited therein.
27. S. Ghodbane and D.E Martire, *J. Phys. Chem.*, **91**, 6410, (1987)
28. D.E. Martire in "The Molecular Physics of Liquid Crystals", G.R. Luckhurst and G.W. Gray (eds.), Academic Press, New York. 1979.
29. J.M. Schnur and D.E. Martire, *Mol. Cryst. Liq. Cryst.*, **26**, 213, (1974)
30. G. A. Oweimreen, G.C. Lin and D.E. Martire, *J. Phys. Chem.*, **83**, 2111 (1979)
31. A. Oweimreen and D.E. Martire, *J. Chem. Phys.*, **72**, 2500, (1980)
32. F.D. Saeva, *Pure Appl. Chem.*, **38**, 25, (1974)
33. E. Sackman, P. Krebs, H.U. Rega, J. Voss and H. Mohwald, *Mol. Cryst. Liq. Cryst.*, **24**, 283, (1973)
34. Z. Luz in "Nuclear Magnetic Resonance of Liquid Crystals", J.W.D. Emsley (ed.), NATO ASI Series, Ser. C, Vol. 141, Reidel Publishing Co., Dordrecht, 1985
35. (a) B. Samori and L. Fiocco, *J. Am. Chem. Soc.*, **104**, 2634, (1982). (b) P. de Maria, A. Lodi, B. Samori, F. Rustichelli and G. Torquati, *J. Am. Chem. Soc.*, **106**, 653, (1984). (c) B. Samori, P De Maria, P. Mariani, F. Rustichelli and P. Zani, *Tetrahedron*, **43**, 1409, (1987) and references cited therein.
36. B.M. Fung and M. Gangoda, *J. Am. Chem. Soc.*, **107**, 3395, (1985).
37. M. Gangoda and B.M. Fung, *Chem. Phys. Lett.*, **120**, 527, (1985)

38. R.L. Treanor and R.G. Weiss, *J. Phys. Chem.*, 91, 5552, (1987)
39. B.J. Fahie, D.S. Mitchell and W.J. Leigh, *Can. J. Chem.*, 67, 148, (1989)
40. B.J. Fahie, D.S. Mitchell, M.S. Workentin and W.J. Leigh, *J. Am. Chem. Soc.*, 111, 2916, (1989)
41. (a) J.M. Nerbonne and R.G. Weiss, *J. Am. Chem. Soc.*, 100, 5953, (1978) (b) J.P. Otruba III and R.G. Weiss, *J. Org. Chem.*, 48, 3448, (1983)
42. V.C. Anderson, B.B. Craig and R.G. Weiss, *J. Phys. Chem.*, 86, 4642, (1982)
43. V.C. Anderson, B.B. Craig and R.G. Weiss, *Mol. Cryst. Liq. Cryst.*, 97, 351, (1983)
44. R.L. Treanor and R.G. Weiss, *J. Am. Chem. Soc.*, 110, 2170, (1988)
45. R.G. Zimmerman, J.H. Liu and R.G. Weiss, *J. Am. Chem. Soc.*, 108, 5264, (1986)
46. S. Ganapathy, R.G. Zimmerman and R.G. Weiss, *J. Org. Chem.*, 51, 2529, (1986)
47. E.G. Cassis Jr. and R.G. Weiss, *Photochem. Photobiol.*, 439, (1982)
48. E. Sackman, *J. Am. Chem. Soc.*, 93, 7088, (1971)
49. S. Melone, V. Mosini, R. Nicoletti, B. Samori and G. Torquati, *Mol. Cryst. Liq. Cryst.*, 98, 399, (1983)
50. W.E. Bacon and G.H. Brown, *Mol. Cryst. Liq. Cryst.*, 12, 229, (1971)
51. M.J.S. Dewar and B.D. Nahlovsky, *J. Am. Chem. Soc.*, 96, 460, (1974)
52. W.J. Leigh, D.T. Frendo and P.J. Klawunn, *Can. J. Chem.*, 63, 2131, (1985)
53. (a) C.S. Yannoni, *J. Am. Chem. Soc.*, 92, 5237, (1970) (b) R. Poupko, H. Zimmerman and Z. Luz, *J. Am. Chem. Soc.*, 106, 5391, (1984)
54. (a) J.M. Anderson and A.C.-F. Lee, *J. Magn. Reson.*, 3, 427, (1970) (b) M.E. Moseley, R. Poupko, Z. Luz, *J. Magn. Reson.*, 48, 354, (1982)
55. R. Poupko and Z. Luz, *J. Chem. Phys.*, 75, 1675, (1981)

56. Z. Luz, R. Naor and E. Meirovitch, *J. Chem. Phys.*, 74, 6624, (1981)
57. R. Poupko and Z. Luz, *Mol. Phys.*, 76, 5662, (1982)
58. B.M. Fung, R.V. Sigh and M.M. Alcock, *J. Am. Chem. Soc.*, 106, 7301, (1984)
59. J.T. Otruba III and R.G. Weiss, *Mol. Cryst. Liq. Cryst.*, 80, 165 (1982)
60. W.J. Leigh and S. Jakobs, *Tetrahedron*, 43, 1393, (1987)
61. W.J. Leigh, *J. Am. Chem. Soc.*, 107, 6114, (1985)
62. W.J. Leigh, *Can. J. Chem.*, 64, 1130, (1986)
63. D.A. Hrovat, J.H. Liu, N.J. Turro and R.G. Weiss, *J. Am. Chem. Soc.*, 106, 7033, (1984)
64. C.D. Hurd and L. Schmerling, *J. Am. Chem. Soc.*, 59, 107, (1937)
65. J.P. Ryan and P.R. O'Connor, *J. Am. Chem. Soc.*, 74, 5866, (1952)
66. A.R. Katritzky and G.J.T. Tiddy, *Org. Magn. Reson.*, 1, 57, (1969)
67. J. Riand, M.-T. Chenon and J. Lumbroso-Bader, *J. Chem. Soc., Perkin Trans.*, 2, 1248, (1979)
68. P.J. Wagner, *Acc. Chem. Res.*, 16, 461, (1983)
69. J.C. Scaiano, W.G. McGimpsey, W.J. Leigh and S. Jakobs, *J. Org. Chem.*, 52, 4540 (1987)
70. P.K. Das, M.V. Encinas and J.C. Scaiano, *J. Am. Chem. Soc.*, 103, 4154, (1981)
71. (a) P.J. Wagner, P.A. Kelso, A.E. Kemppainen, A. Haug and D.R. Graber, *Mol. Photochem.*, 2, 81, (1970) (b) D.G. Whitten and W.E. Punch, *Mol. Photochem.*, 2, 81, (1970). (c) J.C. Scaiano, M.J. Perkins, J.W. Sheppard, M.S. Platz and R.L. Barcus, *J. Photochem.*, 21, 137, (1983).
72. D.A. Hrovat, J.H. Liu, N.J. Turro and R.G. Weiss, *J. Am. Chem. Soc.*, 106, 5291, (1984)

73. G.R. Bauer, F. Dickert and A. Hammerschmidt, *Angew. Chem. Int. Ed. (ENG)*, **25**, 841, (1986)
74. G.B. Sergeev, V.A. Batyuk, T.I. Shabatina, *Kinet. Katal.*, **24**, 538 (1983)
75. K.-I. Okamoto and M.M. Labes, *Mol. Cryst. Liq. Cryst.*, **54**, 9, (1979)
76. W. J. Leigh, *Can. J. Chem.*, **63**, 2736, (1985)
77. V.C. Anderson, B.B. Craig and R.G. Weiss, *J. Am. Chem. Soc.*, **103**, 7169, (1981)
78. V.C. Anderson, B.B. Craig and R.G. Weiss, *J. Am. Chem. Soc.*, **104**, 2972, (1982)
79. J.M. Nerbonne and R.G. Weiss, *J. Am. Chem. Soc.*, **100**, 2571, (1978)
80. J.M. Nerbonne and R.G. Weiss, *J. Am. Chem. Soc.*, **101**, 402, (1979)
81. P. De Maria, B. Samori, A. Tampieri and P. Zani, *Bull. Chem. Soc. Jpn.*, **61**, 1773, (1988)
82. C.N. Sukenik, J.A.P. Bonapace, S.H. Mandel, P. Lou, G. Wood and R.G. Bergman, *J. Am. Chem. Soc.*, **99**, 851, (1977)
83. G. Aviv, J. Sagiv and A. Yogev, *Mol. Cryst. Liq. Cryst.*, **36**, 349, (1976)
84. T. Kunieda, T. Takahashi and M. Hirobe, *Tet. Lett.*, **24**, 5107, (1983)
85. A. van der Gen, J. Lakeman, U.K. Pandit, H.O. Huisman, *Tetrahedron*, **21**, 3641 (1965)
86. Authentic samples of 1/DMAD adducts were prepared in our laboratory by P.J. Klawunn, senior thesis student 1984-85.
87. W.B. Smith, *Orgn. Magn. Reson.*, **9**, 644 1977
88. R.E. Perrier and M.J. McGlinchey, *Can. J. Chem.*, **66**, 3003 (1988)
89. C. Wiegand, *Z. Naturforsch Teil B*, **4**, 249 (1948)
90. E.M. Barrell, *Mol. Cryst. Liq. Cryst.*, **18**, 195 (1972)

91. P.G. de Gennes, "The Physics of Liquid Crystals", Clarendon Press, Oxford (1974) and references cited therein.
92. A.W. Maier and A. Saupe, *Z. Naturforschung*, **15**, 287 (1960)
93. A.W. Maier and A. Saupe, *Z. Naturforschung*, **13**, 564 (1958)
94. A.W. Maier and A. Saupe, *Z. Naturforschung*, **16**, 816 (1961)
95. A.W. Maier and A. Saupe, *Z. Naturforschung*, **14**, 882 (1959)
96. J.H. Davis, *Biochim. Biophys. Acta.*, **737**, 117 (1983)
97. J.W. Emsley, *Isr. J. Chem.*, **28**, 297 (1988)
98. C. Zannoni in, "Nuclear Magnetic Resonance of Liquid Crystals", J.W.D. Emsley (ed.), NATO ASI Series, Ser. C, Vol. 141, Reidel Publishing Co., Dordrecht, 1985
99. J.W. Emsley and J.C. Lindon, "N.M.R. Spectroscopy Using Liquid Crystal Solvents", Pergamon, (1965)
100. G.R. Luckhurst in "Electron Spin Relaxation in Liquids", L.T. Muus and P.W. Atkins eds., Plenum, (1972)
101. E.W. Thulstrup and J. Michl, *J. Phys. Chem.*, **84**, 82 (1980)
102. C. Zannoni, *Mol. Phys.*, **38**, 1813 (1979)
103. C. Zannoni, *Mol. Phys.*, **42**, 1303 (1981)
104. V.A. Batyk, T.N. Boronina, G.E. Chudinov and G.B. Sergeev, *Liquid Crystals*, **4**, 181 (1989)
105. V.A. Batyk, T.I. Shabatina and G.B. Sergeev, *Mol. Cryst. Liq. Cryst.*, **166**, 105 (1989)
106. V.A. Batyk, T.I. Shabatina, Yu.N. Morosov and G.B. Sergeev, *Mol. Cryst. Liq. Cryst.*, **161**, 109 (1988)
107. N.C. Shivaprakash and J.S. Prasad, *J. Chem. Phys.*, **76**, 866 (1982)

108. C.L. Khetrapal, P. Diehl and A.C. Kunwar, **Organic Magnetic Resonance**, 10, 213 (1977)
109. P.J. Collings, T.J. McKee and J.R. McColl, **J. Chem. Phys.**, 65, 3520 (1976)
110. A. Saupe, **Angew. Chem.**, 41, 26 A (1969)
111. J.V. Crivello, **J. of Polymer Science, Polymer Chem. Ed**, 14, 159 (1976)
112. R.G. Splies, **J. Org. Chem.**, 2601 (1961)
113. F.D. Bellamy and K. Ou, **Tetrahedron Letters**, 25, 839 (1984)